

1986

Reactivity of nucleophiles toward phenyl radical

James Louis Anderson Jr.
Iowa State University

Follow this and additional works at: <https://lib.dr.iastate.edu/rtd>

 Part of the [Organic Chemistry Commons](#)

Recommended Citation

Anderson, James Louis Jr., "Reactivity of nucleophiles toward phenyl radical " (1986). *Retrospective Theses and Dissertations*. 8135.
<https://lib.dr.iastate.edu/rtd/8135>

This Dissertation is brought to you for free and open access by the Iowa State University Capstones, Theses and Dissertations at Iowa State University Digital Repository. It has been accepted for inclusion in Retrospective Theses and Dissertations by an authorized administrator of Iowa State University Digital Repository. For more information, please contact digirep@iastate.edu.

INFORMATION TO USERS

While the most advanced technology has been used to photograph and reproduce this manuscript, the quality of the reproduction is heavily dependent upon the quality of the material submitted. For example:

- Manuscript pages may have indistinct print. In such cases, the best available copy has been filmed.
- Manuscripts may not always be complete. In such cases, a note will indicate that it is not possible to obtain missing pages.
- Copyrighted material may have been removed from the manuscript. In such cases, a note will indicate the deletion.

Oversize materials (e.g., maps, drawings, and charts) are photographed by sectioning the original, beginning at the upper left-hand corner and continuing from left to right in equal sections with small overlaps. Each oversize page is also filmed as one exposure and is available, for an additional charge, as a standard 35mm slide or as a 17"x 23" black and white photographic print.

Most photographs reproduce acceptably on positive microfilm or microfiche but lack the clarity on xerographic copies made from the microfilm. For an additional charge, 35mm slides of 6"x 9" black and white photographic prints are available for any photographs or illustrations that cannot be reproduced satisfactorily by xerography.



8703682

Anderson, James Louis, Jr.

REACTIVITY OF NUCLEOPHILES TOWARD PHENYL RADICAL

Iowa State University

Ph.D. 1986

University
Microfilms
International 300 N. Zeeb Road, Ann Arbor, MI 48106

PLEASE NOTE:

In all cases this material has been filmed in the best possible way from the available copy. Problems encountered with this document have been identified here with a check mark .

1. Glossy photographs or pages _____
2. Colored illustrations, paper or print _____
3. Photographs with dark background _____
4. Illustrations are poor copy _____
5. Pages with black marks, not original copy _____
6. Print shows through as there is text on both sides of page _____
7. Indistinct, broken or small print on several pages _____
8. Print exceeds margin requirements _____
9. Tightly bound copy with print lost in spine _____
10. Computer printout pages with indistinct print _____
11. Page(s) _____ lacking when material received, and not available from school or author.
12. Page(s) _____ seem to be missing in numbering only as text follows.
13. Two pages numbered _____. Text follows.
14. Curling and wrinkled pages _____
15. Dissertation contains pages with print at a slant, filmed as received _____
16. Other _____

University
Microfilms
International



Reactivity of nucleophiles toward phenyl radical

by

James Louis Anderson, Jr.

A Dissertation Submitted to the
Graduate Faculty in Partial Fulfillment of the
Requirements for the Degree of
DOCTOR OF PHILOSOPHY

Department: Chemistry
Major: Organic Chemistry

Approved:

Signature was redacted for privacy.

In Charge of Major Work

Signature was redacted for privacy.

For the Major Department

— Signature was redacted for privacy.

For the Graduate College

Iowa State University
Ames, Iowa

1986

TABLE OF CONTENTS

	Page
GENERAL INTRODUCTION	1
PART I. MECHANISTIC STUDY OF THE AROMATIC S_N1 REACTION USING COMPETITIVE REACTION KINETICS	2
INTRODUCTION	3
RESULTS AND DISCUSSION	38
CONCLUSION	123
EXPERIMENTAL	125
PART II. THE DETERMINATION OF ABSOLUTE RATE CONSTANTS FOR THE COUPLING OF PHENYL RADICAL WITH VARIOUS NUCLEOPHILES	138
INTRODUCTION	139
RESULTS AND DISCUSSION	158
CONCLUSION	186
EXPERIMENTAL	187
GENERAL SUMMARY	193
REFERENCES	194
ACKNOWLEDGEMENTS	199

LIST OF TABLES

	Page
Table 1. Absolute rate constants for the dissociation of aryl halide radical anions in various solvents determined either by electrochemical (E) or pulse radiolysis (P)	13
Table 2. Effect of added substances on $S_{RN}1$ reactions	22
Table 3. Nucleophile reactivities relative to pinacolone enolate ion and diethyl phosphite ion in liquid ammonia at -38°C initiated by U.V. light	24
Table 4. Nucleophile reactivity relative to thiophenoxide determined electrochemically in liquid ammonia at -38°C	30
Table 5. Enolate reactivity relative to pinacolone enolate ion for phenyl radical in DMSO at 25°C determined using the competition technique	30
Table 6. Nucleophile reactivity relative to thiophenoxide for phenyl radical in liquid ammonia	31
Table 7. Absolute rate constants for the coupling of aryl radicals with nucleophiles in liquid ammonia determined electrochemically at -38°C	33
Table 8. The yields for 1-phenyl-3,3-dimethyl-2-butanone (<u>25</u>) and diethyl phenylphosphonate (<u>24</u>) from the reaction of pinacolone enolate/diethyl phosphite ion with phenyl radical as a function of time for two experiments	41
Table 9. The yields of 1-phenyl-3,3-dimethyl-2-butanone (<u>25</u>) and diethyl phenylphosphonate (<u>24</u>) from the competition of pinacolone enolate versus diethyl phosphite ion with iodobenzene in DMSO	44

	Page
Table 10. The yields of 1-phenyl-3,3-dimethyl-2-butanone (25) and diethyl phenylphosphonate (24) from the competition of pinacolone enolate versus diethyl phosphite ion with diphenyl sulfide in DMSO	48
Table 11. The yields of 1-phenyl-3,3-dimethyl-2-butanone (25) and diethyl phenylphosphonate (24) from the competition of pinacolone enolate versus diethyl phosphite ion with bromobenzene in DMSO	49
Table 12. The yields of 1-phenyl-3,3-dimethyl-2-butanone (25) and diethyl phenylphosphonate (24) from the competition of pinacolone enolate versus diethyl phosphite ion with phenyltrimethylammonium iodide in DMSO	50
Table 13. Values for k_{e^*}/k_{p^*} and fk_r/k_{p^*} ratios for iodobenzene, bromobenzene, diphenyl sulfide, and phenyltrimethylammonium iodide	50
Table 14. Time study of the decomposition of diethyl phenylphosphonate (24)	59
Table 15. Time study of the decomposition of diethyl phenylphosphonate (24) with slight excess of potassium t-butoxide present	59
Table 16. The relative reactivity of diethyl phosphite ion to ethyl phenylacetate enolate for phenyl radical at 45 °C in DMSO	61
Table 17. The relative reactivity of pinacolone enolate to ethyl phenylacetate enolate for phenyl radical at 45 °C in DMSO	61
Table 18. The yields of 1-phenyl-3,3-dimethyl-2-butanone (25) and diphenyl sulfide (29) from the competition of pinacolone enolate versus thiophenoxide with iodobenzene in DMSO	64
Table 19. The relative reactivity of thiophenoxide to ethyl phenylacetate enolate toward phenyl radical at 45 °C in DMSO	65

	Page
Table 20. The yields of 1-phenyl-3,3-dimethyl-2-butanone (25) and 1,1-diphenyl-3,3-dimethyl-2-butanone (26) from the reaction of pinacolone enolate with iodobenzene as a function of time	71
Table 21. The yields of 1-phenyl-3,3-dimethyl-2-butanone (25), 1,1-diphenyl-3,3-dimethyl-2-butanone (26), and diethyl phenylphosphonate (24) from the reaction of pinacolone enolate/diethyl phosphite ion with iodobenzene as a function of time	78
Table 22. Initial relative rates for the pinacolone enolate/diethyl phosphite ion pair with iodobenzene	79
Table 23. The yields of 1-phenyl-3,3-dimethyl-2-butanone (25), 1,1-diphenyl-3,3-dimethyl-2-butanone (26), and diethyl phenylphosphonate (24) from the reaction of pinacolone enolate/ diethyl phosphite ion in the presence of potassium iodide with iodobenzene as a function of time	85
Table 24. The yields of 1-phenyl-3,3-dimethyl-2-butanone (25), 1,1-diphenyl-3,3-dimethyl-2-butanone (26), and diphenyl sulfide (29) from the reaction of pinacolone enolate/thiophenoxide with iodobenzene	88
Table 25. Initial relative rates for the pinacolone enolate/diethyl phosphite ion pair with iodobenzene	89
Table 26. The yields of 1-phenyl-3,3-dimethyl-2-butanone (25), 1,1-diphenyl-3,3-dimethyl-2-butanone (26), and diphenyl sulfide (29) from the reaction of pinacolone enolate/thiophenoxide with phenyl radical generated from the thermolysis of PAT	94
Table 27. Initial relative rates for the pinacolone enolate/thiophenoxide pair with phenyl radical generated from the thermolysis of PAT	97

	Page
Table 28. The yields of diethyl phenylphosphonate (24) and diphenyl sulfide (29) from the reaction of diethyl phosphite ion/thiophenoxide with iodobenzene as a function of time	98
Table 29. Initial relative rates for the diethyl phosphite ion/thiophenoxide pair with iodobenzene	102
Table 30. The yields of diethyl phenylphosphonate (24) and 1,1-diphenyl-3,3-dimethyl-2-butanone (26) from the reaction of diethyl phosphite ion/1-phenyl-3,3-dimethyl-2-butanone enolate with iodobenzene as a function of time	105
Table 31. Initial relative rates for the 1-phenyl-3,3-dimethyl-2-butanone enolate/diethyl phosphite ion pair with iodobenzene	110
Table 32. The yields of diphenyl sulfide (29) and 1,1-diphenyl-3,3-dimethyl-2-butanone (26) from the reaction of thiophenoxide/1-phenyl-3,3-dimethyl-2-butanone enolate with iodobenzene as a function of time	112
Table 33. Initial relative rates for the thiophenoxide/1-phenyl-3,3-dimethyl-2-butanone enolate pair with iodobenzene	116
Table 34. The yields of 1-phenyl-3,3-dimethyl-2-butanone (25), diethyl phenylphosphonate (24), and diphenyl sulfide (29) from the reaction of pinacolone enolate/diethyl phosphite ion/thiophenoxide with iodobenzene as a function of time	117
Table 35. Initial relative rates for the pinacolone enolate/diethyl phosphite ion/thiophenoxide group with iodobenzene	121
Table 36. Initial relative reactivity of nucleophiles in the aromatic $S_{RN}1$ reaction	122
Table 37. Relative reactivity of phenyl radical toward hydrogen atom abstraction relative to chlorine atom abstraction from carbon tetrachloride	140

	Page
Table 38. Relative reactivity of phenyl radical toward halogen abstraction relative to chlorine atom abstraction from carbon tetrachloride	143
Table 39. Relative reactivity of phenyl radical toward addition relative to chlorine atom abstraction from carbon tetrachloride	146
Table 40. Absolute rate constants for the reaction of phenyl radical with radical scavengers	147
Table 41. Absolute rate constants for hydrogen atom abstraction by phenyl radical at 25 °C	152
Table 42. Absolute rate constants for the reaction of phenyl radical with various substrates in Freon 113 at 25 °C	153
Table 43. Absolute rate constants for the coupling of aryl radicals with nucleophiles determined electrochemically in liquid ammonia at -38 °C	156
Table 44. Absolute rate constants for the reaction of phenyl radical with various substrates in DMSO at 45 °C based on the rate constant of chlorine atom abstraction from carbon tetrachloride	157
Table 45. Relative reactivity of various nucleophiles toward phenyl radical in DMSO at 45 °C	163
Table 46. Mean values of relative reactivities of nucleophiles toward phenyl radical in DMSO at 45 °C	169
Table 47. Calculated relative reactivities	171
Table 48. Time study of the decomposition of diethyl phenylphosphonate in the presence of diethyl phosphite ion and thiophenoxide	171
Table 49. Absolute rate constants for the coupling of phenyl radical with nucleophiles in DMSO at 45 °C	173

	Page
Table 50. The yields of benzene and 1-phenyl-3,3-dimethyl-2-butanone from the reaction of phenyl radical with pinacolone enolate at 45 °C in DMSO	176
Table 51. The yields of benzene and 1-phenyl-3,3-dimethyl-2-butanone from the reaction of phenyl radical with pinacolone enolate when potassium is complexed by 18-crown-6 at 45 °C in DMSO	179
Table 52. Absolute rate constants for the coupling of phenyl radical with nucleophiles in DMSO at 45 °C when potassium is complexed by 18-crown-6	180
Table 53. The basicities of the nucleophiles	182

LIST OF FIGURES

	Page
Figure 1. A plot of the yield ratio of <u>25/24</u> versus $[C]^{-1}$ for the competition of pinacolone enolate versus diethyl phosphite ion with iodobenzene in DMSO for experiments A (circle) and B (square)	45
Figure 2. A plot of the yield ratio of <u>25/24</u> versus $[C]^{-1}$ for the competition of pinacolone enolate versus diethyl phosphite ion with diphenyl sulfide in DMSO for experiments A (circle) and B (square)	51
Figure 3. A plot of the yield ratio of <u>25/24</u> versus $[C]^{-1}$ for the competition of pinacolone enolate versus diethyl phosphite ion with bromobenzene in DMSO for experiments A (circle) and B (square)	52
Figure 4. A plot of the yield ratio of <u>25/24</u> versus $[C]^{-1}$ for the competition of pinacolone enolate versus diethyl phosphite ion with phenyltrimethylammonium iodide in DMSO for the experiment of Table 12	53
Figure 5. A plot of the yield ratio of <u>25/29</u> versus $[C]^{-1}$ for the competition of pinacolone enolate versus thiophenoxide with iodobenzene in DMSO for experiments A (circle) and B (square)	66
Figure 6. A plot of the yield ratio of 1-phenyl-3,3-dimethyl-2-butanone (<u>25</u>) to 1,1-diphenyl-3,3-dimethyl-2-butanone (<u>26</u>) versus time for the reaction of pinacolone enolate with iodobenzene (experiment A, Table 20)	73
Figure 7. A plot of the yield ratio of 1-phenyl-3,3-dimethyl-2-butanone (<u>25</u>) to 1,1-diphenyl-3,3-dimethyl-2-butanone (<u>26</u>) versus time for the reaction of pinacolone enolate with iodobenzene (experiment B, Table 20)	74

	Page
Figure 8. A plot of the yield of diethyl phenylphosphonate (24) (circle) and 1-phenyl-3,3-dimethyl-2-butanone (25) (square) versus time for the reaction of pinacolone enolate/diethyl phosphite ion with iodobenzene (experiment A, Table 21)	80
Figure 9. A plot of the yield of diethyl phenylphosphonate (24) (circle) and 1-phenyl-3,3-dimethyl-2-butanone (25) (square) versus time for the reaction of pinacolone enolate/diethyl phosphite ion with iodobenzene (experiment B, Table 21)	81
Figure 10. A plot of the yield ratio of 1-phenyl-3,3-dimethyl-2-butanone (25) to diethyl phenylphosphonate (24) versus time for the reaction of pinacolone enolate/diethyl phosphite ion with iodobenzene (experiment A, Table 21)	82
Figure 11. A plot of the yield ratio of 1-phenyl-3,3-dimethyl-2-butanone (25) to diethyl phenylphosphonate (24) versus time for the reaction of pinacolone enolate/diethyl phosphite ion with iodobenzene (experiment B, Table 21)	83
Figure 12. A plot of the yield of 1-phenyl-3,3-dimethyl-2-butanone (25) and diethyl phenylphosphonate (24) versus time for the reaction of pinacolone enolate/diethyl phosphite ion with iodobenzene in the presence of potassium iodide (Table 23)	86
Figure 13. A plot of the yield ratio of 1-phenyl-3,3-dimethyl-2-butanone (25) to diethyl phenylphosphonate (24) versus time for the reaction of pinacolone enolate/diethyl phosphite ion with iodobenzene in the presence of potassium iodide (Table 23)	87

	Page
Figure 14. A plot of the yield of 1-phenyl-3,3-dimethyl-2-butanone (25) (circle) and diphenyl sulfide (29) (square) versus time for the reaction of pinacolone enolate/thiophenoxide with iodobenzene (experiment A, Table 24)	90
Figure 15. A plot of the yield of 1-phenyl-3,3-dimethyl-2-butanone (25) (circle) and diphenyl sulfide (29) (square) versus time for the reaction of pinacolone enolate/thiophenoxide with iodobenzene (experiment B, Table 24)	91
Figure 16. A plot of the ratio of yields of 1-phenyl-3,3-dimethyl-2-butanone (25) to diphenyl sulfide (29) versus time for the reaction of pinacolone enolate/thiophenoxide with iodobenzene (experiments A (circle) and B (square), Table 24)	92
Figure 17. A plot of the yield of 1-phenyl-3,3-dimethyl-2-butanone (25) (circle) and diphenyl sulfide (29) (square) versus time for the reaction of pinacolone enolate/thiophenoxide with phenyl radical (experiment A, Table 26)	95
Figure 18. A plot of the yield of 1-phenyl-3,3-dimethyl-2-butanone (25) (circle) and diphenyl sulfide (29) (square) versus time for the reaction of pinacolone enolate/thiophenoxide with phenyl radical (experiment B, Table 26)	96
Figure 19. A plot of the yield of diethyl phenylphosphonate (24) (circle) and diphenyl sulfide (29) (square) versus time for the reaction of diethyl phosphite ion/thiophenoxide with iodobenzene (experiment A, Table 28)	100
Figure 20. A plot of the yield of diethyl phenylphosphonate (24) (circle) and diphenyl sulfide (29) (square) versus time for the reaction of diethyl phosphite ion/thiophenoxide with iodobenzene (experiment B, Table 28)	101

	Page
Figure 21. A plot of the yield of diethyl phenylphosphonate (24) (circle) and 1,1-diphenyl-3,3-dimethyl-2-butanone (26) (square) versus time for the reaction of diethyl phosphite ion/1-phenyl-3,3-dimethyl-2-butanone enolate with iodobenzene (experiment A, Table 30)	107
Figure 22. A plot of the yield of diethyl phenylphosphonate (24) (circle) and 1,1-diphenyl-3,3-dimethyl-2-butanone (26) (square) versus time for the reaction of diethyl phosphite ion/1-phenyl-3,3-dimethyl-2-butanone enolate with iodobenzene (experiment B, Table 30)	108
Figure 23. A plot of the ratio of yields of 1,1-diphenyl-3,3-dimethyl-2-butanone (26) to phenyl phosphonate (24) versus time for the reaction of 1-phenyl-3,3-dimethyl-2-butanone enolate/diethyl phosphite ion with iodobenzene (experiments A (circle) and B (square), Table 30)	109
Figure 24. A plot of the yield of 1,1-diphenyl-3,3-dimethyl-2-butanone (26) and diphenyl sulfide (29) versus time for the reaction of 1-phenyl-3,3-dimethyl-2-butanone enolate/thiophenoxide with iodobenzene (experiment A, Table 32)	113
Figure 25. A plot of the yield of 1,1-diphenyl-3,3-dimethyl-2-butanone (26) and diphenyl sulfide (29) versus time for the reaction of 1-phenyl-3,3-dimethyl-2-butanone enolate/thiophenoxide with iodobenzene (experiment B, Table 32)	114
Figure 26. A plot of the yield ratio of 1,1-diphenyl-3,3-dimethyl-2-butanone (26) to diphenyl sulfide (29) for the reaction of 1-phenyl-3,3-dimethyl-2-butanone/thiophenoxide with iodobenzene (experiments A and B, Table 32)	115

	Page
Figure 27. A plot of the yield of diethyl phenylphosphonate (24) (circle), 1-phenyl-3,3-dimethyl-2-butanone (25) (square), and diphenyl sulfide (29) (triangle) versus time for the reaction of diethyl phosphite ion/pinacolone enolate/thiophenoxide with iodobenzene (experiment A, Table 34)	119
Figure 28. A plot of the yield of diethyl phenylphosphonate (24) (circle), 1-phenyl-3,3-dimethyl-2-butanone (25) (square), and diphenyl sulfide (29) (triangle) versus time for the reaction of diethyl phosphite ion/pinacolone enolate/thiophenoxide with iodobenzene (experiment B, Table 34)	120

GENERAL INTRODUCTION

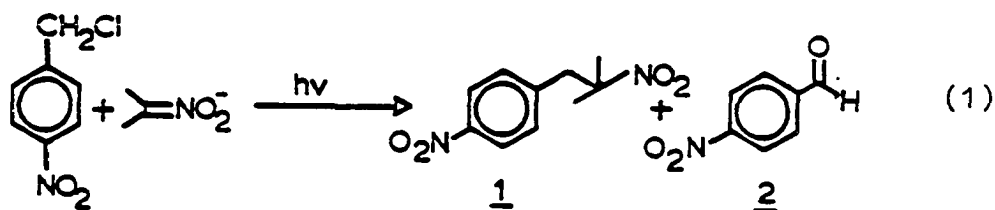
The thesis is divided into two parts. Part I presents the mechanistic study of the aromatic $S_{RN}1$ reaction using competitive reaction kinetics and initial relative rates. Part II presents absolute rate constants for the coupling of phenyl radical with various nucleophiles determined by competitive reaction kinetics.

PART I. MECHANISTIC STUDY OF THE AROMATIC $S_{RN}1$
REACTION USING COMPETITIVE REACTION KINETICS

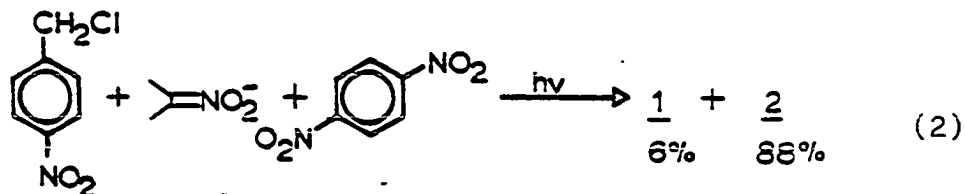
INTRODUCTION

General Background

It was discovered in 1966^{1,2} that *p*-nitrobenzyl chloride reacts with the sodium salt of 2-nitropropane yielding the carbon alkylated product (1) via a free radical chain reaction (Equation 1). Earlier results had shown that the sodium salt of 2-nitropropane reacted with alkyl halides to yield the oxygen alkylated product (2).³

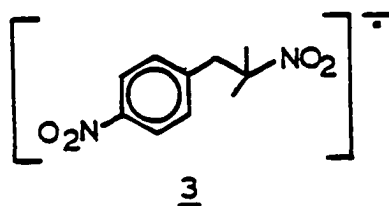
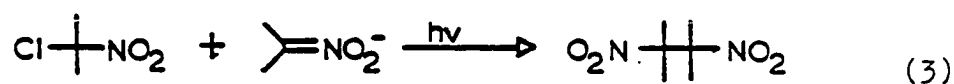


Kornblum et al.¹ discovered that when a good electron acceptor, such as *p*-dinitrobenzene, was present in the reaction mixture, the yield of the carbon alkylated product decreased to 6% while the oxygen alkylated product increased to 88% (Equation 2). Also observed was that the reaction depended on the leaving group and the presence of an *o* or *p*-nitro substituent.



Russell and Danen² also observed that the reactions of

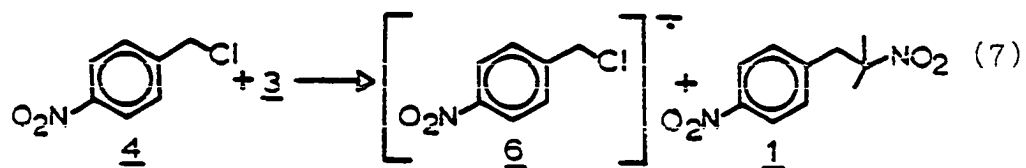
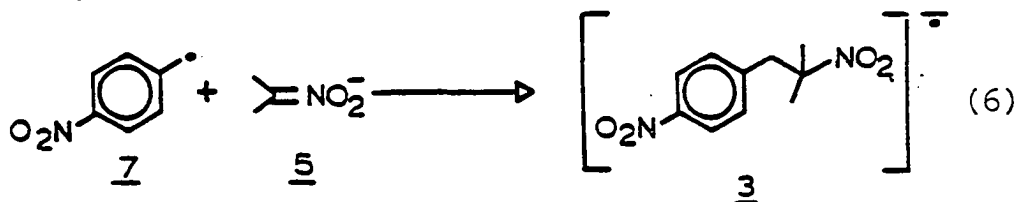
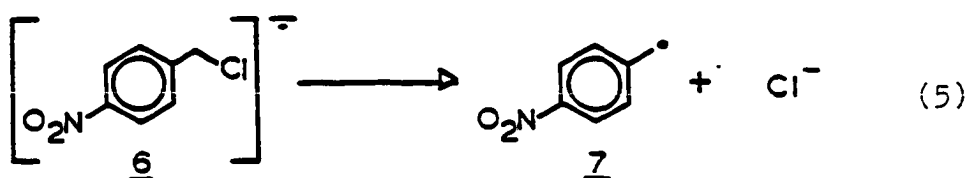
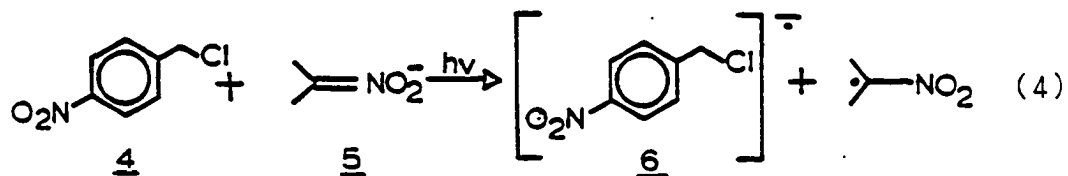
p-nitrobenzyl chloride with 2-nitro-2-propyl anion and 2-chloro-2-nitropropane with 2-nitro-2-propyl anion were catalyzed by light (Equation 3). The electron spin resonance spectrum of the 2-(p-nitrobenzyl)-2-nitropropane radical anion (3), which results from coupling of the radical and nucleophile, was recorded.



Considering the experimental results, a radical chain mechanism involving a single electron transfer and radical anion intermediate was proposed (Scheme 1). The important features of this mechanism are that p-nitrobenzyl chloride (4) accepts an electron from the 2-nitro-2-propyl anion (5) to yield the p-nitrobenzyl chloride radical anion (6) to initiate the chain reaction (Equation 4). Radical anion 6 then dissociates yielding the p-nitrobenzyl radical (7) and chloride ion (Equation 5). Radical 7 is then trapped by the 2-nitro-2-propyl anion (5) to yield 2-(p-nitrobenzyl)-2-nitropropane radical anion (3) (Equation 6). Radical anion 3 then transfers its odd electron to 4 to yield 6 and the

substituted product, 2-(p-nitrobenzyl)-2-nitropropane (1)
(Equation 7).

Scheme 1.



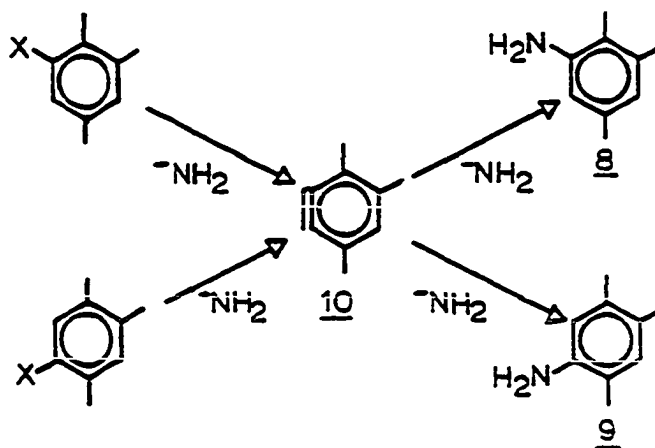
Equation 5, is similar to the classical S_N1 mechanism where the leaving group departs yielding an intermediate, a radical in this case, which is then trapped by a nucleophile (Equation 6), yielding eventually the substituted product.

Due to the similarity of this mechanism to the S_N1 mechanism, the $S_{RN}1$ or Substitution Radical Nucleophilic, Unimolecular term was coined to describe the mechanism.⁴

Kim and Bunnett^{4,5} studied the reaction of sodium amide with 5- and 6-halo 1,2,4-trimethylbenzenes in liquid ammonia. When the halide was either a chloride or bromide, the ratio of the substituted products 8 and 9 was equal to 1.46 (Scheme 2). This result indicated a single intermediate, independent of the halide. The intermediate involved in this reaction was benzyne (10).

Scheme 2.

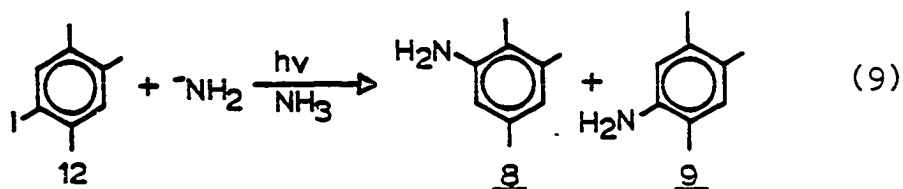
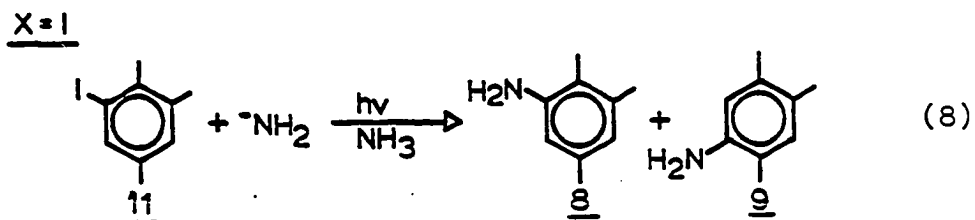
X=Cl, Br



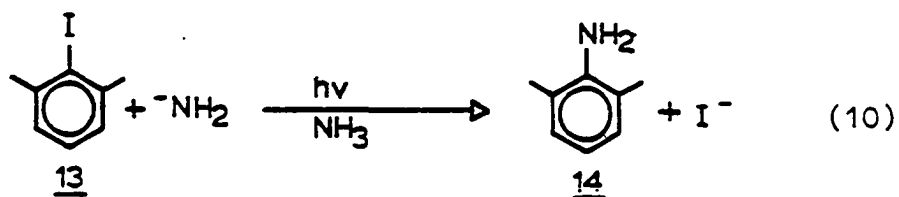
However, when the halide was an iodide, for example, 6-iodo-1,2,4-trimethyl-benzene (11), the major product was 2,3,5-trimethylaniline (8) along with some 2,3,4-trimethylaniline (9) (Scheme 3). The ratio of 8/9 was 5.9 (Equation

8). The same reaction but with 5-iodo-1,2,4-trimethylbenzene (12) resulted in a ratio of 8/9 equaling 0.59 (Equation 9). Thus, when the halide is iodide, substitution without rearrangement predominates. Addition of an inhibitor brought the ratio of 8/9 closer to the ratio obtained for the aryne mechanism.

Scheme 3.



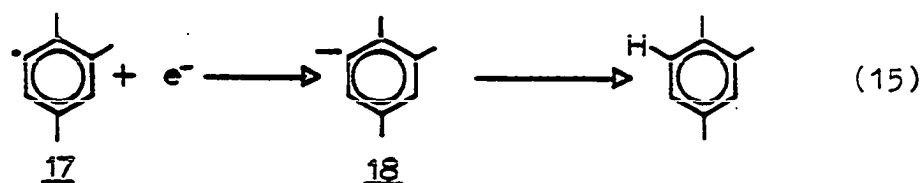
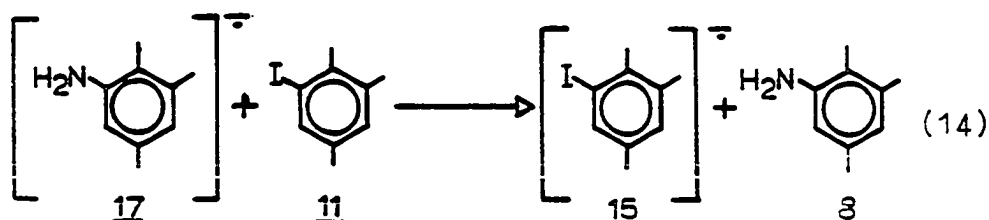
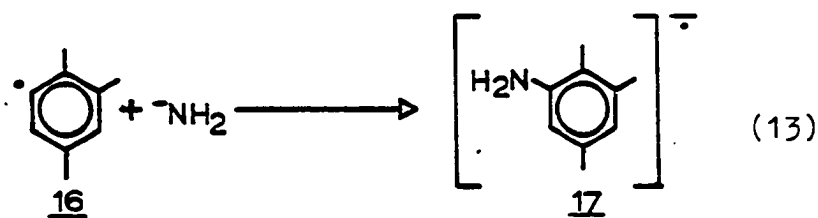
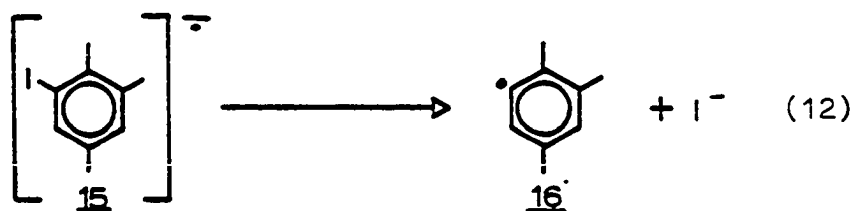
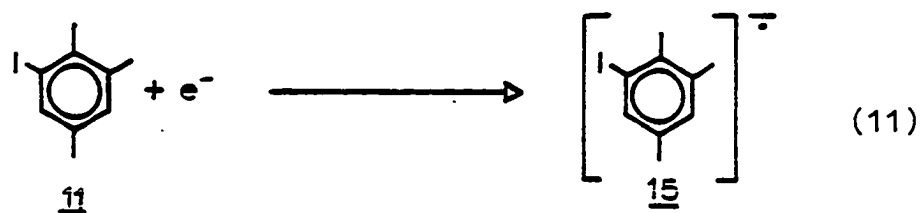
Also noted was that the reaction was catalyzed by solvated electrons in liquid ammonia. For example, 2-iodo-1,3-dimethylbenzene (13) can not react with amide ion to form benzyne. Substitution occurs with amide ion in the presence of potassium metal to yield the product, 2,6-dimethylaniline (14) in 64% yield (Equation 10).



Considering that the reaction was stimulated by solvated electrons and inhibited by using radical scavengers and electron acceptors, Kim and Bunnett^{4,5} proposed the mechanism outlined in Scheme 4. The mechanism was termed aromatic S_{RN}1 because of the similarity to the aliphatic S_{RN}1 mechanism described earlier.

The mechanism is initiated by the one electron reduction of the aryl halide to give radical anion (15) (Equation 11). The radical anion (15) dissociates yielding a phenyl radical (16) and iodide ion (Equation 12). The phenyl radical is then trapped by an amide ion to yield radical anion (17) (Equation 13). The radical anion 17 transfers its odd electron to the substrate 11 to yield the substituted product 8 and radical anion 15 (Equation 14). The major termination step in liquid ammonia is the one electron reduction of the phenyl radical 17 to yield the anion 18 which abstracts a proton from the solvent (Equation 15).

Scheme 4.



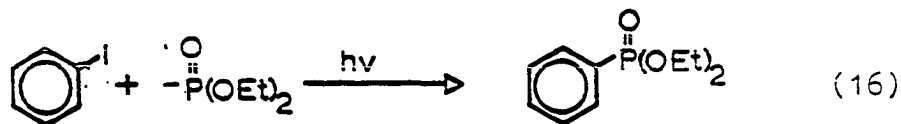
The aromatic $S_{RN}1$ reaction has been reviewed extensively^{6,7,8,9,10} The remaining portion of this chapter will briefly outline the steps in the aromatic $S_{RN}1$ mechanism and

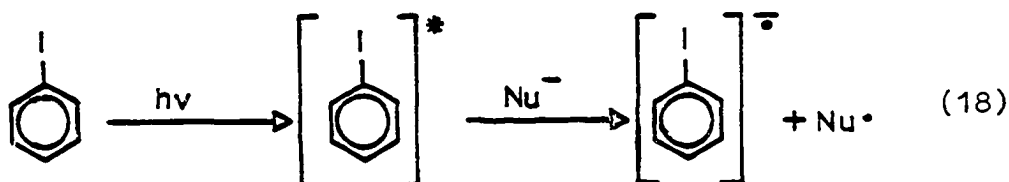
present experimental evidence where important.

Steps of the Aromatic $S_{RN}1$ Mechanism

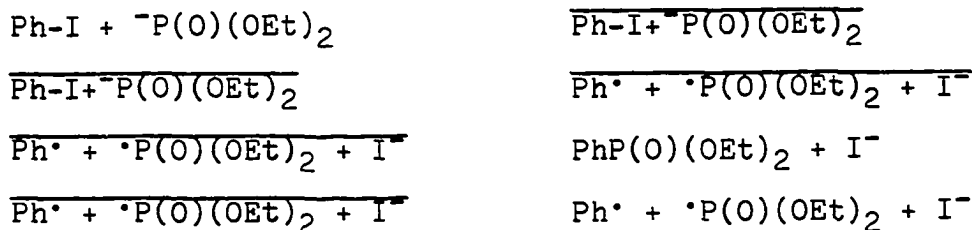
Initiation

The aromatic $S_{RN}1$ reaction can be initiated by a number of different methods which include solvated electrons,⁷ electroreduction of the aryl halide,^{11,12} thermal electron transfer,¹³ and chemical catalysis.¹⁴ The most common and least understood, however, is the photostimulation method. Hoz and Bunnett¹⁵ carried out a quantitative study of the photostimulated reaction of iodobenzene with diethyl phosphite ion in dimethyl sulfoxide (DMSO)(Equation 16). They observed that the quantum yield of the reaction was much greater than unity indicating that the reaction proceeds via a chain mechanism. A charge-transfer complex between iodobenzene and diethyl ester phosphorous acid anion (diethyl phosphite ion) was also observed and was thought to absorb a photon to initiate the reaction (Scheme 5). Other modes of initiation considered was the homolytic cleavage of the aryl-iodine bond (Equation 17) and electron transfer from the anion to the excited iodobenzene generating a radical anion (Equation 18).





Scheme 5.



Fox, Younathan and Fryxell¹⁶ studied the photoinitiation of the aromatic $\text{S}_{\text{RN}}1$ reaction using wavelength-dependent quantum yield measurements. It was suggested that electron transfer within an excited charge-transfer complex was a sufficient photoinitiation mode for the reaction of bromo- and iodobenzene with acetone enolate (Scheme 5) but not with iodobenzene and diethyl phosphite. Fox et al.¹⁶ suggested that in the iodobenzene-diethyl phosphite pair, homolytic cleavage of the aryl-iodine bond competes with photoinduced electron transfer as the primary photoprocess.

Propagation

The first essential step in the propagation cycle of the aromatic $S_{RN}1$ reaction is dissociation of the radical anion to a free radical. Evidence for the decomposition of the aryl halide radical anion to the aryl radical has been reported in the literature. Table 1 lists different aryl halides along with the rate constants for the dissociation of the aryl halide radical anions in various solvents.

Inspection of the results outlined in Table 1 reveal some important trends. The most notable is that the rate of dissociation depends on the halide in the following order: $I > Br > Cl > F$. Another notable trend is that electron releasing substituents destabilize the radical anion, increasing the rate of dissociation while electron withdrawing substituents stabilize the radical anion, decreasing the rate of dissociation.

The solvent also influences the rate of dissociation.⁹ The effect of solvents on the stability of radical anions has been attributed to the solvation of the radical anion. Solvation delocalizes the negative charge resulting in the stabilization of the radical anion.

The dependence of the rate of dissociation of the halide has been noted in the aromatic $S_{RN}1$ reaction.^{17,18} For example, the photostimulated reaction of m-bromo-iodobenzene with diethyl phosphite ion yields mainly the disub-

Table 1. Absolute rate constants for the dissociation of aryl halide radical anions in various solvents determined either by electrochemical (E) or pulse radiolysis (P)



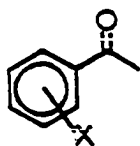
substrate	k (s^{-1})	solvent	method	ref
PhCl	4.0×10^7	NH_3	E	19
PhCl	1.0×10^7	DMF	E	20
<i>p</i> -Ph-PhCl	7.5×10^7	H_2O	P	21
				
X=F	6.0×10^5	H_2O	P	22
X=Cl	4.0×10^7	H_2O	P	22
				
X= <i>p</i> -F	6.5×10^5	H_2O	P	23
<i>o</i> -Cl	9.0×10^6	H_2O	P	23
<i>m</i> -Cl	4.2×10^4	H_2O	P	23
<i>p</i> -Cl	5.0×10^6	H_2O	P	23
<i>m</i> -Br	8.0×10^6	H_2O	P	23
<i>p</i> -Br	3.0×10^7	H_2O	P	23
<i>m</i> -F	10^3	DMF	E	24
<i>p</i> -F	1.1×10^1	DMF	E	25

Table 1. continued

substrate	k (s ⁻¹)	solvent	method	ref
<u>m</u> -Cl	10 ¹⁰	DMF	E	25
<u>p</u> -Cl	10 ¹⁰	DMF	E	25
<u>m</u> -Br	10 ¹⁰	DMF	E	25
<u>p</u> -Br	10 ¹⁰	DMF	E	25
<u>m</u> -I	10 ¹⁰	DMF	E	25
<u>p</u> -Br	10 ¹⁰	DMF	E	25
<u>p</u> -Cl	9.0 X 10 ⁸	NH ₃	E	26
<u>o</u> -Cl	1.4 X 10 ⁸	NH ₃	E	27
<u>m</u> -Cl	9.8 X 10 ⁵	NH ₃	E	27
<u>p</u> -Cl	9.3 x 10 ⁸	NH ₃	E	27
<u>p</u> -Br	2.0 X 10 ⁹	NH ₃	E	27
<u>p</u> -I	2.5 10 ¹⁰	NH ₃	E	27



X= <u>o</u> -Cl	1.5 X 10 ³	H ₂ O	P	22
<u>p</u> -Cl	10 ²	H ₂ O	P	22
<u>o</u> -Br	5.0 x 10 ⁵	H ₂ O	P	22
<u>m</u> -Br	10 ²	H ₂ O	P	22
<u>p</u> -Br	5.0 X 10 ³	H ₂ O	P	22
<u>p</u> -I	1.4 X 10 ⁵	H ₂ O	P	22

Table 1. continued

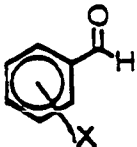
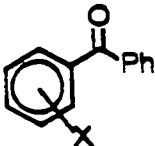
substrate	k (s ⁻¹)	solvent	method	ref
<u>m</u> -Cl	1.0 X 10 ¹	DMF	E	28
<u>p</u> -Cl	10 ⁵	DMF	E	28
				
X= <u>m</u> -Br	4.0 X 10 ²	H ₂ O	P	22
				
X= <u>p</u> -Br	<7	H ₂ O	P	22
<u>m</u> -Cl	1.0 X 10 ⁻¹	DMF	E	28, 29
<u>p</u> -Cl	1.0 X 10 ¹	DMF	E	28, 29
<u>p</u> -Cl	5.1 X 10 ¹	DMF	E	30
<u>m</u> -Br	7.4 X 10 ²	DMF	E	29
<u>p</u> -Br	8.0 X 10 ⁴	DMF	E	29
<u>p</u> -Cl	3.4 X 10 ¹	DMF	E	29
<u>m</u> -Br	9.0	CH ₃ CN	E	29
<u>p</u> -Br	2.4 X 10 ³	CH ₃ CN	E	29
<u>m</u> -Br	3.0 X 10 ¹	Me ₂ CHCN	E	29
<u>p</u> -Br	6.8 X 10 ³	Me ₂ CHCN	E	29

Table 1. continued

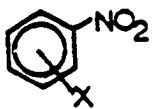
substrate	k (s ⁻¹)	solvent	method	ref
				
X= <u>o</u> -Cl	1.0 X 10 ⁻²	DMF	E	31
<u>m</u> -Cl	<10 ⁻³	DMF	E	28
<u>p</u> -Cl	1.0 X 10 ⁻²	DMF	E	29
<u>p</u> -Cl	1.4 X 10 ⁻²	DMF	E	29
<u>p</u> -Cl	1.0 X 10 ⁻⁶	DMF	E	32
<u>o</u> -Br	1.1 X 10 ²	DMF	E	31
<u>p</u> -Br	4.0 X 10 ⁻³	DMF	E	31
<u>p</u> -Br	1.4 X 10 ⁻³	DMF	E	33
<u>o</u> -I	8.0 X 10 ⁴	DMF	E	31
<u>m</u> -I	3.1 X 10 ⁻¹	DMF	E	31
<u>p</u> -I	9.0 X 10 ⁻¹	DMF	E	31
<u>p</u> -I	6.7	DMF	E	32, 34
<u>m</u> -F	2.0 X 10 ⁻¹	CH ₃ CN	E	35
<u>p</u> -F	3.0 X 10 ⁻³	CH ₃ CN	E	35
<u>p</u> -F	1.4 X 10 ⁻³	CH ₃ CN	E	35
<u>m</u> -Cl	3.0 X 10 ⁻³	CH ₃ CN	E	35
<u>m</u> -Br	5.0 X 10 ⁻³	CH ₃ CN	E	35
<u>p</u> -Br	1.2 X 10 ⁻¹	CH ₃ CN	E	35

Table 1. continued

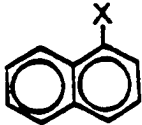

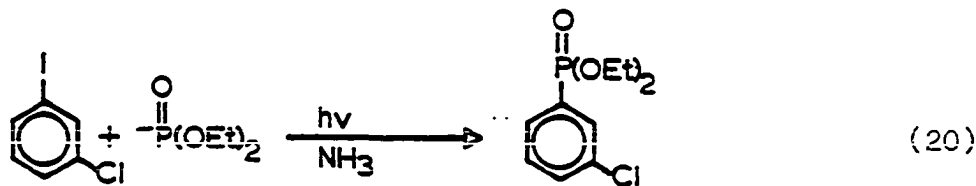
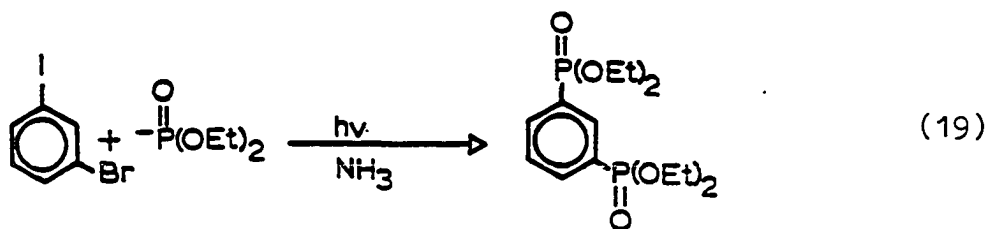
substrate	k (s ⁻¹)	solvent	method	ref
				
X=Cl	1.5 X 10 ⁴	NH ₃	E	36
Cl	1.2 X 10 ⁷	NH ₃	E	27
I	1.6 X 10 ¹¹	NH ₃	E	27
Cl	5.0 X 10 ⁷	DMSO	E	37
Br	3.0 X 10 ⁸	DMSO	E	37
I	6.0 X 10 ⁸	DMSO	E	37
				
X= <u>o</u> -Br	1.7 X 10 ⁴	NH ₃	E	36
<u>o</u> -Cl	1.3 X 10 ⁵	NH ₃	E	36
<u>o</u> -I	3.0 X 10 ⁶	NH ₃	E	36
<u>o</u> -Cl	1.7 X 10 ⁴	NH ₃	E	27
<u>p</u> -Cl	1.9 X 10 ⁶	NH ₃	E	27
<u>m</u> -Br	1.5 X 10 ⁷	NH ₃	E	27
<u>o</u> -I	1.2 X 10 ⁸	NH ₃	E	27

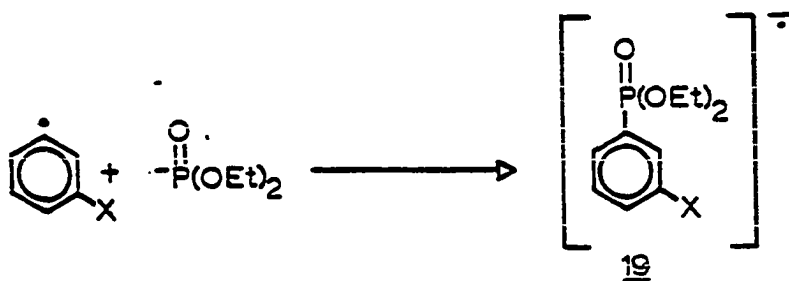
Table 1. continued

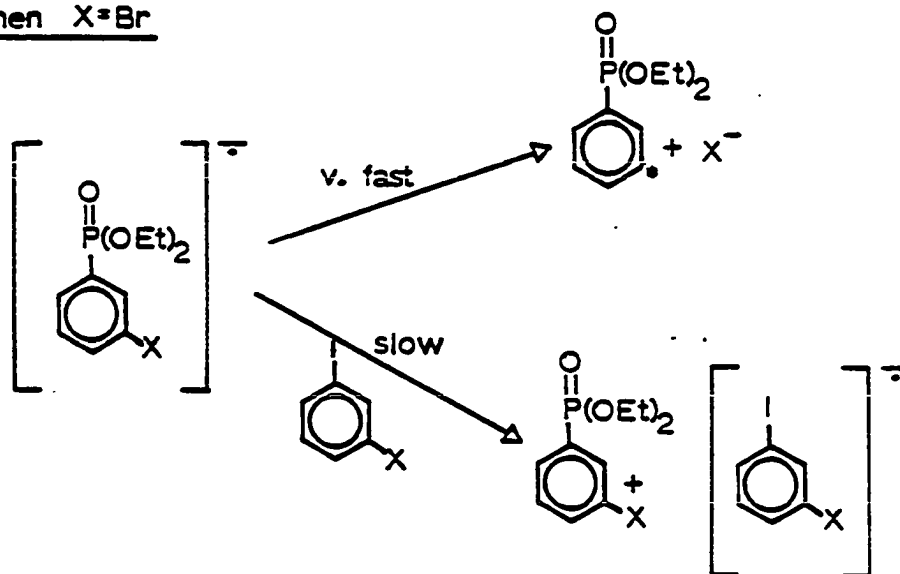
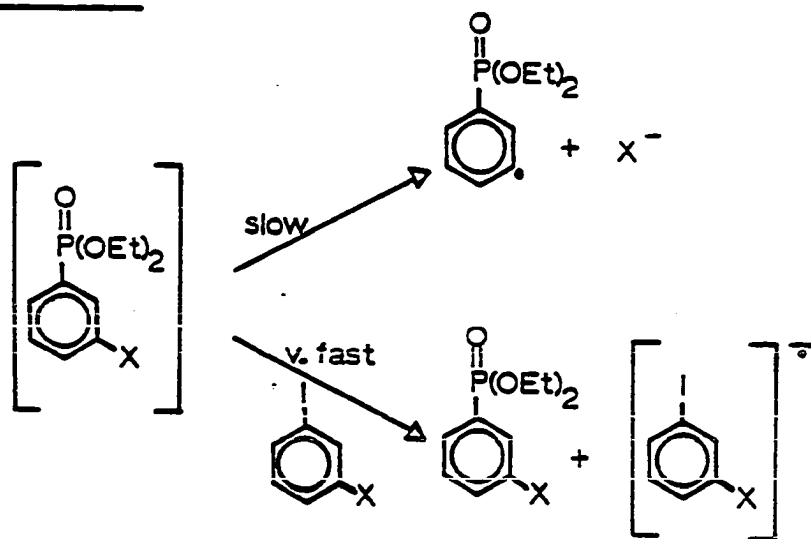
substrate	k (s ⁻¹)	solvent	method	ref
<u>m</u> -I	2.4 X 10 ⁹	NH ₃	E	27
PhSPh	1.1 X 10 ⁴	NH ₃	E	19

stituted product (Equation 19). On the other hand, m-chloro-iodobenzene yields mainly the mono substituted product (Equation 20). This can be explained by relative rates of dissociation of the aryl radical anions (Scheme 6). For both substrates, iodide is substituted first resulting in radical anion 19. When X=Br, dissociation is faster than electron transfer to the substrate. Conversely, when X=Cl, electron transfer is faster than dissociation of the radical anion resulting in the formation of the mono substituted radical anion.



Scheme 6.

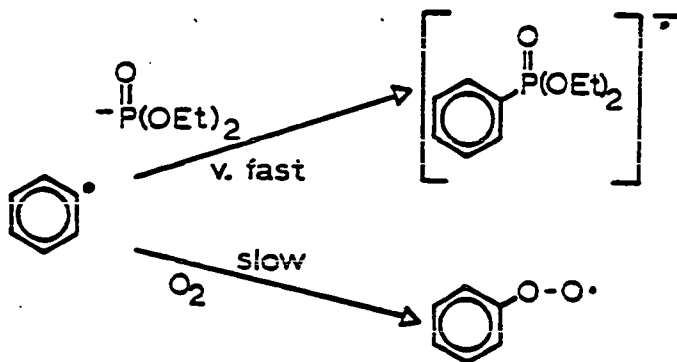


Scheme 6. continuedwhen X=Brwhen X=Cl

The second step in the propagation cycle is the coupling of a phenyl radical with a nucleophile to form a radical anion that eventually yields the product. First, however, the intermediacy of a phenyl radical had to be

established. Hoz and Bunnett¹⁵ studied the effect of inhibitors on the reaction of iodobenzene and diethyl phosphite ion. Dioxygen, a common radical scavenger, was found not to inhibit the reaction. It was postulated that diethyl phosphite ion is exceedingly reactive with phenyl radical, so much so, that dioxygen can not compete with this anion (Scheme 7). The addition of 4.4% mole of di-tert-butyl nitroxide reduced the rate of the reaction by only a factor of three, also indicating the high reactivity of phenyl radical with diethyl phosphite ion. Other electron acceptors and radical scavengers have been used to study the aromatic $S_{RN}1$ mechanism. Table 2 summarizes the inhibitors used and their effects.

Scheme 7.



To gain further evidence for the intermediacy of a phenyl radical in the aromatic $S_{RN}1$ reaction, Galli and Bunnett³⁸ studied the mechanism using the competition

Table 2. Effect of added substances on $S_{RN}1$ reactions

substrate	nucleophile	promoter	inhibiter	effect	solvent	ref
iodotrimethyl benzene	$^{-}NH_2$	dark	Me_3CNO	inhib.	NH_3	5
iodotrimethyl benzene	$^{-}NH_2$	dark	Ph_2NNPh_2	inhib.	NH_3	5
PhBr	$^{-}CH_2COCH_3$	hv	$(tBu)_2NO$	inhib.	NH_3	38
PhBr	$^{-}CH_2COCH_3$	hv	O_2	inhib.	NH_3	38
PhI	$^{-}PO(OEt)_2$	hv	$(tBu)_2NO$	inhib.	DMSO	15
PhI	$^{-}CH_2COtBu$	dark	PhCOPh	inhib.	DMSO	13
PhI	$^{-}CH_2COtBu$	dark	$(tBu)_2NO$	inhib.	DMSO	13
PhI	$^{-}PO(OEt)_2$	hv	$p-(NO_2)_2C_6H_4$	inhib.	NH_3	39
p-iodotoluene	$^{-}PPh_2$	dark	$(tBu)_2NO$	inhib.	DMSO	40
PhBr	$^{-}CH_2CN$	hv	PhCOPh	inhib	NH_3	41

technique. If a phenyl radical is involved in the reaction, there should be no leaving group effect (Scheme 8). Competing diethyl phosphite ion and pinacolone enolate for phenyl radicals, assuming the radical-nucleophile coupling is irreversible and electron transfer to the substrate is fast, the ratio of the rate constants for the coupling process can be determined. The relative product yields are related to the relative rate constants for the coupling reactions by Equation 21. It was determined that the ratio of the rate constants, k_p/k_e , was independent of the leaving group, indicating the existence of a single intermediate, but not demanding it. Table 3 summarizes k_p/k_e values obtained for various substrates.

Scheme 8.

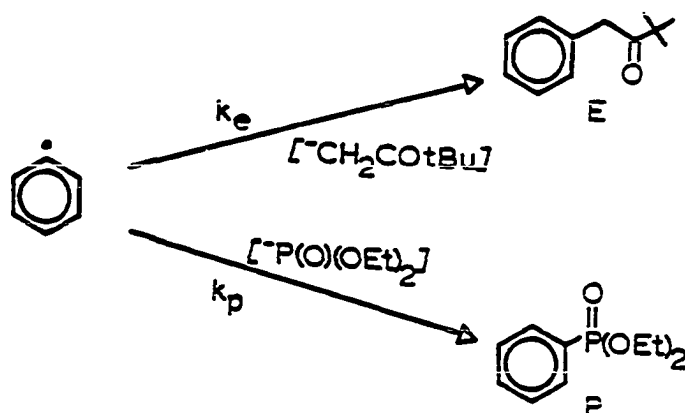


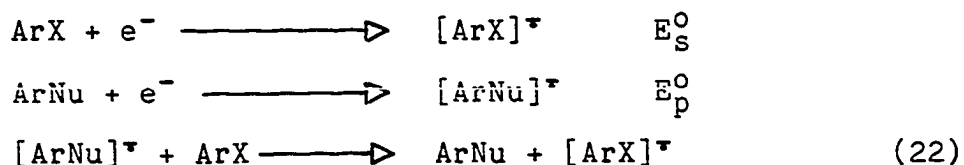
Table 3. Nucleophile reactivities relative to pinacolone enolate ion and diethyl phosphite ion in liquid ammonia at -38°C initiated by U.V. light

substrate	$(\text{EtO})_2\text{PO}^-$	$t\text{-BuCOCH}_2^-$	Ph_2P^-	$\text{Ph}_2\text{P}(\text{O})^-$	PhS^-	ref
PhI	1.33	1	5.19	2.34	0.08	14
PhBr	1.39	1	21.9			14
PhCl	1.47	1	10.1			14
PhF	1.38	1				14
PhSPh	1.46	1				14
$\text{PhNMe}_3^+\text{I}^-$	1.25	1				14
$p\text{-MeC}_6\text{H}_4\text{I}$	1.28	1	5.6			14
$p\text{-MeC}_6\text{H}_4\text{Br}$	6.17	1				14

$$\frac{Y_E}{Y_P} = \frac{k_e [\text{CH}_2\text{COtBu}]^-}{k_p [\text{P(O)(OEt)}_2]^-} \quad (21)$$

The last step of the propagation cycle is the transfer of an electron from the product radical anion to the substrate. This can be best explained by considering Scheme 9.⁹ If the standard reduction potential of the ArX/[ArX]^{•-} couple, E_S⁰, is greater than the standard reduction potential of the ArNu/[ArNu]^{•-} couple, E_P⁰, the electron transfer from [ArNu]^{•-} to ArX is thermodynamically favored (Equation 22). Conversely, if E_P⁰ > E_S⁰, the electron transfer is thermodynamically unfavored and other competing reactions such as disproportionation, protonation or reduction of aryl radicals may occur.

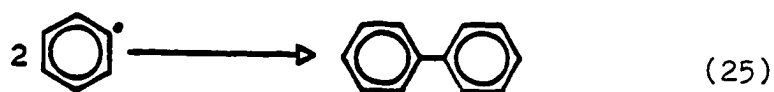
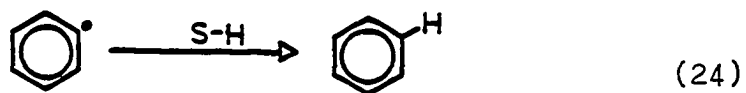
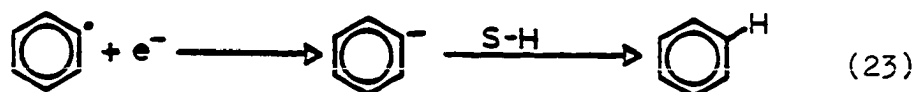
Scheme 9.



Termination

Termination of the radical chain mechanism may occur by a number of routes depending on the method of initiation or the nucleophile present.⁹ Under electrochemical initiation, reduction of the aryl radical to the anion is the major termination step (Equation 23). When photostimulation is employed to initiate the reaction, termination can occur by

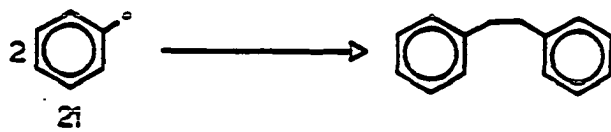
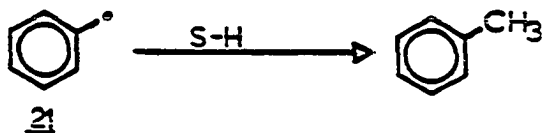
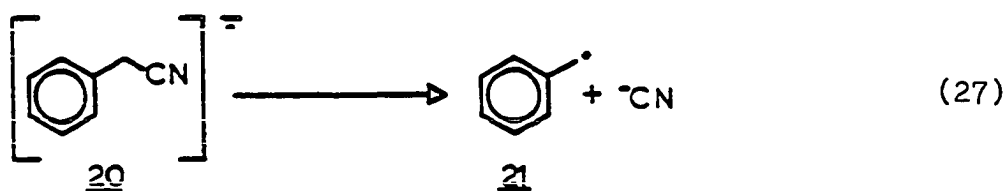
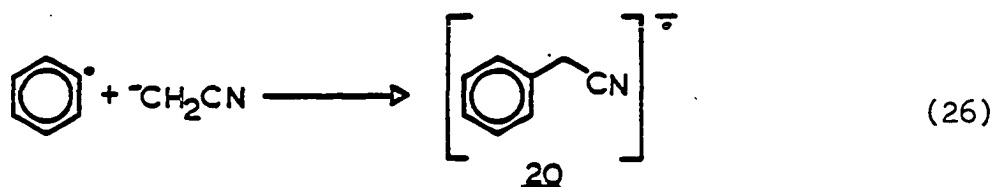
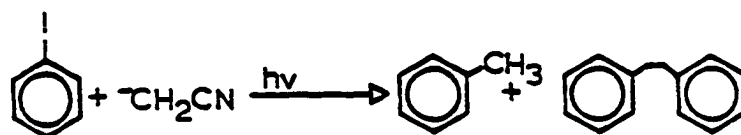
hydrogen atom abstraction from the solvent and/or nucleophile (Equation 24). Radical coupling can also be a possible mode of termination (Equation 25), however, in the case where iodobenzene is the substrate, no biphenyl has been detected.⁴²



Fragmentation of the product radical anion before electron transfer to the substrate can also be a termination step. The two largest groups of nucleophiles that exhibit this type of behavior are the cyanomethyl anions and the alkanethiolate ions.⁹ For example, the reaction of iodobenzene and cyanomethyl anion yield as the major products toluene and bibenzyl⁴³ (Scheme 10). What occurs is that the phenyl radical couples with the nucleophile to yield the radical anion of benzyl cyanide (20) (Equation 26). Radical

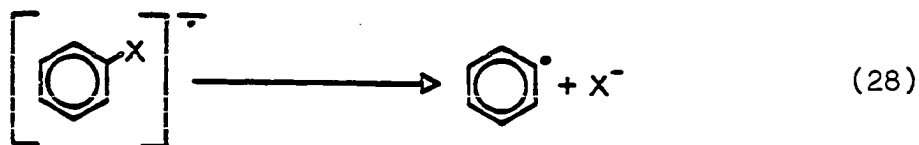
anion 20 does not transfer its electron to iodobenzene, but dissociates to give the benzyl radical (21) and the cyanide ion (Equation 27). The benzyl radical either dimerizes to give bibenzyl or is reduced to an anion which eventually yields toluene. What is notable is that an electron was not transferred back to the substrate, thus, the dissociation of the radical anion was a termination step.

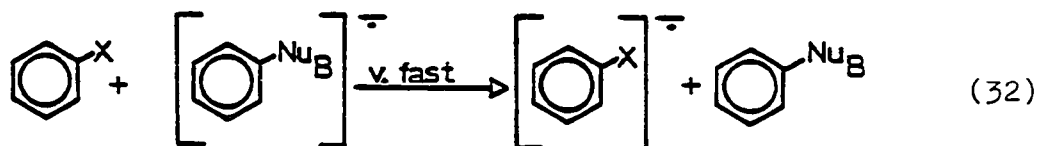
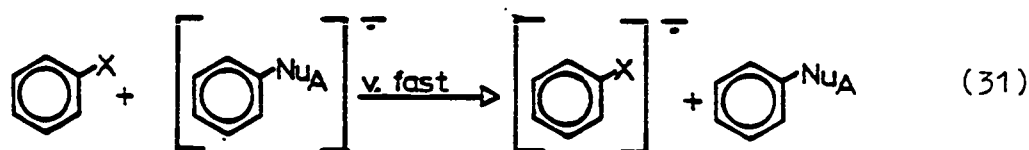
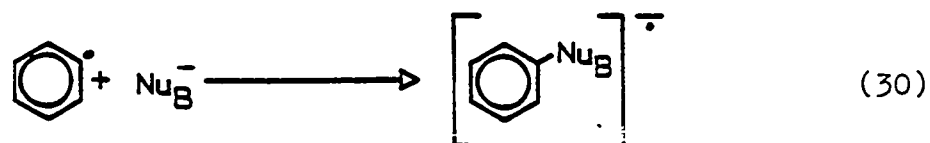
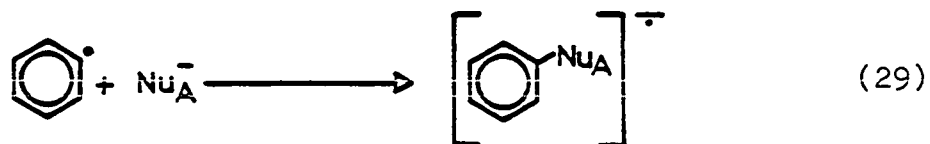
Scheme 10.



Reactivity

Recently, the comparative reactivity of nucleophiles employed in the aromatic $S_{RN}1$ reaction has gained some attention.^{27,38,44,45} Consider Scheme 11 where reactions 28-32 outline the propagation steps for a $S_{RN}1$ reaction when two nucleophiles, Nu_A and Nu_B , are present. If the chain length of the reaction is high and if electron transfer back to the substrate is fast and irreversible, the relative yields of the coupled products are related to the relative rate constants for Equations 29 and 30 via Equation 33. Knowing the initial concentrations of the nucleophiles, the relative rate constants can be calculated. Electrochemical determination of relative rate constants are based on the same assumptions as above but use product currents in place of product yields for the calculation of the ratio of rate constants (Equation 34). Tables 4-6 summarize all the relative reactivities of various nucleophiles toward a host of substrates that have appeared in the literature.

Scheme 11.

Scheme 11. continued.

$$\frac{Y_{\text{ArNuA}}}{Y_{\text{ArNuB}}} = \frac{k_A [\text{Nu}_A]}{k_B [\text{Nu}_B]} \quad (33)$$

$$\frac{i_{\text{p29}}}{i_{\text{p30}}} = \frac{k_A [\text{Nu}_A]}{k_B [\text{Nu}_B]} \quad (34)$$

Table 4. Nucleophile reactivity relative to thiophenoxide determined electrochemically in liquid ammonia at -38°C

Radical	PhS^-	$(\text{EtO})_2\text{PO}^-$	$^-\text{CH}_2\text{COCH}_3$	ref
4-cyanophenyl	1	0.4	0.8	27
2-cyanophenyl	1	0.6	0.6	27
3-cyanophenyl	1	0.5	1.8	27
2-quinolyl	1	1.9	6.6	27
3-quinolyl	1	0.4	2.0	27
4-quinolyl	1	0.5	1.7	27
3-pyridyl	1	0.7	1.6	27
1-naphthyl	1	1.6	2.1	27
2-naphthyl	1	2.0	2.2	27

Table 5. Enolate reactivity relative to pinacolone enolate ion for phenyl radical in DMSO at 25°C determined using the competition technique

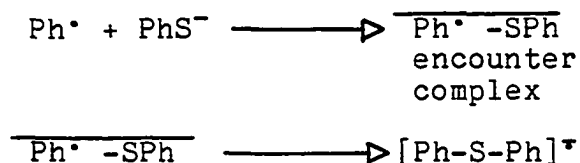
ketone	relative rate	ref
pinacolone	1.00	44
acetone	1.09	44
cyclohexane	0.67	44
2-butanone	1.10	44
3-pentanone	1.40	44
phenyl acetone	0.39	44

Table 6. Nucleophilic reactivity relative to thiophenoxide for phenyl radical in liquid ammonia

nucelophile	relative rate	ref
PhO ⁻	0.0	45
PhS ⁻	1.0	45
PhSe ⁻	5.8	45
PhTe ⁻	28.0	45

The most notable feature is that the reactivity of all of the nucleophiles, with the exception of thiophenoxide, are similar. A possible reason for such a reactivity pattern is that the phenyl radical reacts with the nucleophiles at diffusion controlled rates. However, this is inconsistent with reported absolute rate constants.¹⁷ In the case of thiophenoxide, it has been postulated that an encounter complex between phenyl radical and thiophenoxide forms reversibly (Scheme 12). Carbon-sulfur bond formation to yield diphenyl sulfide radical anion is slower than dissociation of the encounter complex.

Scheme 12.



A few absolute rate constants for the coupling of aryl radicals with various nucleophiles have been determined using electrochemical techniques. Table 7 summarizes the rate constants that have been determined.

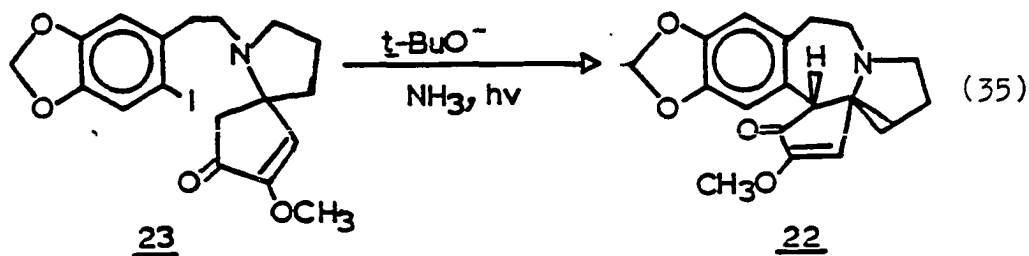
Synthetic Applications

The most widely used aromatic $S_{RN}1$ reaction in synthesis is the intramolecular enolate arylation.⁹ For example, cephalotaxinone (22) was synthesized from iodo-ketone (23) using potassium *t*-butoxide in liquid ammonia

Table 7. Absolute rate constants for the coupling of aryl radicals with nucleophiles in liquid ammonia determined electrochemically at $-38\text{ }^{\circ}\text{C}$

radical	PhS^-	$(\text{EtO})_2\text{PO}^-$	$\text{CH}_3\text{COCH}_2^-$	ref
2-cyanophenyl	1.4×10^{10}	8.0×10^9	2.4×10^{10}	27
3-cyanophenyl	1.5×10^{10}	7.5×10^9	9.0×10^9	27
4-cyanophenyl	3.4×10^9	1.4×10^9	2.6×10^9	27
1-naphthyl	2.0×10^{10}	3.2×10^{10}	4.2×10^{10}	27
2-quinolyl	1.4×10^7	2.6×10^7	9.1×10^7	27
3-quinolyl	1.9×10^9	7.6×10^8	3.8×10^9	27
4-quinolyl	3.2×10^9	1.6×10^9	5.4×10^9	27
3-pyridyl	1.0×10^{10}	7.0×10^9	1.6×10^{10}	27
2-pyridyl	1.0×10^8			27
phenyl	2.6×10^7	3.8×10^8		19

under photostimulation (Equation 35). Using the intramolecular $S_{RN}1$ reaction lead to product 22 in 94% yield.⁴⁶ Other approaches, such as the aryne reaction and Ni(0) catalyzed reaction gave the product in less than 35% yield.

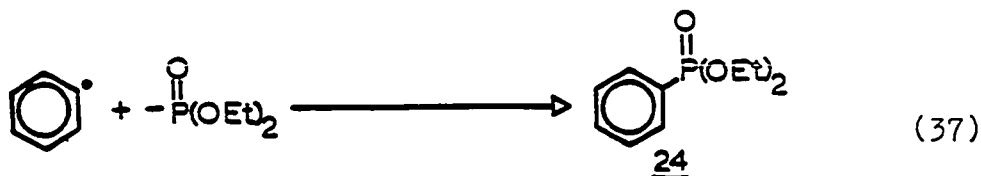
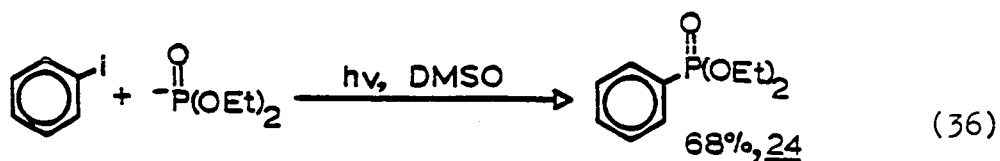


Statement of Research Problem

An earlier study presented evidence for a second kinetically significant intermediate in the aromatic $S_{RN}1$ reaction.¹⁰ The mechanism of the aromatic $S_{RN}1$ was studied using two approaches: 1) comparing phenyl radical reactivity with nucleophiles when generated from an unambiguous source or from the aromatic $S_{RN}1$ reaction; 2) an intramolecular radical rearrangement.

In the earlier study it was found that diethyl phosphite ion reacted with iodobenzene via the $S_{RN}1$ reaction to yield diethyl ester phenylphosphonic acid (diethyl phenylphosphonate, 24) in 68% yield (Equation 36). However, when phenyl radical was generated from the thermolysis of phenylazotriphenylmethane (PAT) in the presence of the diethyl phosphite ion, no diethyl phenylphosphonate was formed

(Equation 37).

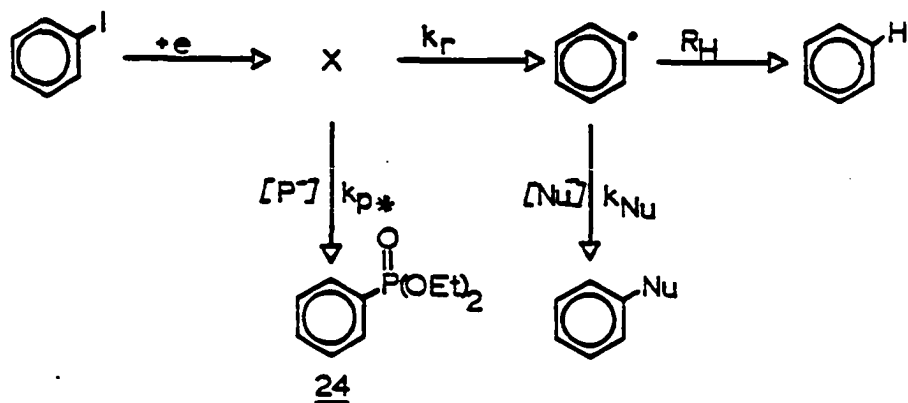


Based on the above experimental facts, it was postulated that the diethyl phosphite ion reacted with some intermediate other than a sigma phenyl radical to yield the diethyl phenylphosphate. The requirements for this intermediate, X, were that it must be paramagnetic and a precursor to a free aryl radical. The identity of the intermediate was discussed with respect to several possibilities; a haloarene radical anion, an excited state aryl radical and an excited state aryl radical/halide complex.

The mechanism proposed is outlined in Scheme 13 where the intermediate is represented by X. The key reaction is the reduction of iodobenzene by one electron to yield X. It was proposed that intermediate X could be trapped by diethyl phosphite ion (P^-) to eventually yield the diethyl phenyl-

phosphonate or could decompose/relax to a sigma phenyl radical which was trapped by certain nucleophiles but not by the diethyl phosphite anion. Another fate of the phenyl radical is the abstraction of a hydrogen atom from the solvent. Competition studies between diethyl phosphite and nitronate anions in the aromatic $S_{RN}1$ led to an assignment of the k_r/k_{p^*} ratio as 0.16 M.

Scheme 13



This section presents the extension of the above problem to nucleophiles other than diethyl phosphite and nitronate ions. The problem was approached from two perspectives. The aryl radical intermediate in the aromatic $S_{RN}1$ reaction and the aryl radical generated from an unambiguous source (PAT) will be compared with respect to their reactivity toward various nucleophiles. The other approach

was the measurement of k_r/k_{p^*} via competition studies pitting two nucleophiles against each other in the aromatic $S_{RN}1$ reaction. If Scheme 13 is correct, the fraction of PhI reacting by the k_{p^*} rate should increase with the concentration of nucleophile (e.g., $P^-(EtO)_2PO^-$).

RESULTS AND DISCUSSION

Competition Studies

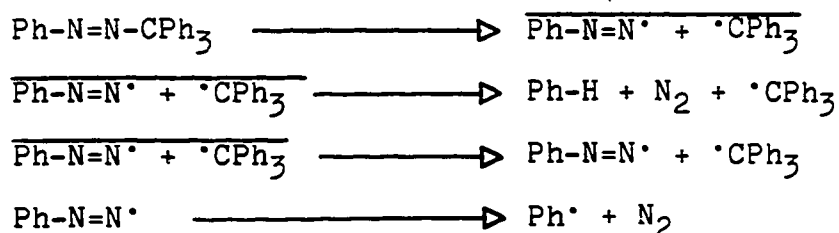
In this section, competition studies pitting two nucleophiles versus each other in the aromatic $S_{RN}1$ reaction are reported. The objective of the study was to gain evidence for or against the existence of a second kinetically significant intermediate in the aromatic $S_{RN}1$ reaction. The relative reactivity of the nucleophiles competing for intermediates in the aromatic $S_{RN}1$ reaction and phenyl radicals generated from the thermolysis of phenylazotriphenylmethane were measured and compared.

Reactivity of nucleophiles toward phenyl radicals generated from PAT

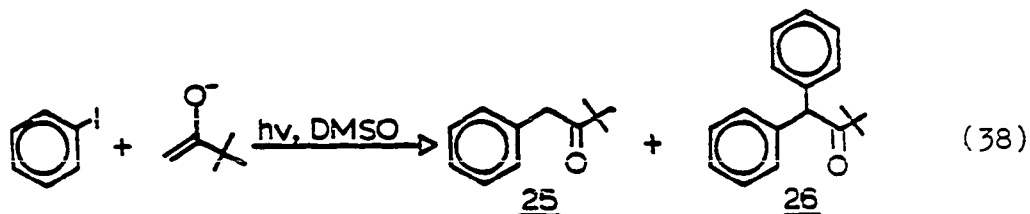
The thermolysis of phenylazotriphenylmethane (PAT) generates greater than 90% yield of phenyl radicals.⁴⁷⁻⁵⁰ Scheme 14 outlines the mechanism for the thermolysis of PAT. The cleavage of the nitrogen-triphenylmethyl bond occurs first yielding the diazenyl radical and trityl radical pair in a solvent cage. The radical pair can diffuse out of the solvent cage yielding a phenyl radical after the loss of nitrogen from the diazenyl radical. The loss of nitrogen from the diazenyl radical to give the phenyl radical can also occur in the solvent cage. It is reported that hydrogen atom abstraction occurs within the solvent cage to yield benzene in 5.4%. Thus, the yields of benzene reported

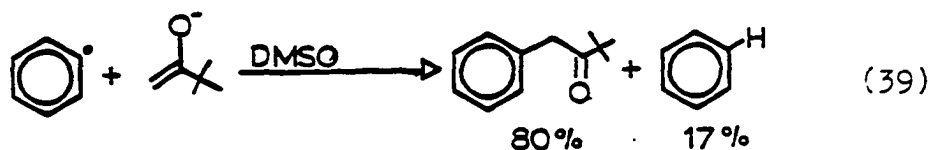
are the differences between the measured yield and 5.4%.

Scheme 14.



Pinacolone enolate reacts with iodobenzene in DMSO under photostimulation to give 1-phenyl-3,3-dimethyl-2-butanone (25) and 1,1-diphenyl-3,3-dimethyl-2-butanone (26) in 79% and 9% yields respectively (Equation 38). When phenyl radicals were generated by the thermolysis of PAT in the presence of pinacolone enolate in DMSO, 1-phenyl-3,3-dimethyl-2-butanone was the major product along with some benzene (Equation 39). The results indicate that pinacolone enolate reacts with the aryl intermediates in the aromatic $S_{RN}1$ reaction and sigma phenyl radical to yield the substituted product. However, the two experiments do not give completely identical results.





Results for the competition of diethyl phosphite ion and pinacolone enolate for the phenyl radical generated from PAT are presented in Table 8. No diethyl phenylphosphonate was formed, suggesting that phenyl radical and diethyl phosphite ion do not couple to yield the substituted product. This was consistent with the earlier results.¹⁰ It is notable, however, that the mass balance of the reaction is below 40%.

Competition with iodobenzene

Considering the experimental facts presented above, the mechanism outlined in Scheme 15 was proposed for the reaction of pinacolone enolate/diethyl phosphite ion with iodobenzene. In the first step, iodobenzene is reduced by one electron to yield intermediate X. Intermediate X can be trapped by diethyl phosphite ion to eventually yield the diethyl phenylphosphonate or relax/decompose to sigma phenyl radical (Ph[•]). The sigma phenyl radical can either be trapped by pinacolone enolate or abstract a hydrogen atom to form benzene.

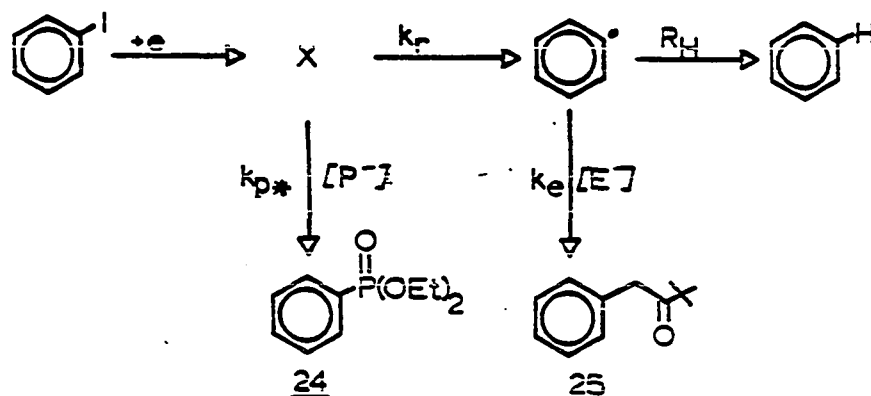
Table 8. The yields for 1-phenyl-3,3-dimethyl-2-butanone (25) and diethyl phenylphosphonate (24) from the reaction of pinacolone enolate/diethyl phosphite ion with phenyl radical as a function of time for two experiments

time (min.)	% yield		
	<u>25</u>	<u>26</u>	<u>24</u>
exp A ^a			
30	6.1	-	-
60	12.1	-	-
90	15.1	-	-
120	20.5	-	-
180	29.0	-	-
240	30.7	-	-
300	34.0	-	-
360	39.0	-	-
exp B ^a			
30	6.1	-	-
60	13.4	-	-
90	20.0	-	-
120	21.1	-	-
180	30.9	-	-
240	32.3	-	-
300	34.0	-	-

^a[PAT]=0.027 M, [⁻CH₂COtBu]=0.35 M,
[(EtO)₂PO⁻]=0.31 M.

Applying the steady state approximation for Ph^\bullet in Scheme 15, it is possible to derive a rate expression for the formation of products 24 and 25 (Equations 40 and 41). The concentration of pinacolone enolate is represented by $[\text{E}^-]$ and the concentration of diethyl phosphite ion by $[\text{P}^-]$. The ratio of concentrations of the two nucleophiles were constant for all competition experiments. Integrating the rate expression to time equal infinity gives Equations 42 and 43, relating the product yields to the kinetic expression. The steady state concentration of Ph^\bullet is given by Equation 44. Substituting Equation 44 into Equation 43 gives Equation 45 relating the yield of 25 to the concentration of intermediate X. Dividing Equation 45 by 40 allows the ratio of yields of 25/24 to be related to a kinetic expression (Equation 46), which is simplified to Equation 47.

Scheme 15.



$$d\underline{24}/dt = k_{p*} [P^-][X] \quad (40)$$

$$d\underline{25}/dt = k_e [E^-][Ph\cdot]_{ss} \quad (41)$$

$$Y_{\underline{24}} = k_{p*} [P^-][X] \quad (42)$$

$$Y_{\underline{25}} = k_e [E^-][Ph\cdot]_{ss} \quad (43)$$

$$[Ph\cdot]_{ss} = \frac{k_r [X]}{k_e [E^-] + R_H} \quad (44)$$

$$Y_{\underline{25}} = \frac{k_r k_E [E^-][X]}{k_e [E^-] + R_H} \quad (45)$$

$$\frac{Y_{\underline{25}}}{Y_{\underline{24}}} = \frac{k_e k_r [E^-]}{k_{p*} [P^-](k_e [E^-] + R_H)} \quad (46)$$

$$\frac{Y_{\underline{25}}}{Y_{\underline{24}}} = \frac{k_r f}{k_{p*} [P^-]} \quad (47)$$

$$\text{where } f = \frac{k_e [E^-]}{k_e [E^-] + R_H}$$

The results of competing pinacolone enolate (E^-) versus diethyl phosphite ion (P^-) with iodobenzene under photo-stimulation by a sunlamp in DMSO for 3 minutes is presented in Table 9. If the mechanism outlined in Scheme 15 was correct, a plot of the yield ratio of $\underline{25}/\underline{24}$ versus $[P^-]^{-1}$ should result in a straight line with a slope equaling $k_r f/k_{p*}$ and a y-intercept of zero. A plot of the yield ratio of $\underline{25}/\underline{24}$ versus $[P^-]^{-1}$ is presented by Figure 1. The plots presented do not have a y-intercept of zero. The average intercept value for the two experiments was 1.1.

Table 9. The yields of 1-phenyl-3,3-dimethyl-2-butanone (25) and diethyl phenylphosphonate (24) from the competition of pinacolone enolate versus diethyl phosphite ion with iodobenzene in DMSO

[C] ⁻¹	% yield		
	<u>25</u>	<u>24</u>	<u>25/24</u>
exp A ^a			
3.03	61.5	43.2	1.42
4.66	63.1	38.1	1.66
6.06	63.2	36.6	1.73
8.66	64.8	31.6	2.07
10.10	64.6	31.4	2.06
exp B ^b			
3.23	58.5	43.8	1.34
4.96	62.7	43.2	1.45
6.45	60.2	36.4	1.65
8.06	61.6	34.6	1.78

^a[Ph-I]=4.5 X 10⁻³ M, [⁻CH₂CotBu]=0.33 M,
[(EtO)₂PO⁻]=0.31 M.

^b[Ph-I]=4.5 X 10⁻³ M, [⁻CH₂Cot-Bu]=0.31 M,
[(EtO)₂PO⁻]=0.31 M.

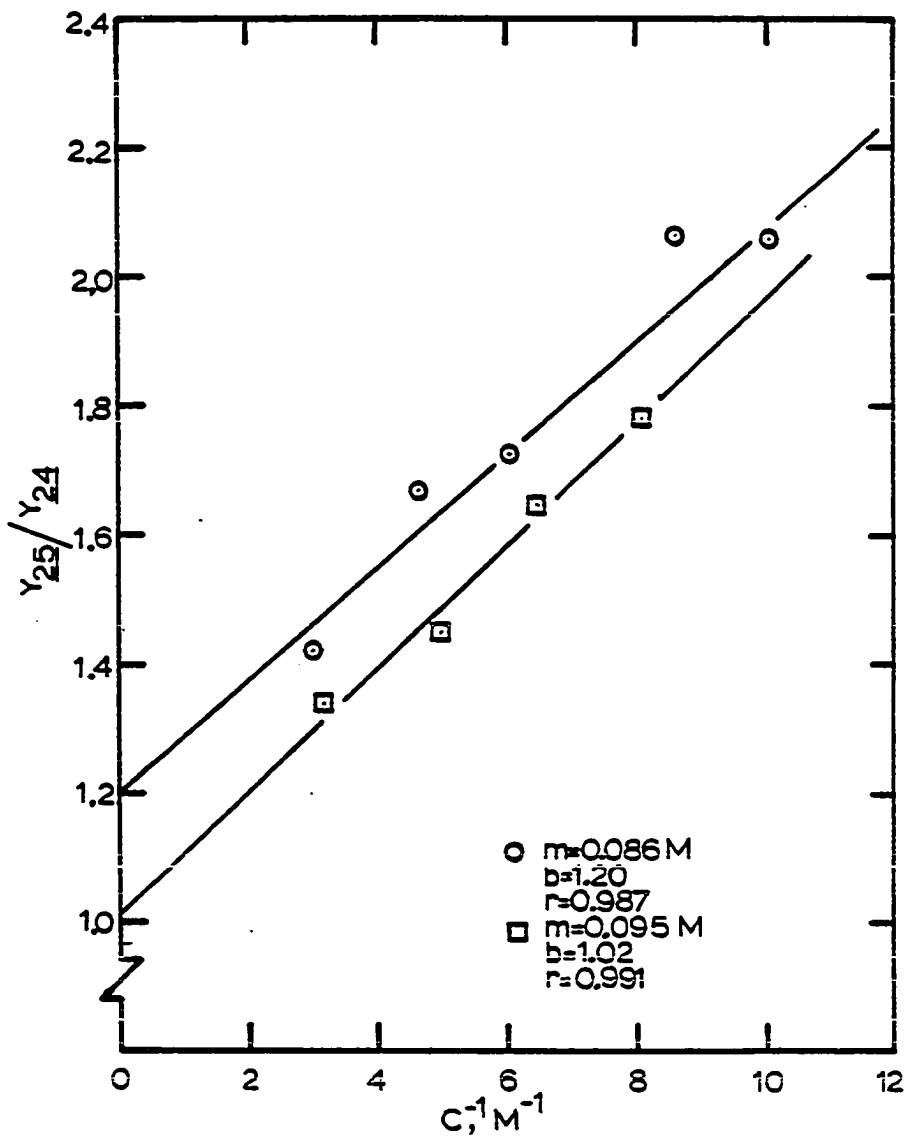
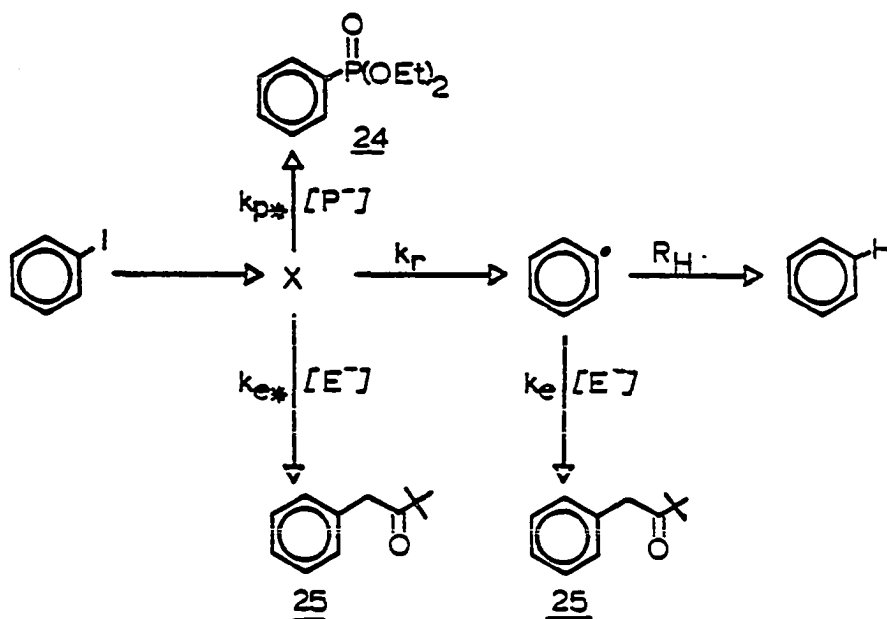


Figure 1. A plot of the yield ratio of 25/24 versus $[C]^{-1}$ for the competition of pinacolone enolate versus diethyl phosphite ion with iodobenzene in DMSO for experiments A (circle) and B (square)

The average slope of the plots was 0.092.

The mechanism outlined in Scheme 14 was revised in light of the above results and is presented in Scheme 16. The only revision is that pinacolone not only attacks sigma phenyl radical, but also traps intermediate X. Applying the steady state approximation for Ph[•] in Scheme 16 as described earlier, results in Equation 48. Fitting Equation 48 to the data plotted, the y-intercept, k_{e^*}/k_{p^*} , equals 1.1 while the slope of the line, 0.092, equals $f_e k_r/k_{p^*}$.

Scheme 16.



$$\frac{Y_{\underline{25}}}{Y_{\underline{24}}} = \frac{k_{e^*}}{k_{p^*}} + \frac{fk_r}{k_{p^*}} \frac{1}{[P^{\bullet}]} \quad (48)$$

Substrates other than iodobenzene were also used for the competition study to investigate a possible leaving group effect on the $f_e k_r / k_{p^*}$ and k_{e^*} / k_{p^*} ratios. The substrates employed were bromobenzene, diphenyl sulfide, and phenyltrimethylammonium iodide. The results of the competition studies are presented in Tables 10, 11, and 12. The results were plotted and are presented in Figures 2, 3 and 4. The average values for the four substrates are summarized in Table 13. For all four substrates, the y-intercept and slope of the plotted data are within experimental error of each other.

The small dependence of the yield ratios on the concentration of the nucleophiles (i.e., a small slope) and no leaving group effect (i.e., no change in the y-intercept) indicated an error in the analysis of the mechanism of the aromatic $S_{RN}1$ reaction. If one intermediate was involved, namely a sigma phenyl radical, the yield ratios would be independent of the nucleophile concentration (Scheme 17, Equation 49). Plotting the yield ratio versus $[C]^{-1}$ would result in a horizontal line with a y-intercept equaling k_e / k_p , the ratio of rate constants for the attack of pinacolone enolate and diethyl phosphite ion on the phenyl radical.

Table 10. The yields of 1-phenyl-3,3-dimethyl-2-butanone (25) and diethyl phenylphosphonate (24) from the competition of pinacolone enolate versus diethyl phosphite ion with diphenyl sulfide in DMSO

[C] ⁻¹	% yield		
	<u>25</u>	<u>24</u>	<u>25/24</u>
exp A ^a			
3.22	51.4	22.0	2.34
5.0	58.1	23.1	2.52
8.33	60.5	22.1	2.74
10.75	57.5	19.4	2.96
exp B ^b			
3.45	57.3	24.9	2.3
8.33	55.7	21.5	2.56
10.0	55.6	19.9	2.79
11.5	60.5	19.8	3.05

^a[Ph-I]=4.3 X 10⁻³ M, [⁻CH₂COtBu]=0.31 M,
[(EtO)₂PO⁻]=0.30 M.

^b[Ph-I]=4.3 X 10⁻³ M, [⁻CH₂COtBu]=0.29 M,
[(EtO)₂PO⁻]=0.30 M.

Table 11. The yields of 1-phenyl-3,3-dimethyl-2-butanone (25) and diethyl phenylphosphonate (24) from the competition of pinacolone enolate versus diethyl phosphite ion with bromobenzene in DMSO

[C] ⁻¹	% yield		
	<u>25</u>	<u>24</u>	<u>25/24</u>
exp A ^a			
3.33	12.2	11.3	1.08
5.13	12.9	11.0	1.17
7.41	12.6	10.3	1.22
8.33	13.2	10.3	1.28
11.1	12.4	8.4	1.43
exp B ^b			
3.33	18.5	17.3	1.07
6.67	20.7	15.8	1.31
8.33	19.3	14.2	1.36
9.52	18.7	12.6	1.48

^a[Ph-Br]=1.0 X 10⁻¹ M, [⁻CH₂COtBu]=0.30 M,
[(EtO)₂PO⁻]=0.30 M.

^b[Ph-Br]=4.2 X 10⁻³ M, [⁻CH₂COtBu]=0.30 M,
[(EtO)₂PO⁻]=0.30 M.

Table 12. The yields of 1-phenyl-3,3-dimethyl-2-butanone (25) and diethyl phenylphosphonate (24) from the competition of pinacolone enolate versus diethyl phosphite ion with phenyltrimethylammonium iodide in DMSO

[C] ⁻¹	% yield		
	<u>25</u>	<u>24</u>	<u>25/24</u>
3.23	30.0	12.9	2.1
4.96	39.4	18.3	2.1
7.17	38.7	18.7	2.2
10.75	42.7	19.4	2.2

^a[PhNMe₃⁺I⁻]=5.0 X 10⁻³ M, [⁻CH₂COtBu]=0.30 M, [(EtO)₂PO⁻]=0.31 M.

Table 13. Values for k_{e*}/k_{p*} and fk_r/k_{p*} ratios for iodobenzene, bromobenzene, diphenyl sulfide, and phenyltrimethylammonium iodide

substrate	k _{e*} /k _{p*}	fk _r /k _{p*}
Ph-I	1.1	0.092
Ph-Br	0.91	0.052
Ph ₂ S	2.02	0.083
PhNMe ₃ ⁺ I ⁻	2.05	0.015

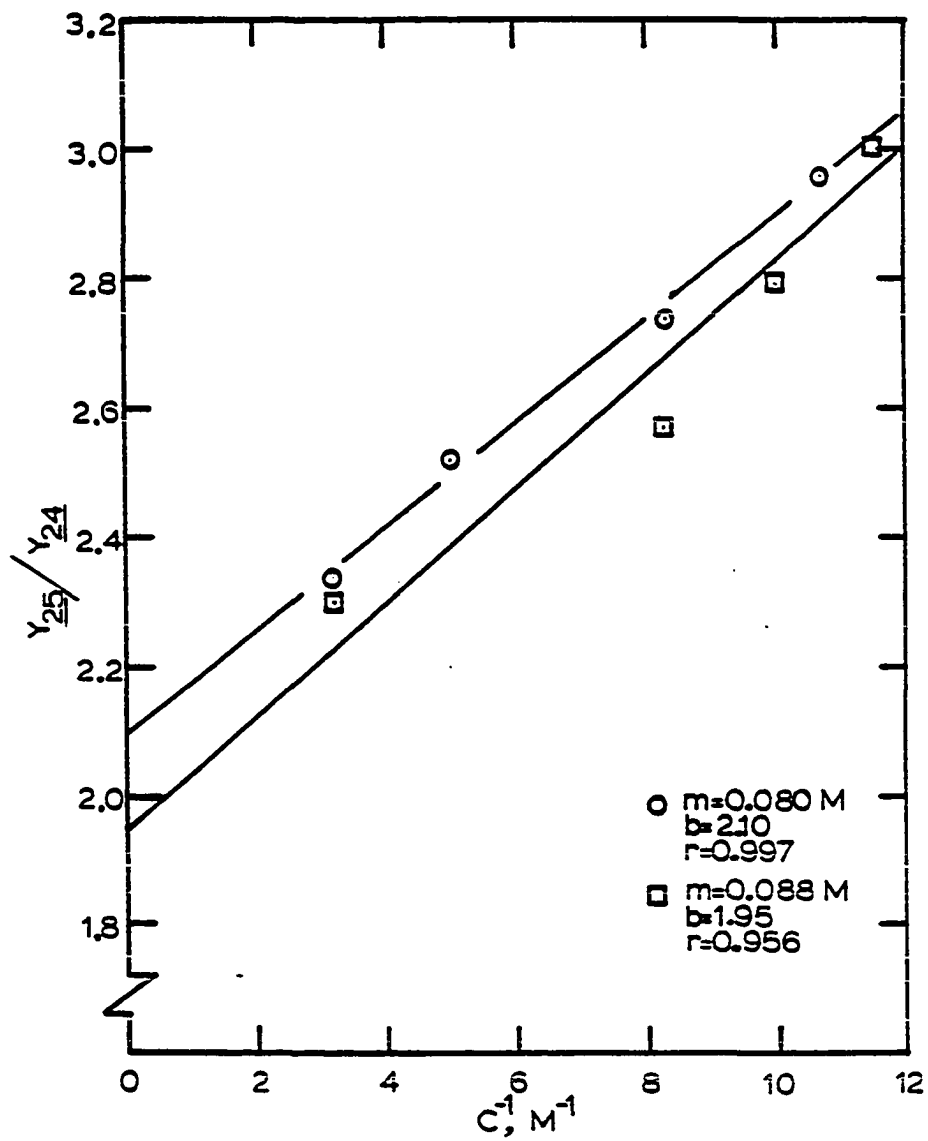


Figure 2. A plot of the yield ratio of 25/24 versus $[C]^{-1}$ for the competition of pinacolone enolate versus diethyl phosphite ion with diphenyl sulfide in DMSO for experiments A (circle) and B (square)

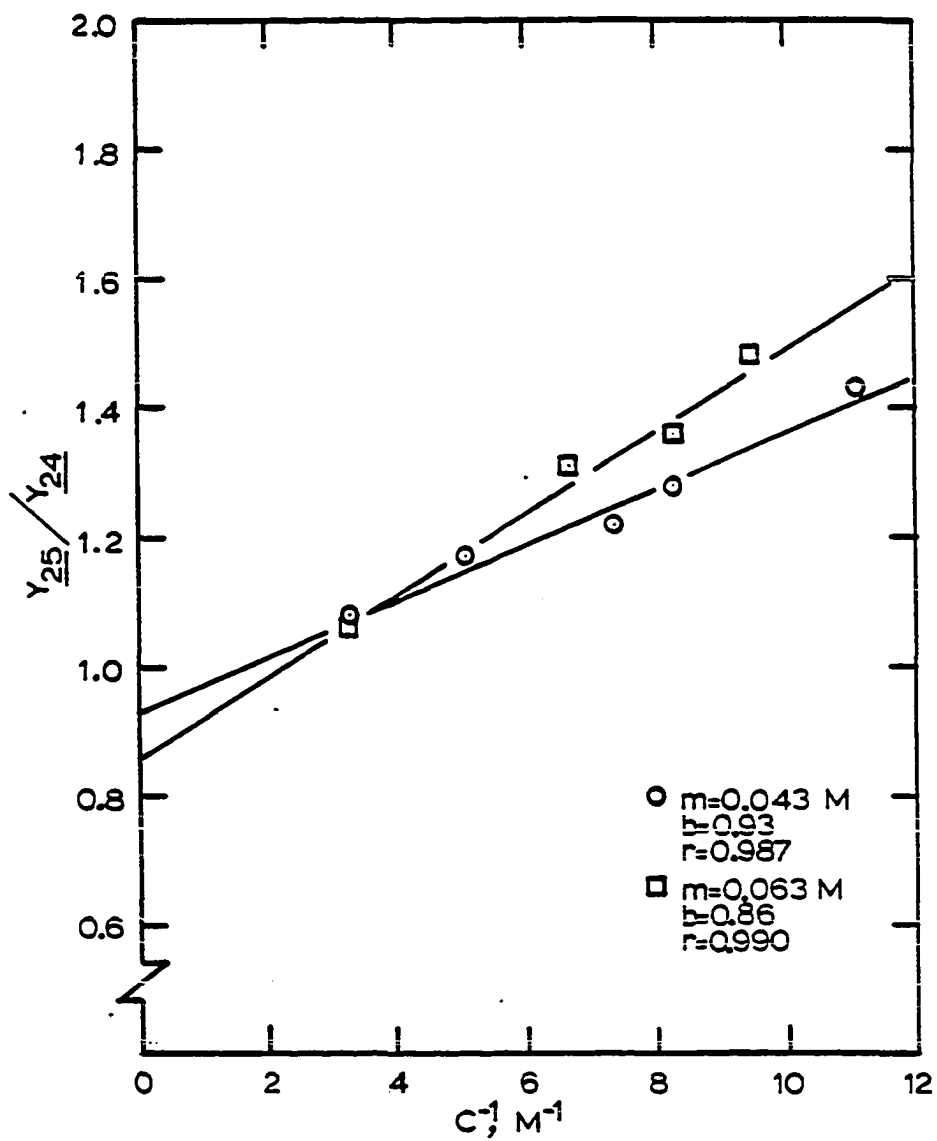


Figure 3. A plot of the yield ratio of 25/24 versus $[C]^{-1}$ for the competition of pinacolone enolate versus diethyl phosphite ion with bromobenzene in DMSO for experiments A (circle) and B (square)

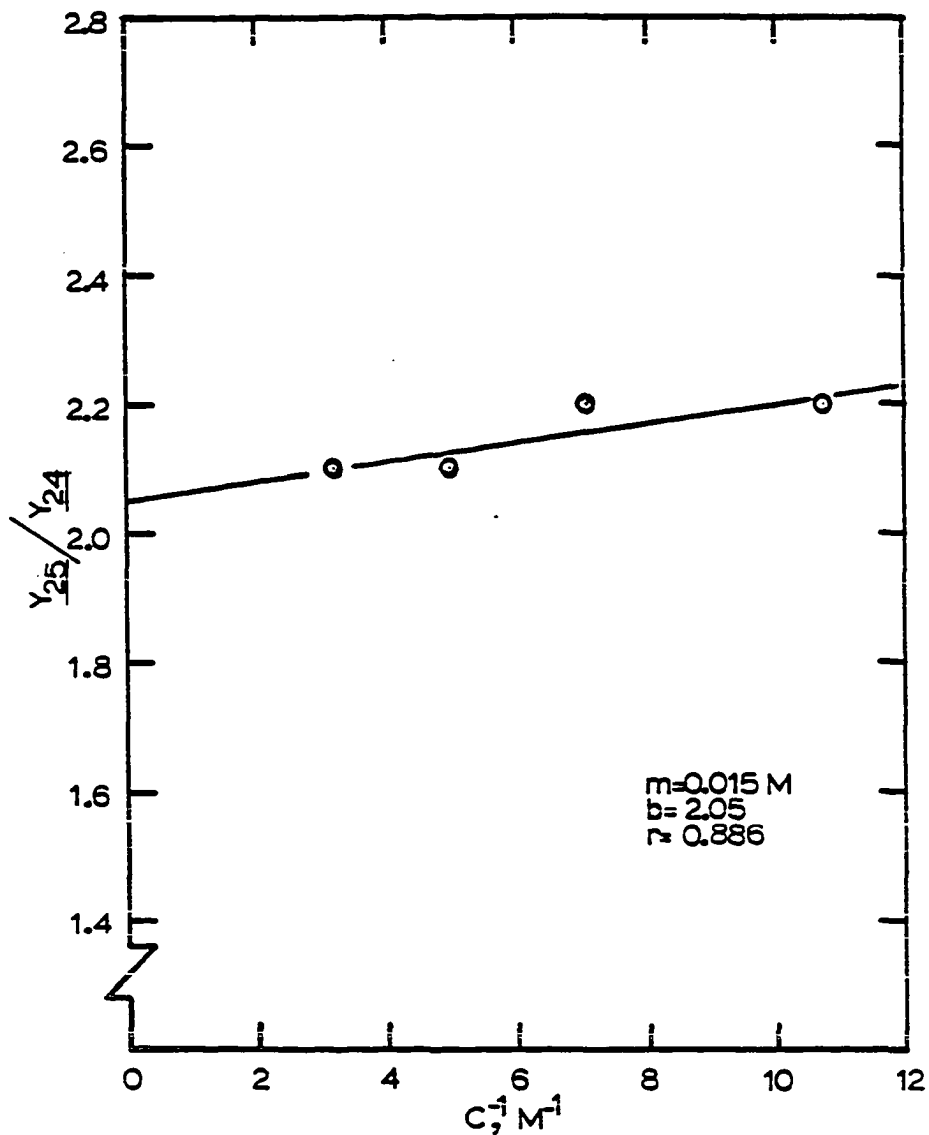
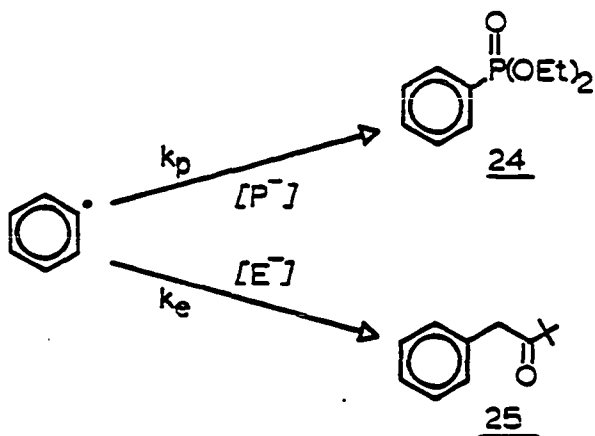


Figure 4. A plot of the yield ratio of $\frac{25}{24}$ versus $[C]^{-1}$ for the competition of pinacolone enolate versus diethyl phosphite ion with phenyltrimethylammonium iodide in DMSO for the experiment of Table 12

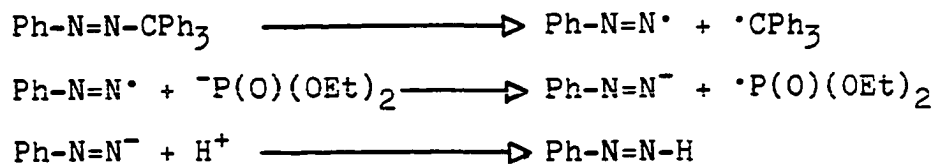
Scheme 17.

$$\frac{Y_{25}}{Y_{24}} = \frac{k_e}{k_p} \quad (49)$$

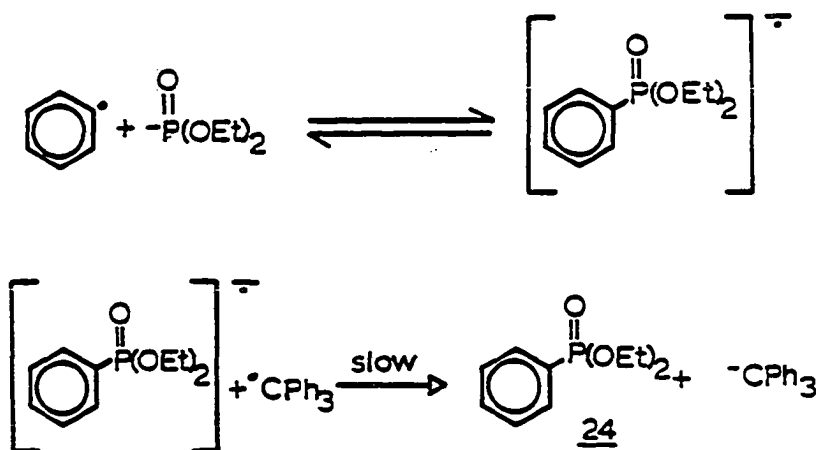
The earlier studies¹⁰ had been interpreted as showing that sigma phenyl radical and diethyl phosphite ion did not couple to form diethyl phenylphosphonate. The observation that the mass balances of the PAT thermolyses were always below 40% when diethyl phosphite ion was present indicated that one of three processes was occurring: 1) the diethyl phosphite ion reduces the diazenyl radical before loss of nitrogen to give the phenyl radical (Scheme 18); 2) the attack of phenyl radical on diethyl phosphite ion is reversible because the trityl radical can not oxidize the radical ion formed (Scheme 19); 3) the product of the

coupling (PhP(O)(OEt)_2) is destroyed during the reaction.

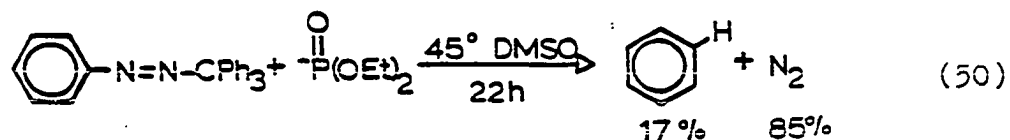
Scheme 18.



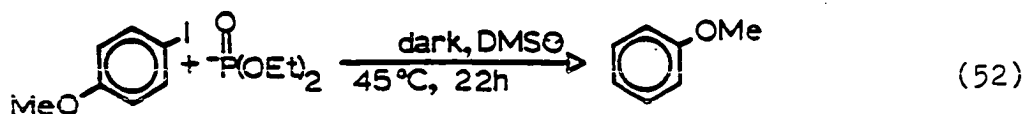
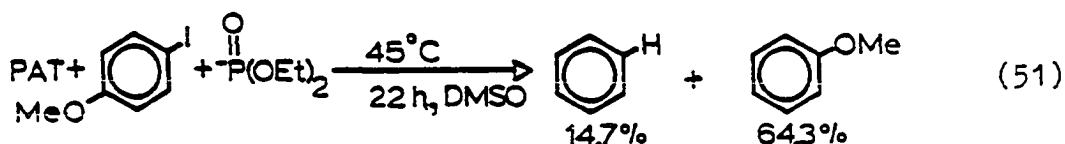
Scheme 19.

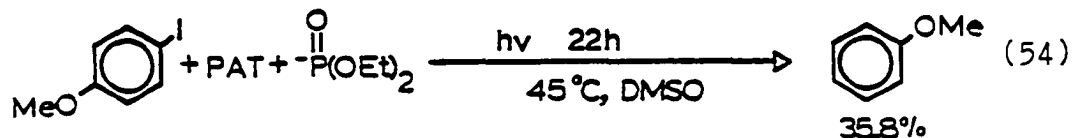
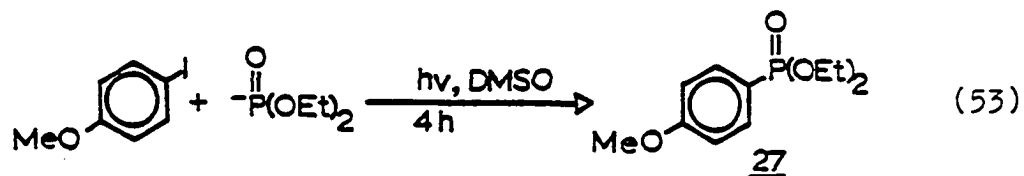


Process one was easily be checked by measuring the amount of nitrogen produced during the reaction (Equation 50). The yield of nitrogen produced was well over 80%. This result indicated that the diazenyl radical does decompose to yield phenyl radical in greater than 80% yield.

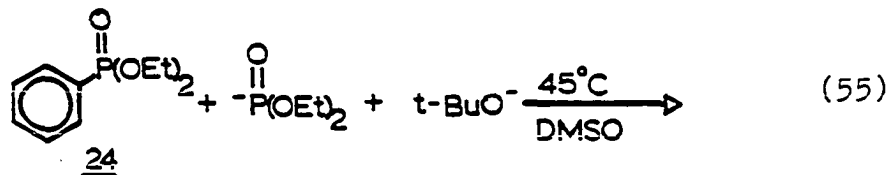


Process two was investigated by adding an electron acceptor, 4-iodoanisole, to the reaction mixture. The only products formed were benzene (14.7%) and anisole (64.3%) (Equation 51). None of the diethyl phosphite ion substituted products were detected. The anisole formed during the reaction is from a dark reaction between 4-iodoanisole and diethyl phosphite ion (Equation 52). As a control experiment, diethyl phosphite ion was reacted with 4-iodoanisole under $S_{RN}1$ conditions (Equation 53). The reaction gave the *p*-methoxyphenylphosphonate (27) in 40% yield and no anisole was detected. This result prompted the running of the PAT, 4-iodoanisole, and diethyl phosphite ion reaction under $S_{RN}1$ conditions (Equation 54). The temperature inside the photochemical reactor was 45 °C, high enough to decompose the PAT, and the ultra-violet irradiation would initiate the aromatic $S_{RN}1$ reaction between 4-iodoanisole and diethyl phosphite ion. Anisole was formed in 35.8% yield, benzene was not quantified. Significantly, *p*-methoxyphenyl phosphonate was not detected.



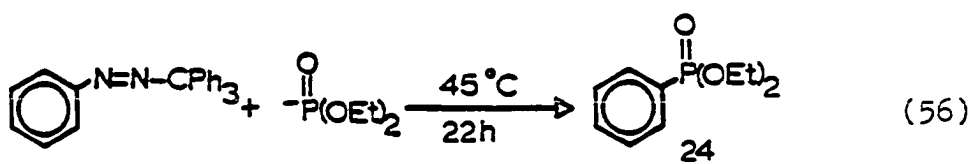


The results indicated that the diethyl phenylphosphonate must be formed but is destroyed under the conditions of the PAT reaction, process three. To check this hypothesis, a solution containing diethyl phenylphosphonate, diethyl phosphite ion and potassium t-butoxide was studied as a function of time under thermolysis conditions (Equation 55). The results are presented in Table 14. The diethyl phenylphosphonate decomposes very quickly under the conditions employed for the PAT thermolysis reactions. It was discovered, however, that if the amount of t-butoxide in the reaction mixture is decreased, the diethyl phenylphosphonate is stable (Table 15).



Determining that the reaction condition played a major

role in the stability of the diethyl phenylphosphonate, phenyl radical was generated in the presence of diethyl phosphite ion without excess t-butoxide in solution. This was achieved by adding an excess of diethyl phosphite to protonate all of the t-butoxide (Equation 56). The results show that phenyl radical will couple with diethyl phosphite ion in high yield (80%).



The relative reactivity of pinacolone enolate to diethyl phosphite ion toward phenyl radical generated from PAT was measured and compared with the y-intercept of the competition plots presented earlier. However, the relative reactivity between these two nucleophiles could not be measured directly. The pinacolone enolate is too basic resulting in the decomposition of the diethyl phenylphosphonate. Therefore, the relative reactivity of the two nucleophiles had to be calculated via a relay nucleophile. The relay nucleophile chosen was the enolate of ethyl phenylacetate. Tables 16 and 17 present the results pitting diethyl phosphite versus ethyl phenylacetate enolate Table 14. Time study of the decomposition of diethyl

Table 14. Time study of the decomposition of diethyl phenylphosphonate (24)^a

time (min.)	% of <u>24</u>
30	64.2
60	49.0
120	34.0
310	8.3
640	1.6

^a[(EtO)₂PO⁻]=0.31 M, [tBuO⁻]=0.03 M,
at t=0, [PhPO(OEt)₂]=0.03 M.

Table 15. Time study of the decomposition of diethyl phenylphosphonate (24) with slight excess of potassium t-butoxide present^a

time (min.)	% of <u>24</u>
15	108.0
30	100.8
70	108.3
120	111.0
180	108.3
345	103.6
1320	100.0

^a[(EtO)₂PO⁻]=0.29 M, [tBuO⁻]=8.4 X 10⁻³ M,
at t=0, [PhPO(OEt)₂]=0.028 M.

(k_p/k_{acet}) and pinacolone enolate versus ethyl phenylacetate enolate (k_e/k_{acet}). The relative rate constants determined were $k_p/k_{\text{acet}}=1.8$ and $k_e/k_{\text{acet}}=2.8$ (Scheme 20). The calculated relative reactivity of pinacolone enolate to diethyl phosphite ion was 1.6 ($k_e/k_p=1.6$). This value agrees very well with the y-intercepts of Figures 1, 2, 3, and 4. The agreement of the two values obtained indicate only one intermediate exists in the aromatic $S_{\text{RN}}1$ reaction, a sigma phenyl radical.

Scheme 20.

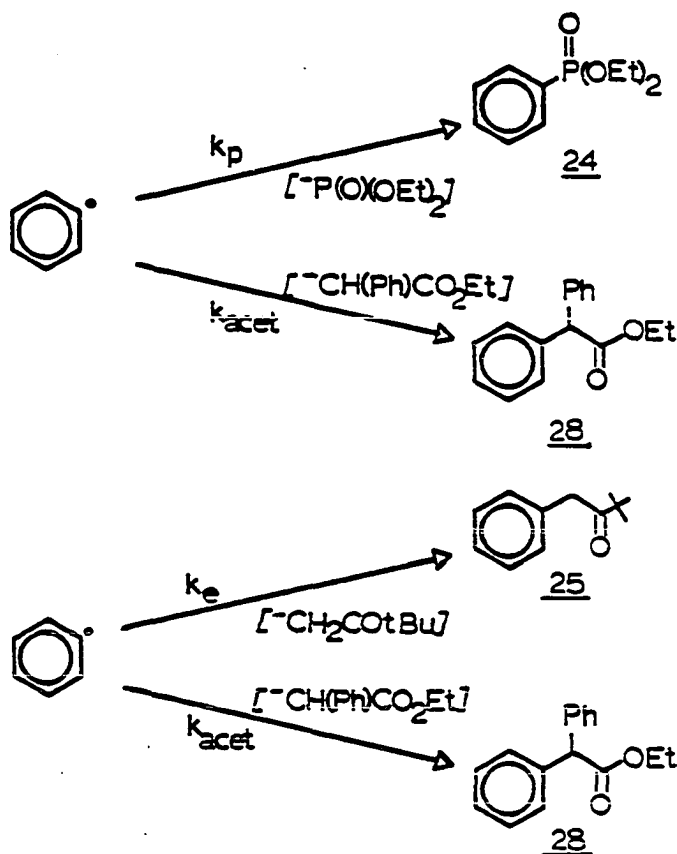


Table 16. The relative reactivity of diethyl phosphite ion to ethyl phenylacetate enolate for phenyl radical at 45 °C in DMSO

% yield ^a			k_p/k_{acet}
<u>24</u>	<u>28</u>		
32.8	13.3		1.8
34.0	13.2		1.9
		ave	1.85

^a $[(EtO)_2PO^-]=0.11$ M, $[-CH(Ph)CO_2Et]=0.093$
 $[PAT]=0.0075$ M.

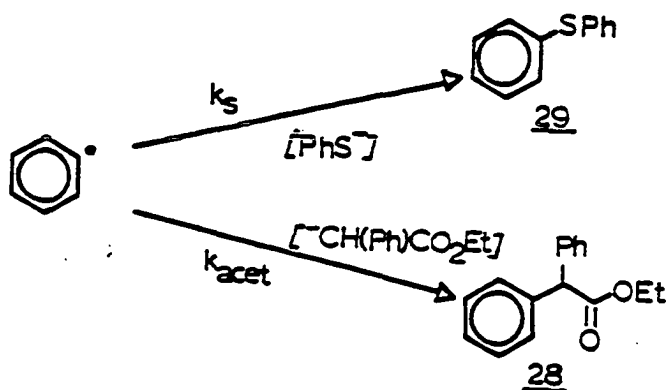
Table 17. The relative reactivity of pinacolone enolate to ethyl phenylacetate enolate for phenyl radical at 45 °C in DMSO

% yield ^a			k_e/k_{acet}
<u>25</u>	<u>28</u>		
45.8	17.1		2.94
43.4	18.4		2.59
		ave	2.77

^a $[-CH_2COtBu]=0.098$ M, $[-CH(Ph)CO_2Et]=0.11$ M
 $[PAT]=0.0075$ M.

Further evidence for a single intermediate can be presented. The results from the competition of pinacolone enolate versus thiophenoxide in the $S_{RN}1$ process is presented in Table 18. The ratio of the yields of 25/29 versus $[C]^{-1}$ are plotted in Figure 5. The plot exhibits a slight curvature at small $[C]^{-1}$. The y-intercept is 3.3.

The relative reactivity of this pair toward sigma phenyl radical from PAT can not be measured directly. Since diphenyl sulfide reacts with pinacolone enolate via the aromatic $S_{RN}1$ reaction to yield 1-phenyl-3,3-dimethyl-2-butanone, which is also the product from phenyl radical coupling with pinacolone enolate. Thus, the relative reactivity was calculated via the relay method described earlier. The results of the thiophenoxide versus ethyl phenylacetate enolate (k_s/k_{acet}) is presented in Table 19 (Scheme 21). The relative reactivity of thiophenoxide to ethyl phenylacetate enolate was 0.64. Since the relative reactivity of pinacolone enolate to ethyl phenylacetate enolate was 2.77 (Table 17), the calculated relative reactivity of pinacolone enolate to thiophenoxide ion is 3.3. This value agrees very well with the value of the y-intercept from the $S_{RN}1$ competition studies indicating the same intermediate in the PAT and $S_{RN}1$ experiments.

Scheme 21.

Initial Relative Reactivities

In this section, the initial relative reactivities of several nucleophiles have been determined. Each reaction competed two or three nucleophiles against each other and was studied as a function of time. Aliquots were removed at set time intervals and worked up as described in the experimental section. The yields of the products, as determined by gas chromatography, were plotted versus time. Smooth curves were drawn for each set of product points. Tangents were drawn by reflection to the smooth curves at time equaling zero ($t=0$) using a tangent meter.

The ratio of the slopes of the tangents are related to the initial rate constants by Equation 57. Equation 57 can then be rearranged to give the ratio of rate constants, k_A/k_B , as a function of experimentally measured parameters, concentration of nucleophiles and the slope of the tangents

Table 18. The yields of 1-phenyl-3,3-dimethyl-2-butanone (25) and diphenyl sulfide (29) from the competition of pinacolone enolate versus thiophenoxide with iodobenzene in DMSO

$[C]^{-1}$	<u>25/29</u>
exp A ^a	
2.04	4.15
3.14	4.41
5.10	5.05
5.83	5.01
8.16	5.85
10.20	5.77
exp B ^b	
3.44	4.58
5.31	5.20
6.90	5.43
8.62	5.72
9.85	5.95

^a[Ph-I]= 4.8×10^{-3} M, [⁻CH₂COtBu]=0.49 M, [PhS⁻]=0.49 M.

^b[Ph-I]= 4.8×10^{-3} M, [⁻CH₂COtBu]=0.29 M, [PhS⁻]=0.29 M.

Table 19. The relative reactivity of thiophenoxide to ethyl phenylacetate enolate toward phenyl radical at 45 °C in DMSO

% yield ^a			k_s/k_{acet}
<u>28</u>	<u>29</u>		
28.2	32.3	0.83	
28.5	32.0	0.85	
		ave 0.84	

^a[PhS⁻]=0.10 M, [⁻CH(Ph)CO₂Et]=0.095 M
[PAT]=0.0085 M.

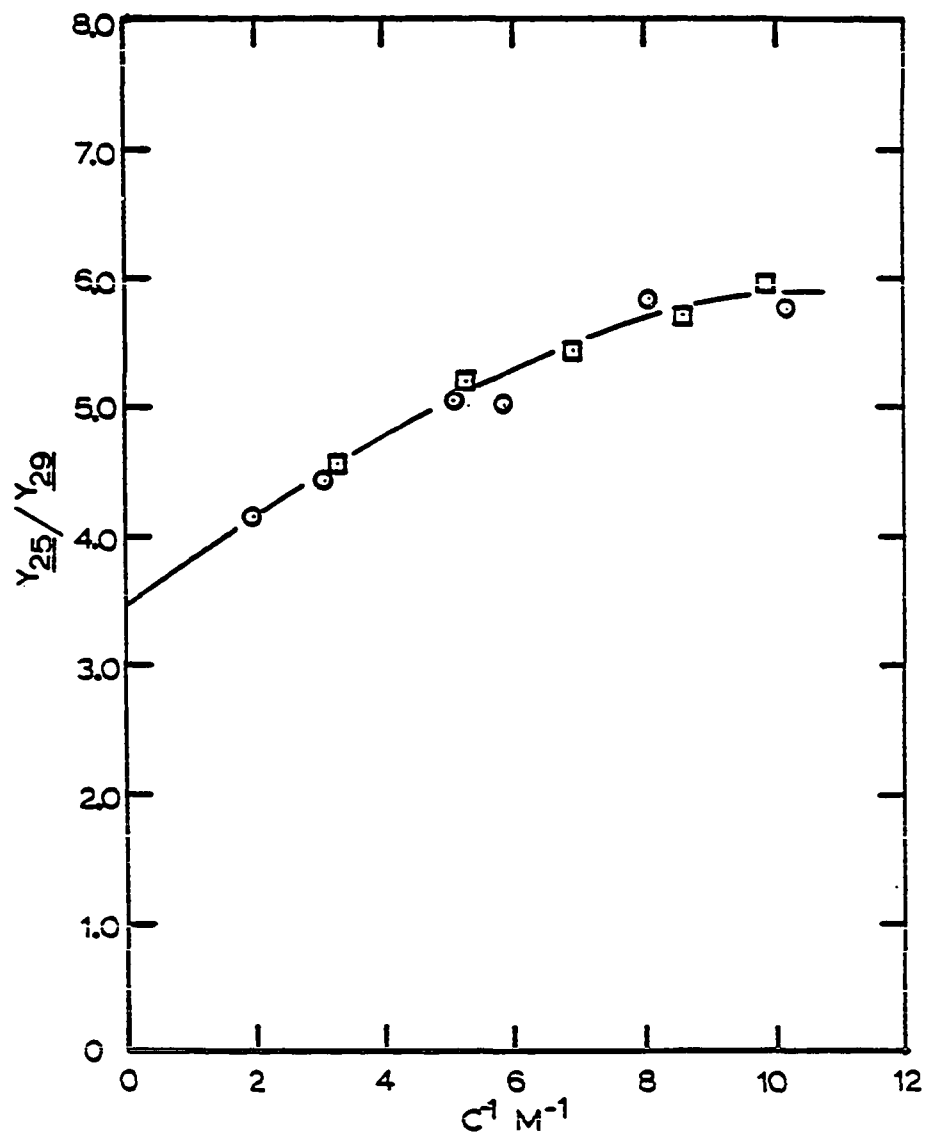


Figure 5. A plot of the yield ratio of 25/29 versus $[C]^{-1}$ for the competition of pinacolone enolate versus thiophenoxide with iodobenzene in DMSO for experiments A (circle) and B (square)

at $t=0$ (Equation 58).

$$\frac{[dA/dt]}{[dB/dt]} = \frac{k_A [Nu_A]}{k_B [Nu_B]} \quad (57)$$

$$\frac{k_A}{k_B} = \frac{[dA/dt] [Nu_B]}{[dB/dt] [Nu_A]} \quad (58)$$

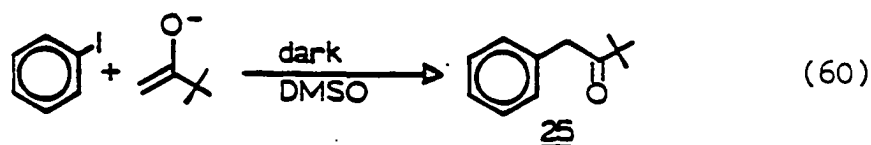
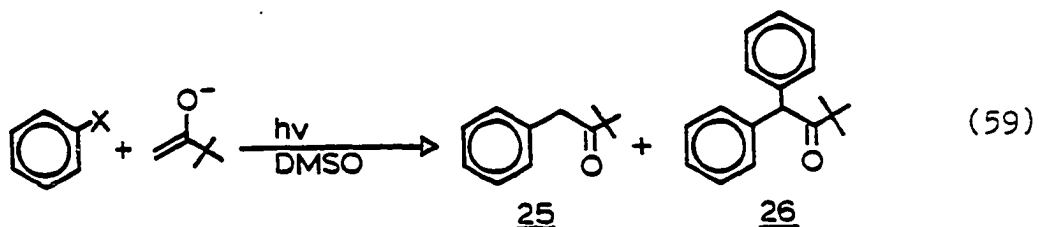
where $[dA/dt]$ =slope of tangent at $t=0$ for product A
 $[dB/dt]$ =slope of tangent at $t=0$ for product B
 $[Nu_A]$ =concentration of nucleophile that yields product A
 $[Nu_B]$ =concentration of nucleophile that yields product B

All reactions were preformed in dry, deoxygenated DMSO. The aromatic $S_{RN}1$ reactions were photostimulated using ultra-violet light at 45°C (350 nm through Pyrex). Phenylazotriphenylmethane was thermolyzed 45°C . The counter ion of the nucleophiles, potassium, was complexed with 18-crown-6.

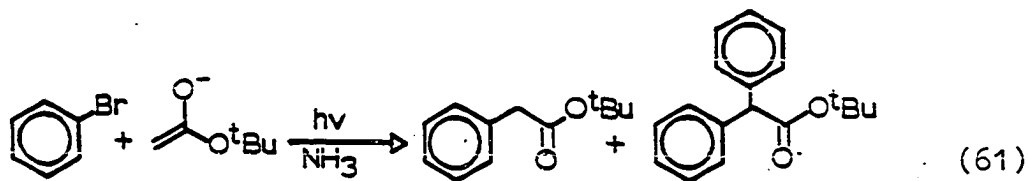
Time study of the reaction of pinacolone enolate with iodobenzene

The photostimulated reaction of pinacolone enolate with halobenzenes in DMSO is a well documented reaction yielding the mono phenylated product (70-80%) along with some diphenylated product (4-19%)(Equation 59).⁵¹ However, in the dark, the only product formed was 1-phenyl-3,3-dimethyl-2-butanone (25) in quantitative yield after 105 minutes (Equation 60).¹³ The generation of phenyl radical by the

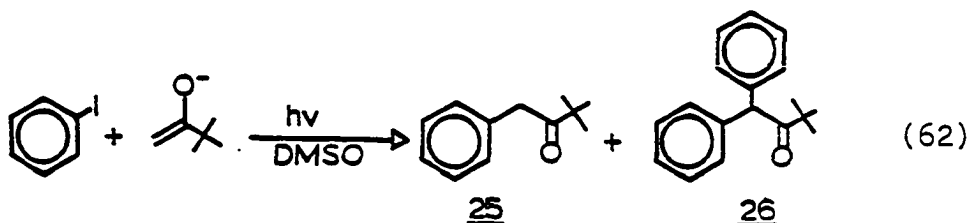
thermolysis of PAT in the presence of pinacolone enolate yields 1-phenyl-3,3-dimethyl-2-butanone (25) in high yield. Only a trace of 1,1-diphenyl-3,3-dimethyl-2-butanone (26) is detected.



Enolates of esters have also exhibited high yields of diphenylated products in liquid ammonia.⁹ For example, the potassium enolate of t-butyl acetate reacted with bromobenzene under photostimulation in liquid ammonia to yield the mono-substituted and disubstituted products in very high yields. The most striking feature of this reaction is the significant yield of the diphenylated product (Equation 61).



In an attempt to understand this reaction, a time study of the photostimulated reaction of pinacolone enolate with iodobenzene was carried out (Equation 62). The results of the study are summarized in Table 20. The ratio of 1-phenyl-3,3-dimethyl-2-butanone (25) to 1,1-diphenyl-3,3-dimethyl-2-butanone (26) is plotted versus time (figures 6 and 7).



In the early stages of the reaction (0-10 min.), the amount of diphenylated product is larger than expected causing the ratio of 25/26 to increase with time. As the reaction proceeded, the ratio reached a maximum (10-15 mins.) and then decreased reaching a plateau of approximately 17 after 60 min.

Assuming that the relative reactivity of 1-phenyl-3,3-dimethyl-2-butanone enolate (30) to pinacolone enolate (31) is similar to the phenylacetone-acetone enolate pair, the ratio of the products can be calculated. For example, at t=50 min., the concentration of 1-phenyl-3,3-dimethyl-2-

butanone is 0.038 M. The concentration of pinacolone enolate is 0.17 M. The relative reactivity of 31/30, making the above assumption, is 2.8. Substituting these values into Equation 63 yields Equation 64 resulting in a ratio of 31/30 equaling 12. This is in good agreement with the experimental result of 15 at t=50 min.

$$\frac{Y_{\underline{25}}}{Y_{\underline{26}}} = \frac{k_e [E^-]}{k_{e'} [E'^-]} \quad (63)$$

$$Y_{\underline{25}}/Y_{\underline{26}} = 12 \quad (64)$$

The large amount of 26 produced in the early stages of the reaction can perhaps be explained by considering the initiation step of the reaction. As discussed in the introduction, Fox¹⁶ and coworkers found that a charge transfer complex exists between iodobenzene and pinacolone enolate. A similar charge transfer complex may also exist between the enolate of 26 and iodobenzene (Scheme 22). Photolysis of the charge transfer complex results in an electron transfer yielding a phenyl radical, iodide ion, and an alpha-keto radical in a solvent cage. Before the radicals diffuse apart, they can couple yielding the substituted product.

Table 20. The yields of 1-phenyl-3,3-dimethyl-2-butanone (25) and 1,1-diphenyl-3,3-dimethyl-2-butanone (26) from the reaction of pinacolone enolate with iodobenzene as a function of time

time (min.)	% yield		
	<u>25</u>	<u>26</u>	<u>[25+26]/26</u>
exp A ^a			
2	6.9	1.1	6.3
4	12.7	1.0	12.6
6	22.8	1.2	23.8
8	27.7	1.5	24.1
10	35.3	1.5	24.5
15	54.3	2.2	25.7
20	51.6	2.4	22.5
30	64.9	3.2	21.3
35	58.0	3.3	18.6
40	71.5	4.0	18.9
45	45.1	3.2	15.1
50	63.1	3.8	17.6
55	63.2	3.8	17.6
60	58.2	3.6	17.2

^a[Ph-I]=0.03 M, [⁻CH₂C(O)t-Bu]=0.20 M.

Table 20. continued

time (min.)	% yield		[<u>25+26</u>]/ <u>26</u>
	<u>25</u>	<u>26</u>	
exp B ^b			
4	14.7	0.7	22.9
6	23.1	0.8	30.6
8	27.4	0.9	33.2
10	38.2	1.4	28.3
15	53.4	2.6	21.5
20	49.9	2.5	21.0
25	83.4	5.1	17.4
30	76.1	4.8	16.9
35	74.1	4.6	17.1
40	88.0	5.9	15.9
50	71.4	4.5	16.9
55	70.8	5.1	14.9
60	66.6	4.5	15.8

^b[Ph-I]=0.03 M, [⁻CH₂C(O)t-Bu]=0.17 M.

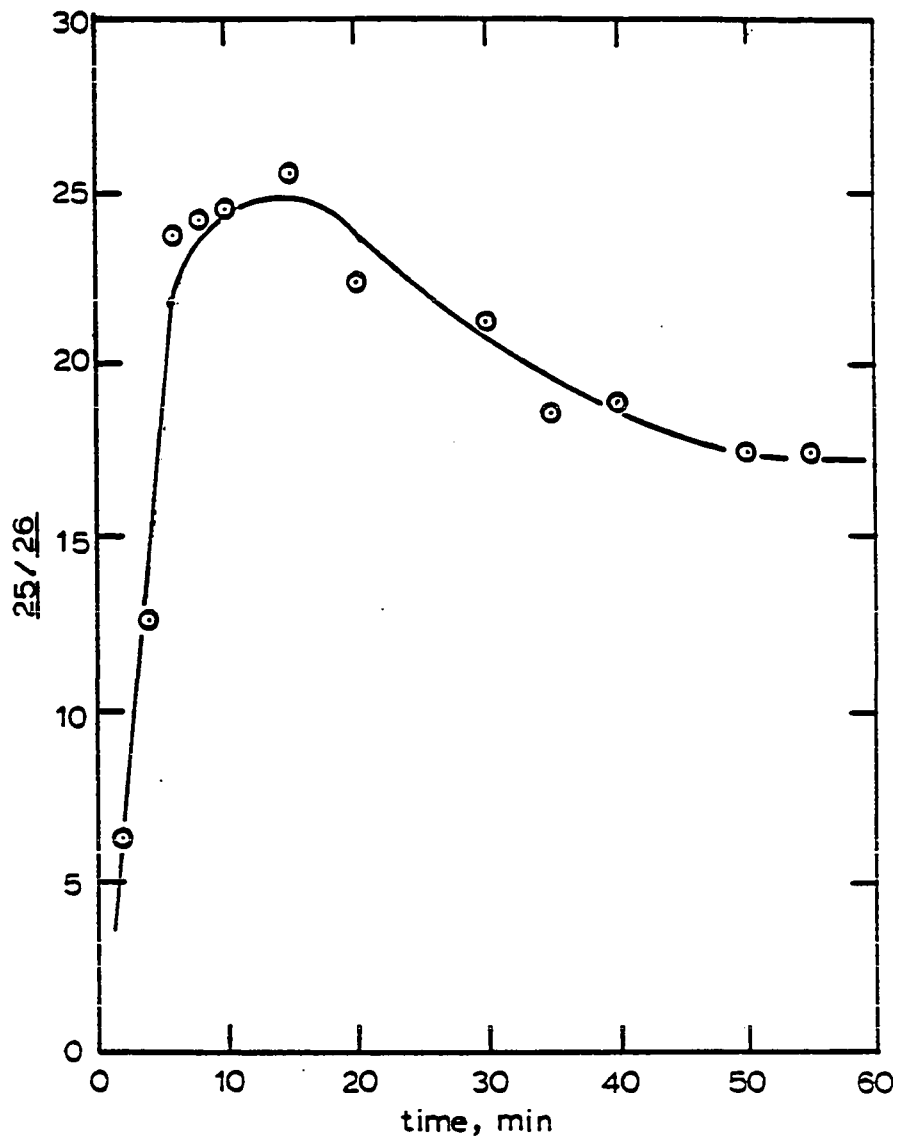


Figure 6. A plot of the yield ratio of 1-phenyl-3,3-dimethyl-2-butanone (25) to 1,1-diphenyl-3,3-dimethyl-2-butanone (26) versus time for the reaction of pinacolone enolate with iodobenzene (experiment A, Table 20)

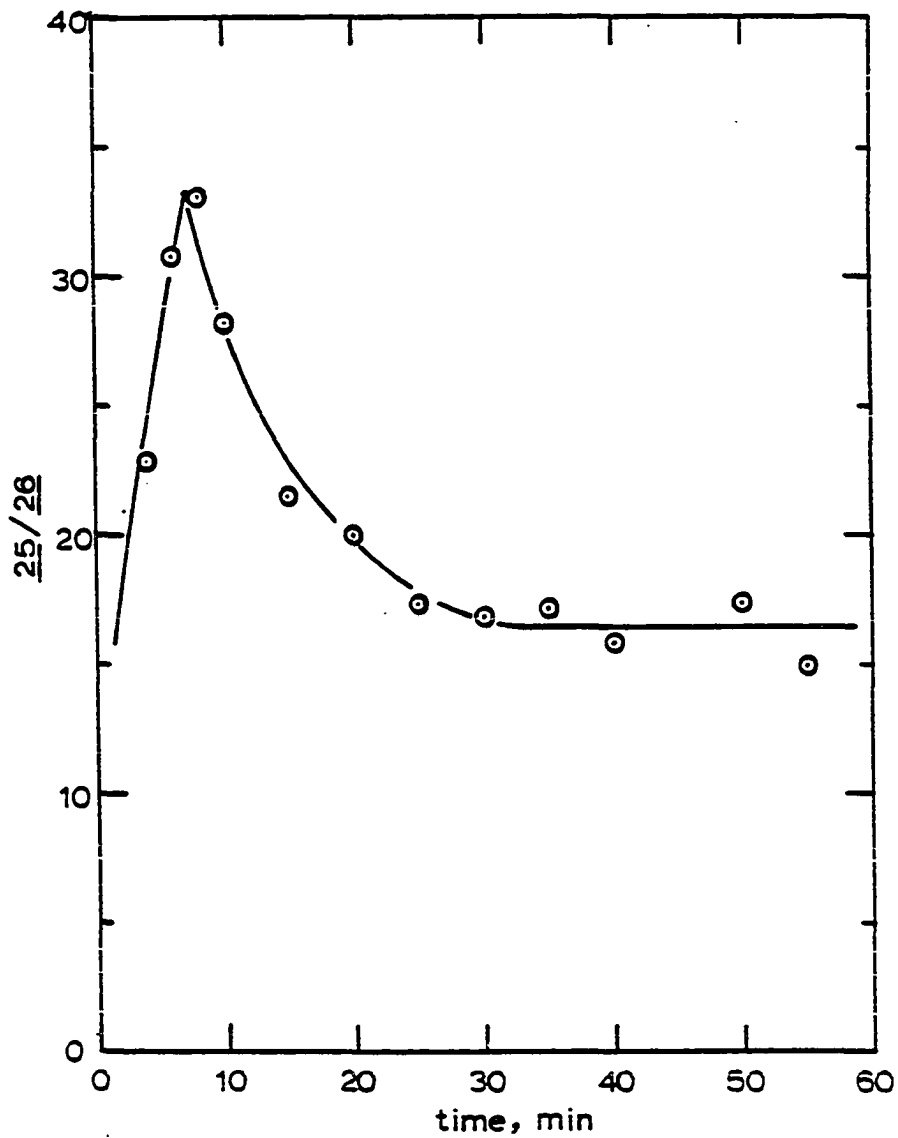
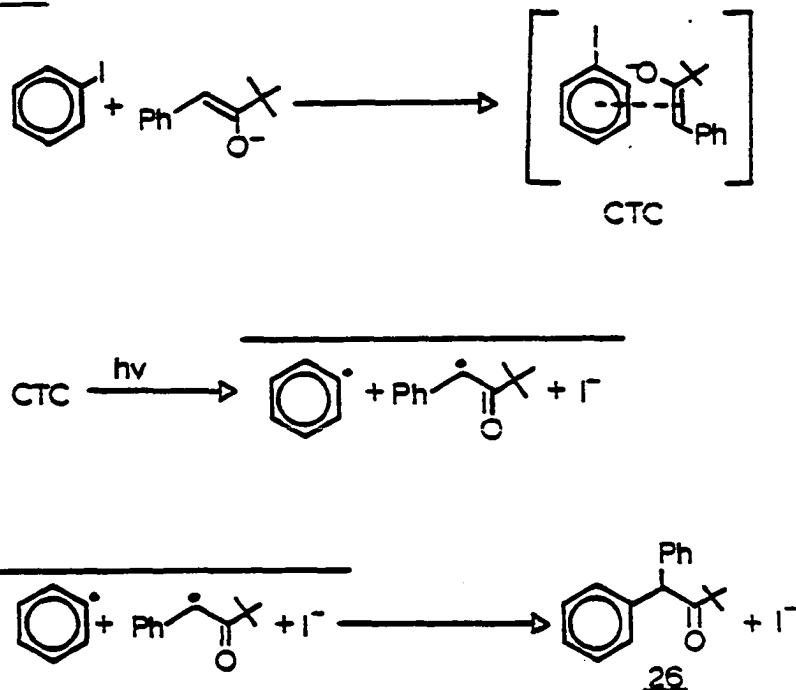


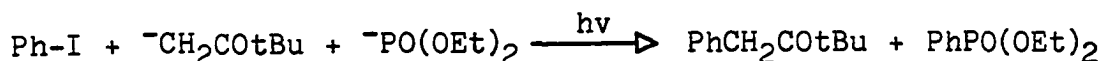
Figure 7. A plot of the yield ratio of 1-phenyl-3,3-dimethyl-2-butanone (25) to 1,1-diphenyl-3,3-dimethyl-2-butanone (26) versus time for the reaction of pinacolone enolate with iodobenzene (experiment B, Table 20)

Scheme 22.



The coupling of the phenyl radical and alpha-keto radical in the solvent cage may be the major product formation step in the first 5 to 10 mins. of the reaction. As the reaction time increases, the kinetic chain length apparently increases until the propagation steps of the reaction become the major product forming step. This occurs at the inflection point of the curve after 10-15 min. This explanation assumes that 31 forms a stronger charge transfer complex with iodobenzene than 32.

Pinacolone enolate versus diethyl phosphite ion with iodobenzene



The initial rate results for the pinacolone enolate, diethyl phosphite couple are summarized in Table 21. Figures 8 and 9 are the curves resulting from plotting the product yields versus time. The initial relative rates were calculated from these curves as described earlier and are summarized in Table 22. The average initial relative rate for the pinacolone/diethyl phosphate pair is 3.8.

Figures 10 and 11 are the curves resulting from plotting the ratio of $[\underline{25} + \underline{26}] / \underline{24}$ versus time. Ideally, a line with a slope of nearly zero and y-intercept having the value of the initial relative rate should occur. The plot has two distinct curves. The curve from $t=0$ to 15 min. suggests that a product, 25, is formed from another process other than radical-nucleophile coupling, and the importance of this process decreases over time. One explanation is that at the beginning of the reaction, product 25 arises from radical coupling after electron transfer in the charge-transfer complex. As the reaction proceeds, the propagation steps become the dominant processes. After $t=15$ min., the ratio of $\underline{25} / \underline{24}$ increases dramatically. This sharp increase of the ratio is the result of the destruction of the diethyl phenylphosphonate during the reaction.

Addition of iodide ion to the reaction mixture changes the initial relative rates. Table 23 summarizes the yields of the products and the plotted results are given in Figures 12 and 13. The initial relative rates for the pinacolone/diethyl phosphite pair in the presence of iodide ion is 1.7 (Figure 12). Plotting $\frac{25}{24}$ versus time gives a horizontal line with a small slope and a y-intercept of 1.95 (Figure 13).

Addition of iodide inhibits the formation of 25 in the early stages of the reaction. One possible explanation is that iodide ion destroys the charge-transfer complex between iodobenzene and pinacolone enolate, preventing the formation of 25 from radical-radical coupling in the solvent cage.

Pinacolone enolate versus thiophenoxide with iodobenzene



Table 24 summarizes the results from the initial relative rate study for the pinacolone enolate/thiophenoxide pair with iodobenzene. Figures 14 and 15 are yield versus time plots from which the initial relative rates were calculated. The average value for the relative rates for pinacolone enolate to thiophenoxide was 3.2 (Table 25).

Figure 16 is a plot of the ratio of yield of 25/29 versus time. Each plot has a slight curvature toward higher

Table 21. The yields of 1-phenyl-3,3-dimethyl-2-butanone (25), 1,1-diphenyl-3,3-dimethyl-2-butanone (26), and diethyl phenylphosphonate (24) from the reaction of pinacolone enolate/diethyl phosphite ion with iodobenzene as a function of time

time (min.)	% yield			[<u>25</u> + <u>26</u>]/ <u>24</u>
	<u>25</u>	<u>26</u>	<u>24</u>	
exp A ^a				
5	18.3	-	5.2	3.5
10	30.9	0.6	9.0	3.5
15	40.9	0.8	13.8	3.0
20	57.9	1.3	17.2	3.4
25	64.4	1.4	17.6	3.7
30	65.8	1.4	15.6	4.3
35	69.4	1.5	13.3	5.3
exp B ^b				
5	17.4	-	4.7	3.7
10	28.1	0.7	8.3	3.5
15	42.3	0.9	13.8	3.1
20	54.5	1.0	14.7	3.8
25	58.3	1.5	14.9	4.0
30	59.7	1.7	12.1	5.0

^a[Ph-I]=0.05 M, [⁻CH₂C(O)t-Bu]=0.30 M,
[(EtO)₂PO⁻]=0.28 M.

^b[Ph-I]=0.054 M, [⁻CH₂C(O)t-Bu]=0.26 M,
[(EtO)₂PO⁻]=0.26 M.

Table 21. continued

time (min.)	% yield			[<u>25+26</u>]/ <u>24</u>
	<u>25</u>	<u>26</u>	<u>24</u>	
35	63.6	1.5	11.2	5.8
40	62.4	1.3	8.3	7.7
45	66.2	1.4	7.0	9.7

Table 22. Initial relative rates for the pinacolone enolate/diethyl phosphite ion pair with iodobenzene

exp	d <u>25</u> /dt	d <u>24</u> /dt	[E ⁻]	[P ⁻]	k _e /k _p
A	4.2	1.1	0.30	0.28	3.7
B	4.2	1.1	0.26	0.26	3.8
				ave	3.75

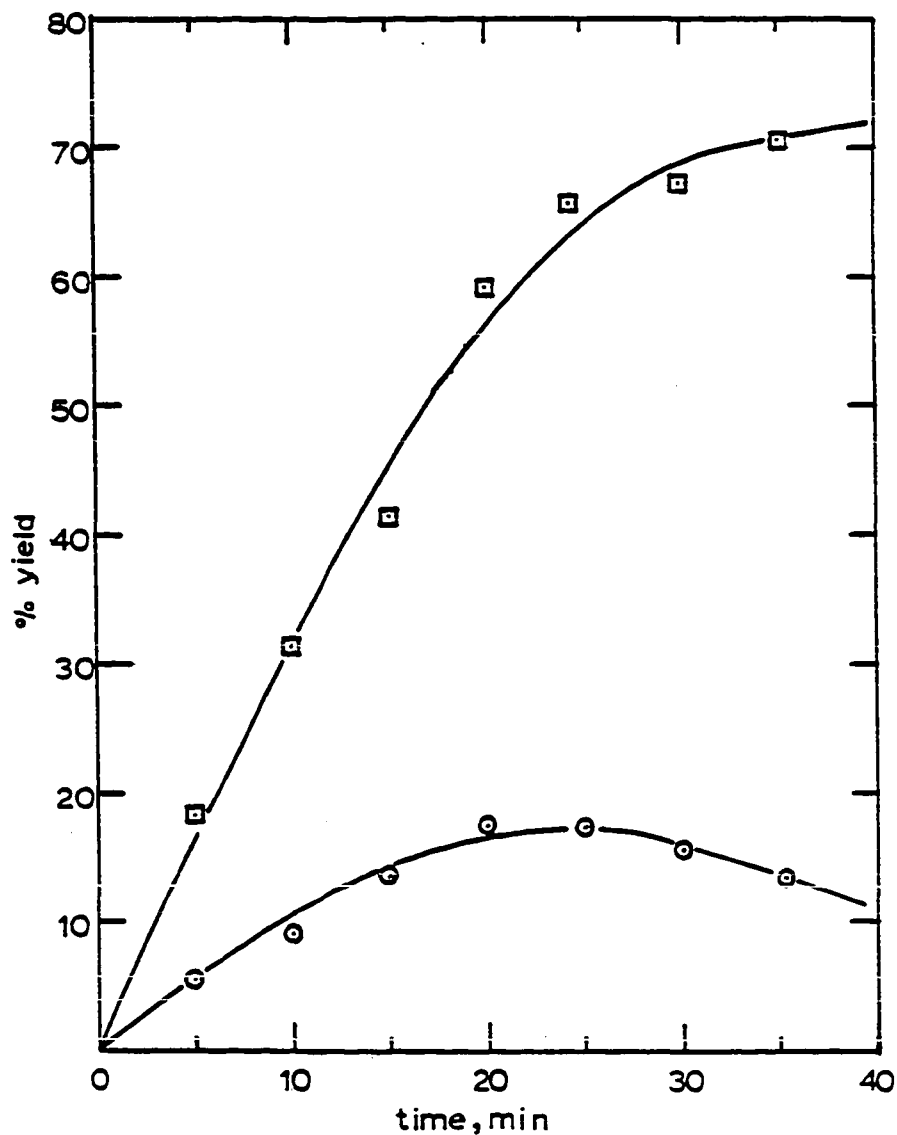


Figure 8. A plot of the yield of diethyl phenylphosphonate (24) (circle) and 1-phenyl-3,3-dimethyl-2-butanone (25) (square) versus time for the reaction of pinacolone enolate/diethyl phosphite ion with iodobenzene (experiment A, Table 21)

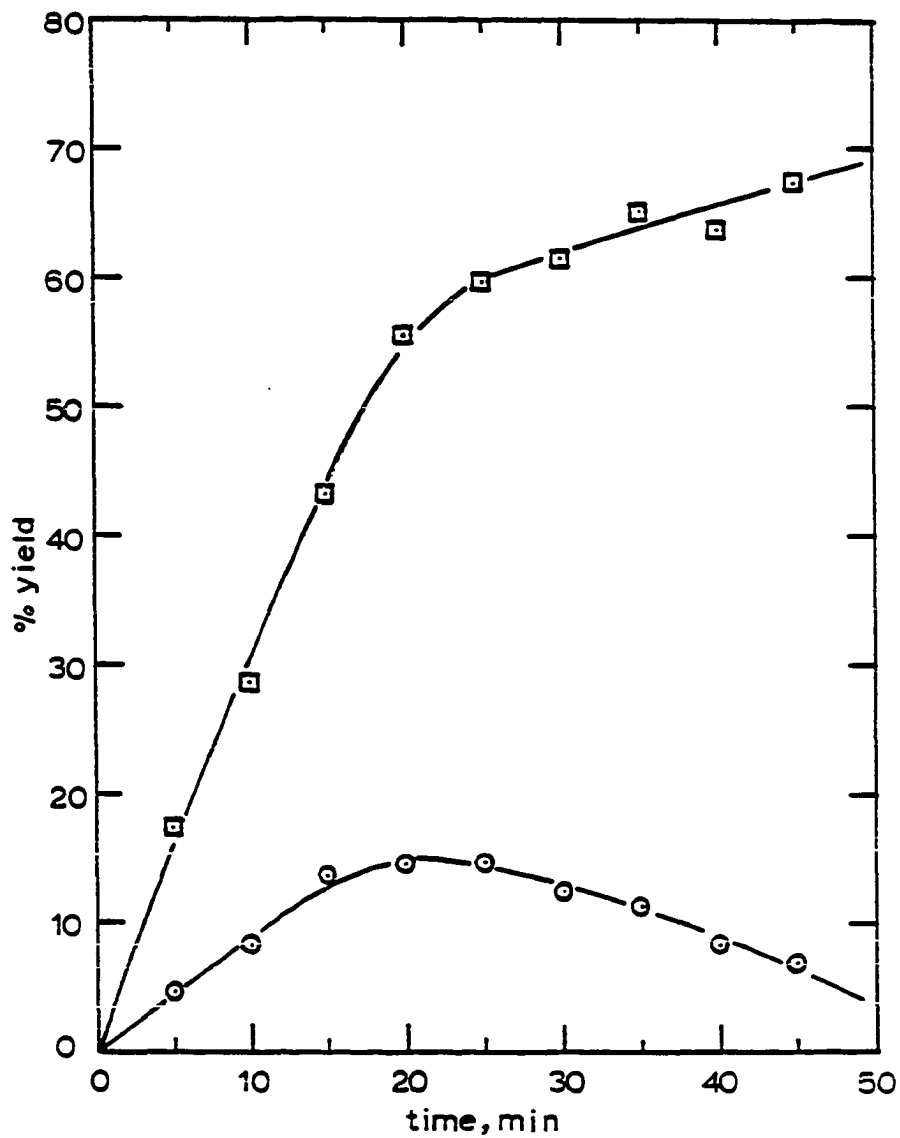


Figure 9. A plot of the yield of diethyl phenylphosphonate (24) (circle) and 1-phenyl-3,3-dimethyl-2-butanone (25) (square) versus time for the reaction of pinacolone enolate/diethyl phosphite ion with iodobenzene (experiment B, Table 21)

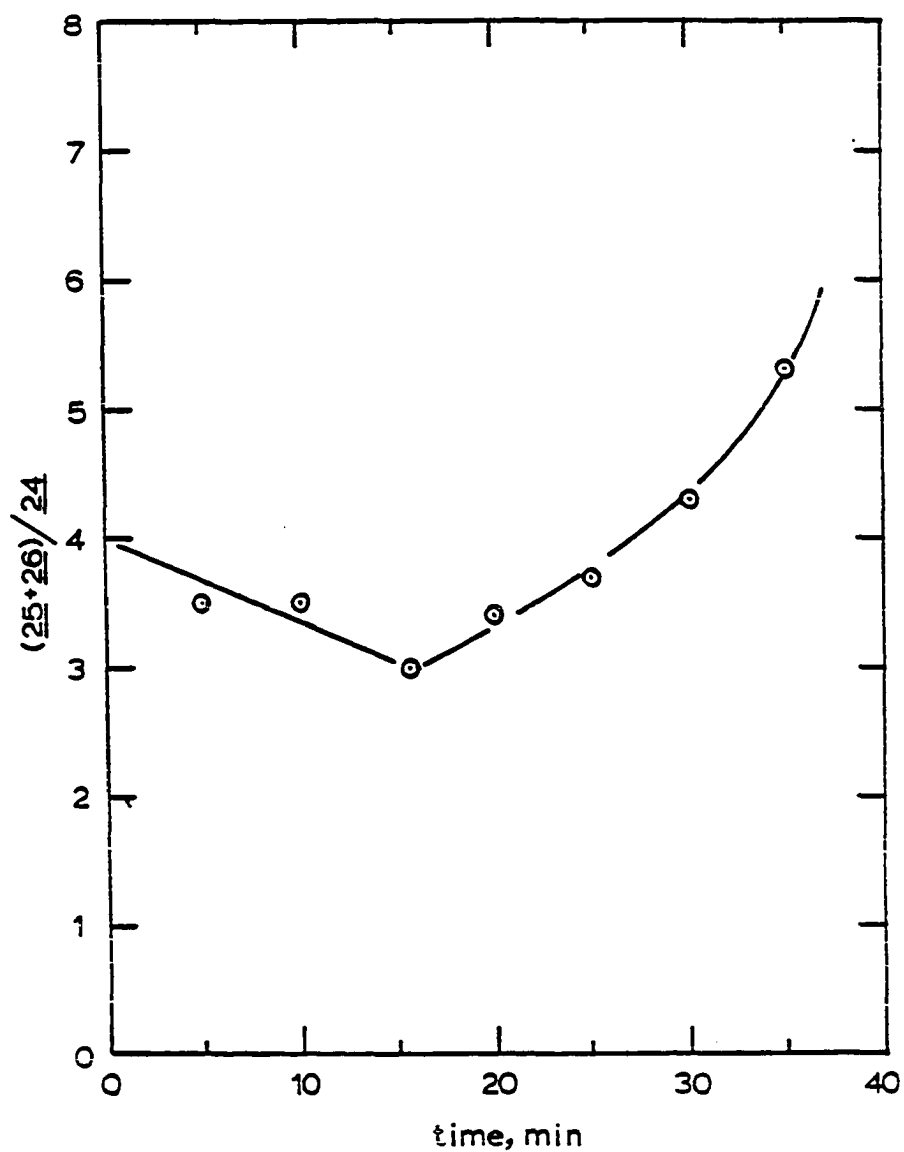


Figure 10. A plot of the yield ratio of 1-phenyl-3,3-dimethyl-2-butanone (25) to diethyl phenylphosphonate (24) versus time for the reaction of pinacolone enolate/diethyl phosphite ion with iodobenzene (experiment A, Table 21)

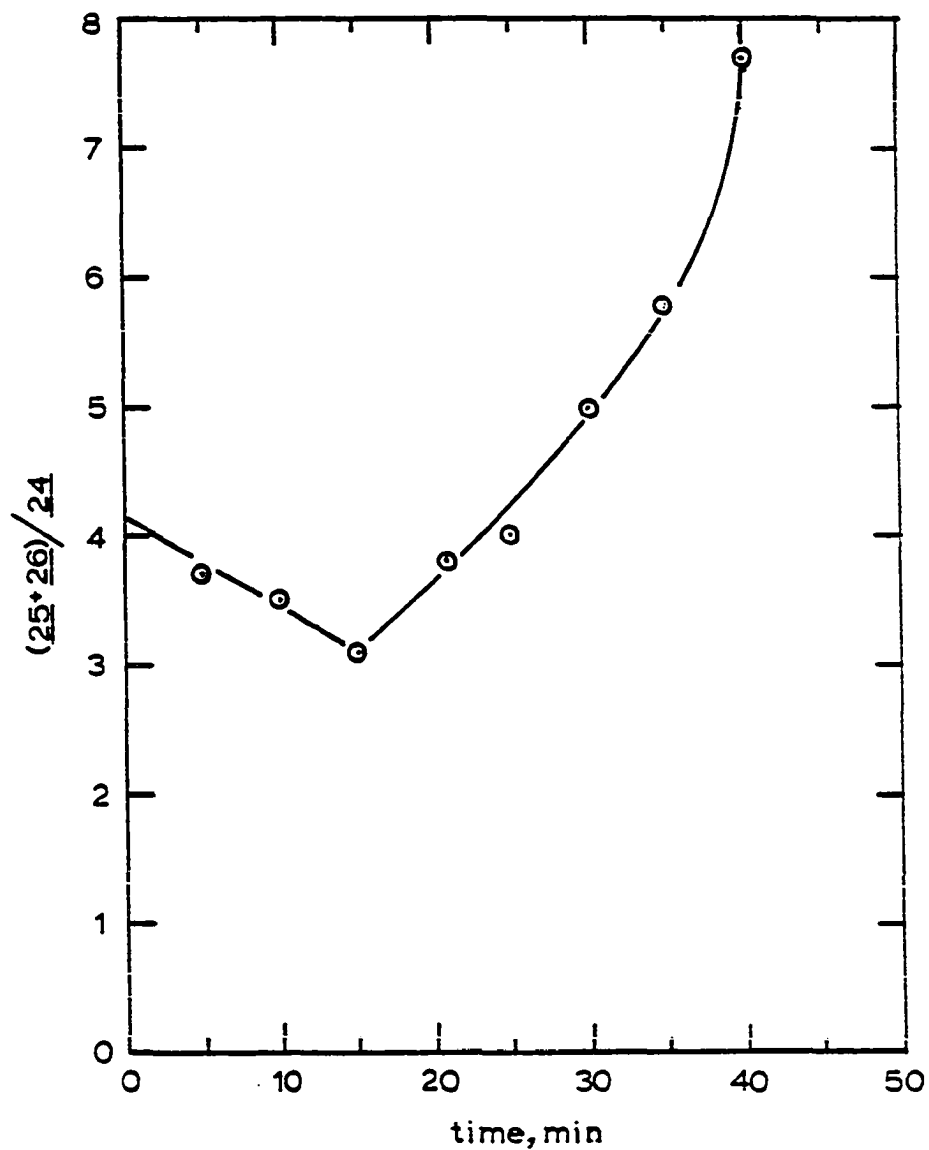


Figure 11. A plot of the yield ratio of 1-phenyl-3,3-dimethyl-2-butanone (25) to diethyl phenylphosphonate (24) versus time for the reaction of pinacolone enolate/diethyl phosphite ion with iodobenzene (experiment B, Table 21)

25 yield at short times. This curvature can be justified when considering the initiation and cage recombination processes discussed earlier. The amount of change is not as pronounced as in the pinacolone enolate/diethyl phosphite pair. A few explanations can be given. One possibility is that thiophenoxide behaves like iodide ion, and destroys the charge transfer complex between the enolate and iodobenzene. Another possibility to consider is that initiation of the reaction by thiophenoxide is faster than with diethyl phosphite ion. Thus, electron transfer and cage recombination by the enolate anion may play a lesser role in this competition reaction.

Pinacolone enolate versus thiophenoxide with phenyl radical



Table 26 summarizes the results from the initial relative rate study for the pinacolone enolate/thiophenoxide pair with phenyl radical generated from PAT. Figures 17 and 18 are yield versus time plots from which the initial relative rates were calculated. The average relative rates for the pinacolone enolate to thiophenoxide is 2.2 toward phenyl radical (Table 27).

Table 23. The yields of 1-phenyl-3,3-dimethyl-2-butanone (25), 1,1-diphenyl-3,3-dimethyl-2-butanone (26), and diethyl phenylphosphonate (24) from the reaction of pinacolone enolate/diethyl phosphite ion in the presence of potassium iodide with iodobenzene as a function of time

time (min.)	% yield			[<u>25</u> + <u>26</u>]/ <u>24</u>
	<u>25</u>	<u>26</u>	<u>24</u>	
5	11.3	0.2	6.3	1.8
10	24.4	0.4	11.0	2.3
15	32.5	0.9	15.0	2.2
20	45.6	1.6	17.9	2.6
25	54.0	1.9	21.5	2.6
30	55.1	1.3	21.2	2.6
35	63.0	1.4	24.1	2.7
40	66.4	1.5	25.7	2.6
45	67.7	2.3	22.2	3.1

^a[Ph-I]=0.054 M, [⁻CH₂C(O)t-Bu]=0.37 M,
[(EtO)₂PO⁻]=0.32 M, [I⁻]=0.10 M.

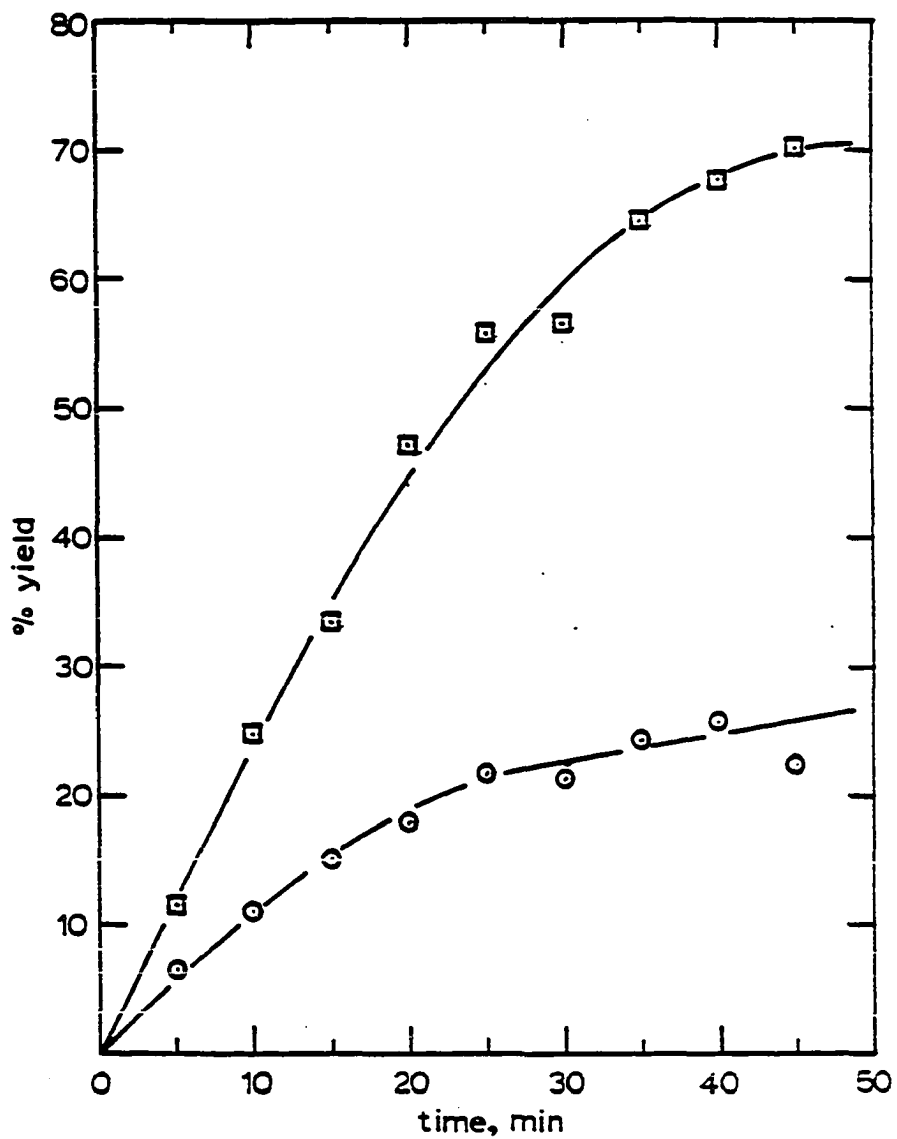


Figure 12. A plot of the yield of 1-phenyl-3,3-dimethyl-2-butanone (25) and diethyl phenylphosphonate (24) versus time for the reaction of pinacolone enolate/diethyl phosphite ion with iodobenzene in the presence of potassium iodide (Table 23)

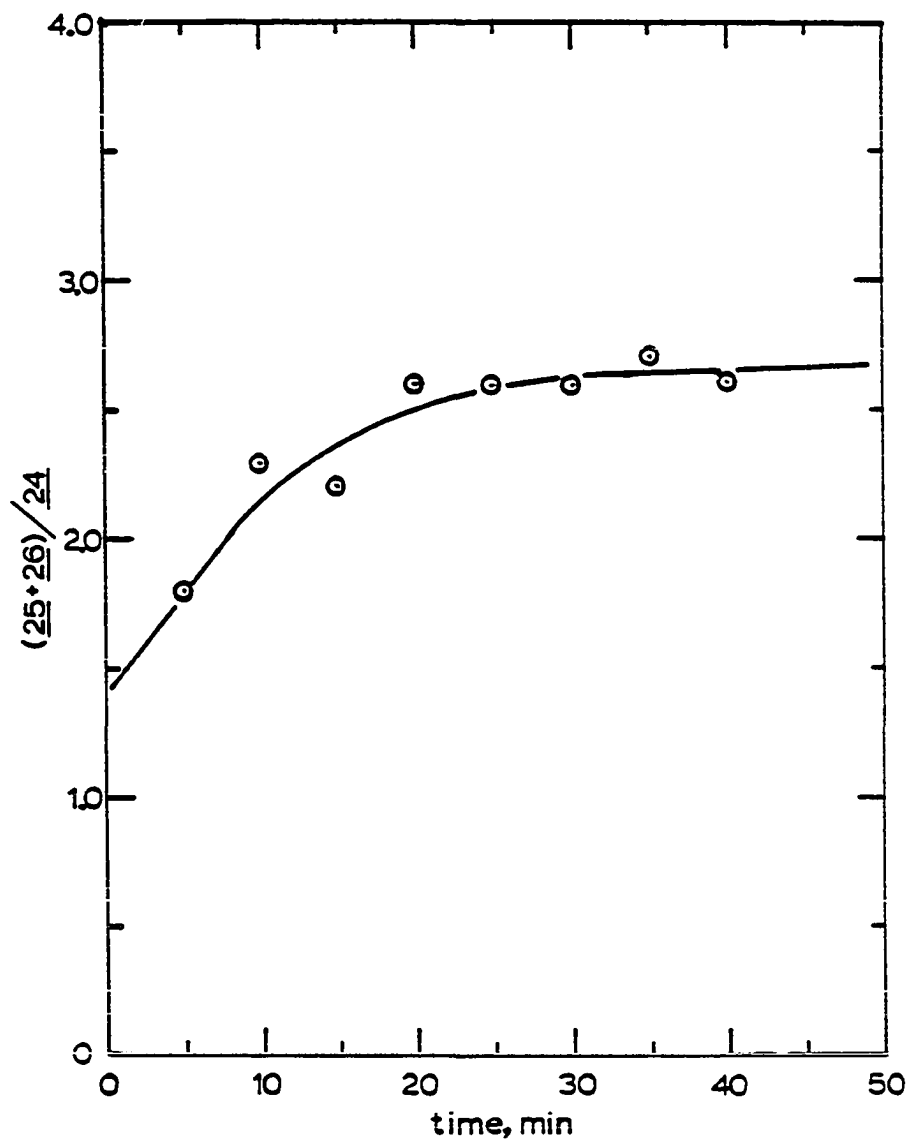


Figure 13. A plot of the yield ratio of 1-phenyl-3,3-dimethyl-2-butanone (25) to diethyl phenylphosphonate (24) versus time for the reaction of pinacolone enolate/diethyl phosphite ion with iodobenzene in the presence of potassium iodide (Table 23)

Table 24. The yields of 1-phenyl-3,3-dimethyl-2-butanone (25), 1,1-diphenyl-3,3-dimethyl-2-butanone (26), and diphenyl sulfide (29) from the reaction of pinacolone enolate/thiophenoxide with iodobenzene

time (min.)	% yield			[25+26]/29
	25	26	29	
exp A ^a				
5	5.2	0.6	4.5	1.3
10	10.2	0.6	11.7	0.98
15	14.0	0.7	15.7	0.94
20	16.5	1.1	18.4	0.96
25	20.2	1.2	23.9	0.90
30	19.6	1.1	21.4	0.97
35	25.9	2.2	29.1	0.97
40	23.9	2.3	31.2	0.84
45	25.6	2.1	30.7	0.90
50	27.0	2.3	32.9	0.89
55	27.8	2.1	34.2	0.87
60	25.4	2.3	32.7	0.85
65	26.8	1.9	33.0	0.87
70	29.3	2.8	35.2	0.91

^a[Ph-I]=0.17 M, [⁻CH₂CotBu]=0.29 M, [PhS⁻]=0.27 M.

Table 24. continued

time (min.)	% yield			[<u>25+26</u>]/ <u>29</u>
	<u>25</u>	<u>26</u>	<u>29</u>	
exp B ^b				
10	14.0	0.7	12.8	1.2
20	20.8	1.7	19.4	1.2
30	28.0	2.0	26.7	1.1
40	32.9	2.4	29.8	1.2
50	32.2	2.4	29.8	1.2
60	40.3	3.2	37.9	1.2
70	43.0	3.6	38.5	1.2
80	40.0	3.2	35.8	1.2
90	44.7	3.6	41.6	1.2

^b[Ph-I]=0.16 M, [⁻CH₂COtBu]=0.30 M,
[PhS⁻]=0.32 M.

Table 25. Initial relative rates for the pinacolone enolate/diethyl phosphite ion pair with iodobenzene

exp	d <u>25</u> /dt	d <u>29</u> /dt	[E ⁻]	[S ⁻]	k _e /k _s
A	3.00	1.35	0.30	0.32	2.68
B	3.50	1.20	0.29	0.27	3.52
				ave	3.10

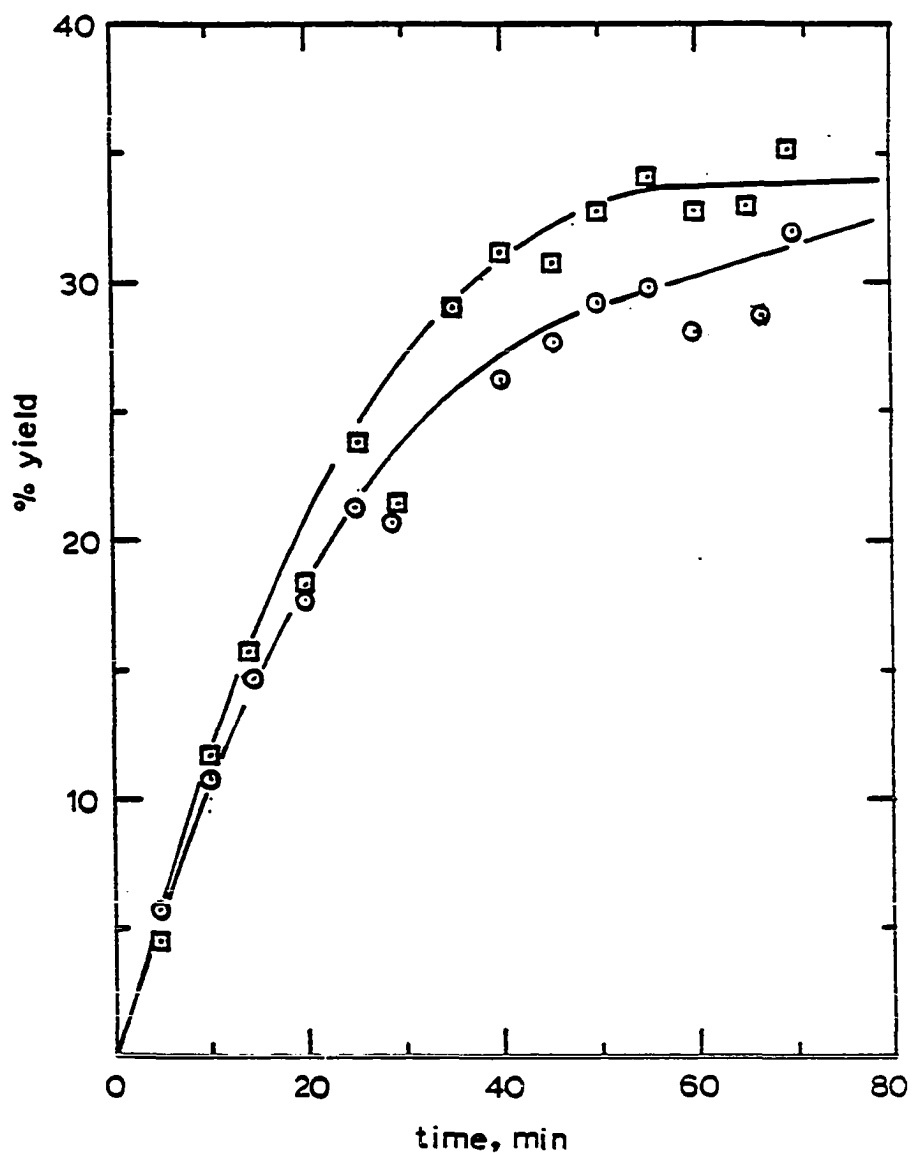


Figure 14. A plot of the yield of 1-phenyl-3,3-dimethyl-2-butanone (25) (circle) and diphenyl sulfide (29) versus time for the reaction of pinacolone enolate/thiophenoxide with iodo-benzene (experiment A, Table 24)

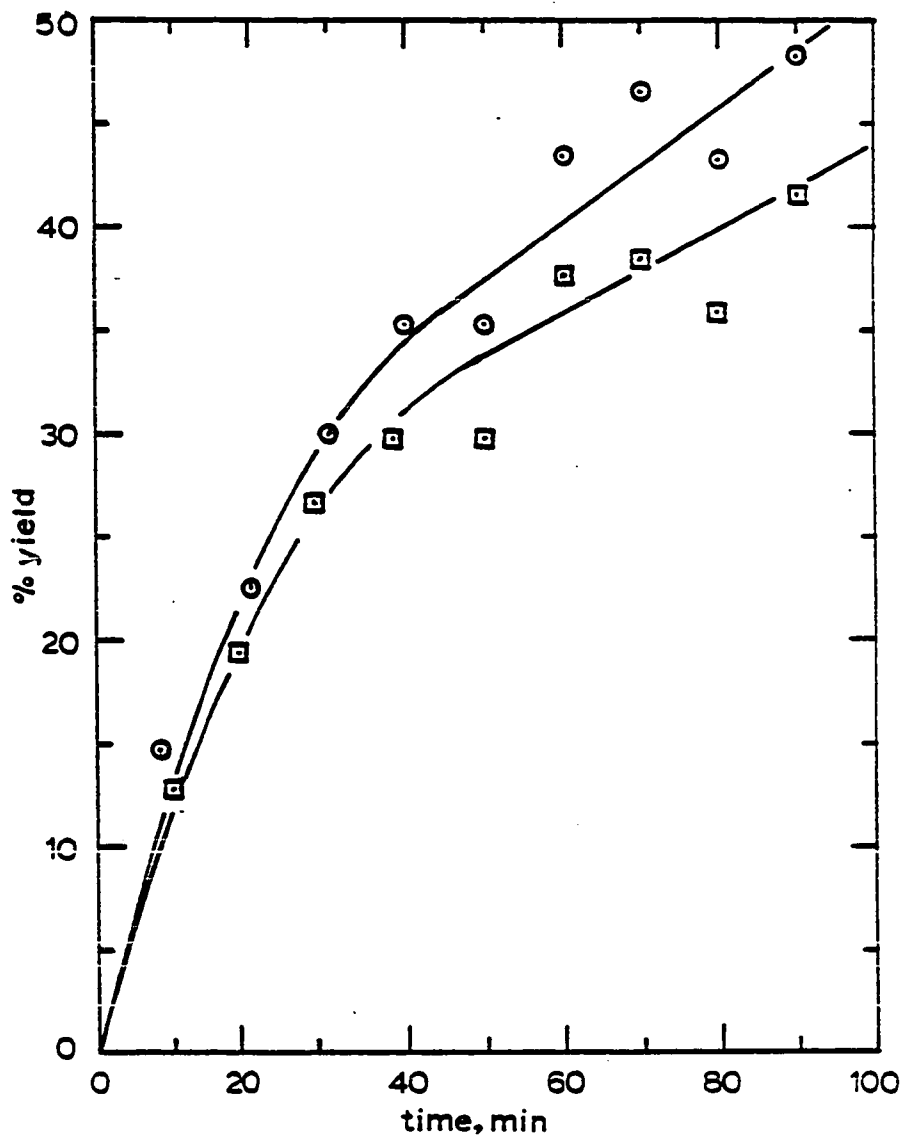


Figure 15. A plot of the yield of 1-phenyl-3,3-dimethyl-2-butanone (25) (circle) and diphenyl sulfide (29) (square) versus time for the reaction of pinacolone enolate/thiophenoxide with iodobenzene (experiment B, Table 24)

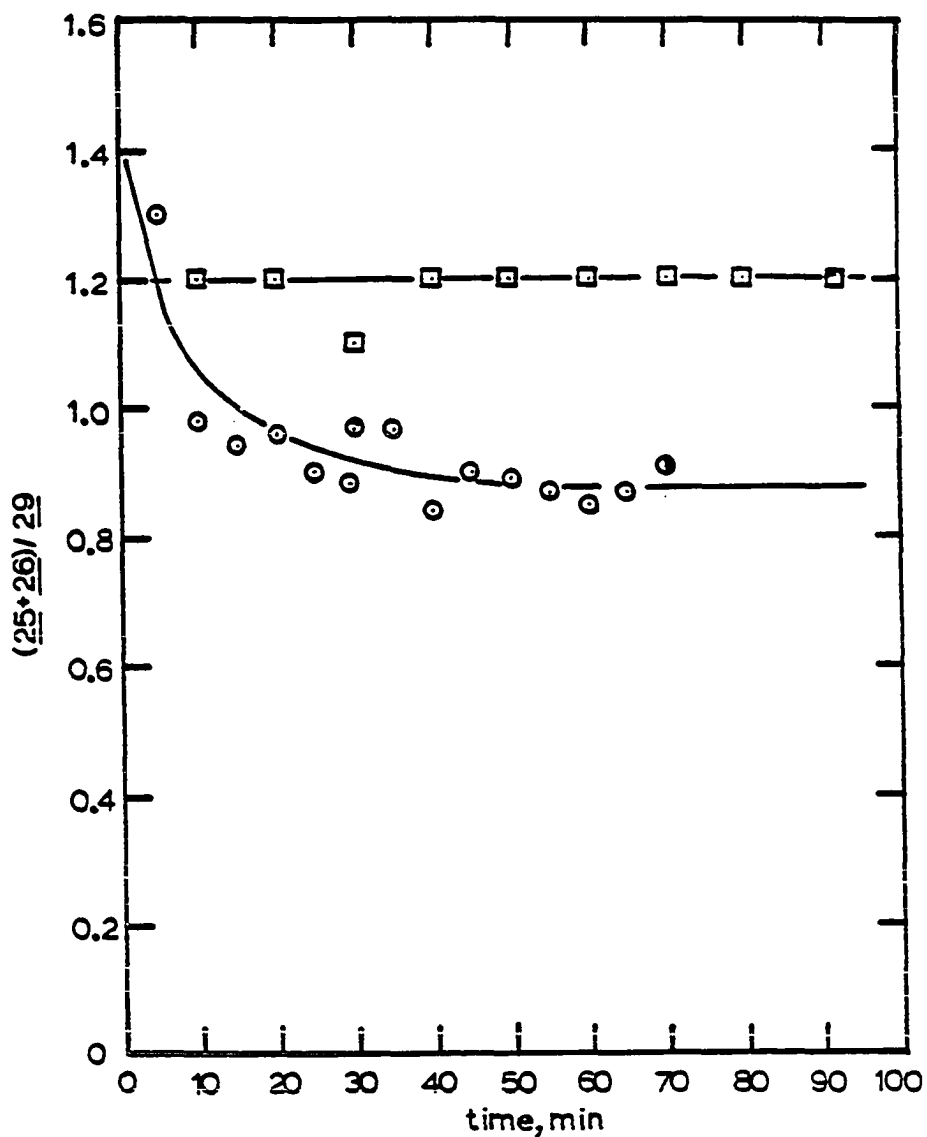


Figure 16. A plot of the ratio of yields of 1-phenyl-3,3-dimethyl-2-butanone (25) to diphenyl sulfide (29) versus time for the reaction of pinacolone enolate/thiophenoxide with iodobenzene (experiments A (circle) and B (square), Table 24)

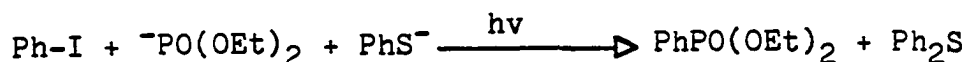
Diethyl phosphite ion versus thiophenoxide with iodobenzene

Table 28 summarizes the results for the initial relative rates for the diethyl phosphite, thiophenoxide pair with iodobenzene. Figures 19 and 20 are the plots for the yield versus time from which the relative rates were calculated. The average initial relative rate value for this pair was 1.9 (Table 29).

A few observations should be noted. First, the overall yield for the reaction decreases when the amount of iodobenzene increases. Second, the products decompose faster when less iodobenzene is used.

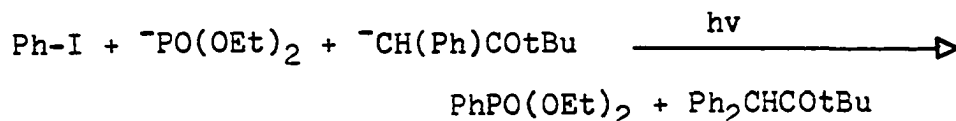
Diethyl phosphite ion versus 1-phenyl-3,3-dimethyl-2-butanone enolate with iodobenzene

Table 30 summarizes the results for the initial relative rate of diethyl phosphite ion/ 1-phenyl-3,3-dimethyl-2-butanone enolate pair with iodobenzene under photostimulation with U.V. irradiation. Figures 21 and 22 are the yield versus time plots from which the initial relative rates were calculated. The initial relative rates are measured for Figures 21 and 22 are 1.1 and 3.8 respectively

Table 26. The yields of 1-phenyl-3,3-dimethyl-2-butanone (25), 1,1-diphenyl-3,3-dimethyl-2-butanone (26), and diphenyl sulfide (29) from the reaction of pinacolone enolate/thiophenoxide with phenyl radical generated from the thermolysis of PAT

time (min.)	% yield		
	<u>25</u>	<u>26</u>	<u>29</u>
exp A ^a			
60	16.7	-	8.5
120	25.9	-	12.5
180	34.6	-	15.3
240	35.9	-	19.8
300	39.2	-	22.0
exp B ^b			
60	14.8	-	6.5
120	26.8	-	11.1
180	30.8	-	12.5
240	35.1	-	16.0
300	40.4	-	15.4
420	50.8	-	26.5

^a[PAT]=0.058 M, [⁻CH₂COt-Bu]=0.27 M, [PhS⁻]=0.26 M.

^b[PAT]=0.058 M, [⁻CH₂COt-Bu]=0.29 M, [PhS⁻]=0.25 M.

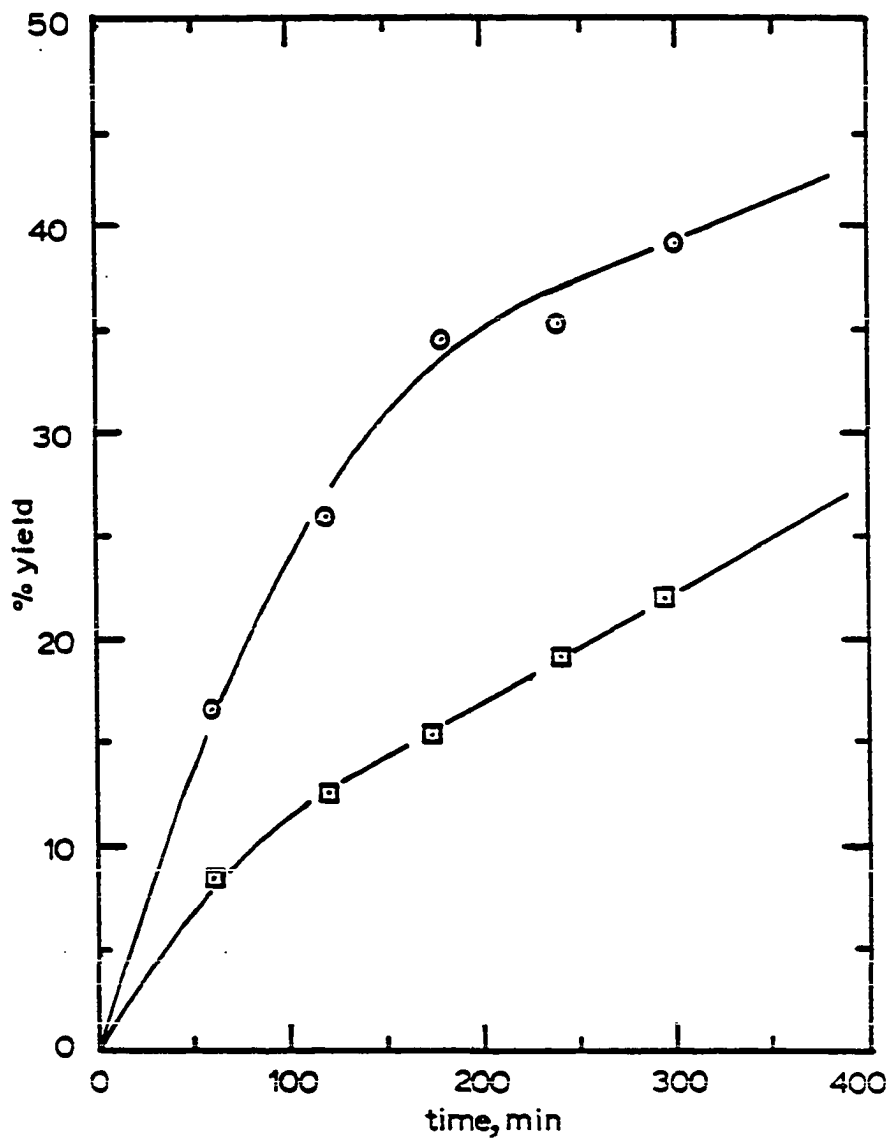


Figure 17. A plot of the yield of 1-phenyl-3,3-dimethyl-2-butanone (25) (circle) and diphenyl sulfide (29) (square) versus time for the reaction of pinacolone enolate/thiophenoxide with phenyl radical (experiment A, Table 26)

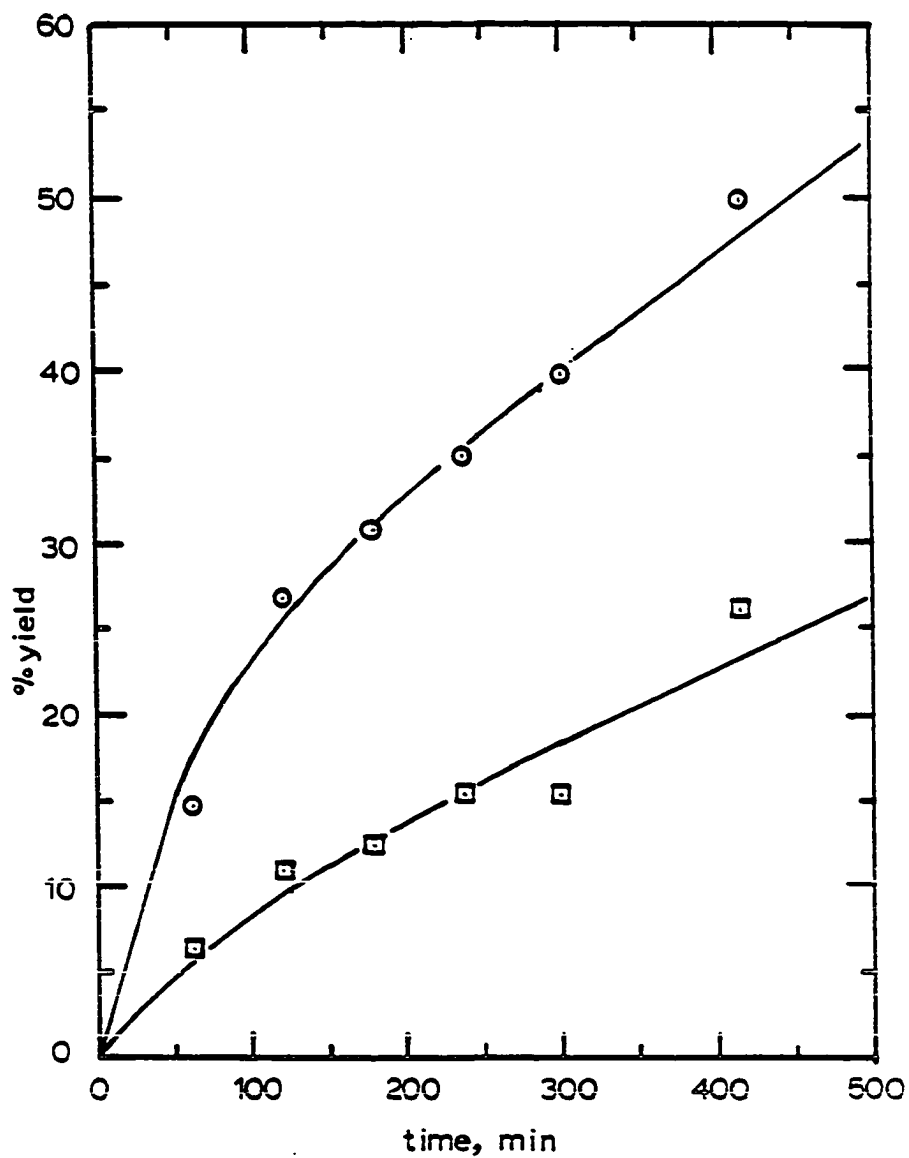


Figure 18. A plot of the yield of 1-phenyl-3,3-dimethyl-2-butanone (25) (circle) and diphenyl sulfide (29) (square) versus time for the reaction of pinacolone enolate/thiophenoxide with phenyl radical (experiment B, Table 26)

Table 27. Initial relative rates for the pinacolone enolate/thiophenoxide pair with phenyl radical generated from the thermolysis of PAT

exp	$\frac{d25}{dt}$	$\frac{d29}{dt}$	$[E^-]$	$[S^-]$	k_e/k_p
A	0.33	0.18	0.27	0.26	1.81
B	0.30	0.10	0.29	0.25	2.65
				ave	2.23

Table 28. The yields of diethyl phenylphosphonate (24) and diphenyl sulfide (29) from the reaction of diethyl phosphite ion/thiophenoxide with iodobenzene as a function of time

time (min.)	% yield		
	<u>24</u>	<u>29</u>	<u>24/29</u>
exp A ^a			
5	11.2	8.2	1.4
10	16.7	12.0	1.4
15	24.2	17.8	1.4
20	28.8	21.5	1.3
25	32.7	25.1	1.3
30	32.5	24.5	1.3
40	32.5	26.1	1.2
45	32.8	25.6	1.3
exp B ^b			
5	16.6	9.3	1.8
10	31.7	16.7	1.9
15	41.6	19.2	2.2
20	58.5	26.1	2.2
25	60.8	23.9	2.5

^a[Ph-I]=0.054 M, [PhS⁻]=0.34 M, [(EtO)₂PO⁻]=0.32 M.

^b[Ph-I]=0.16 M, [PhS⁻]=0.33 M, [(EtO)₂PO⁻]=0.30 M.

Table 28. continued

time (min.)	% yield		
	<u>24</u>	<u>29</u>	<u>24/29</u>
30	62.0	23.0	2.7
35	54.6	17.9	3.1
40	57.1	14.5	3.9

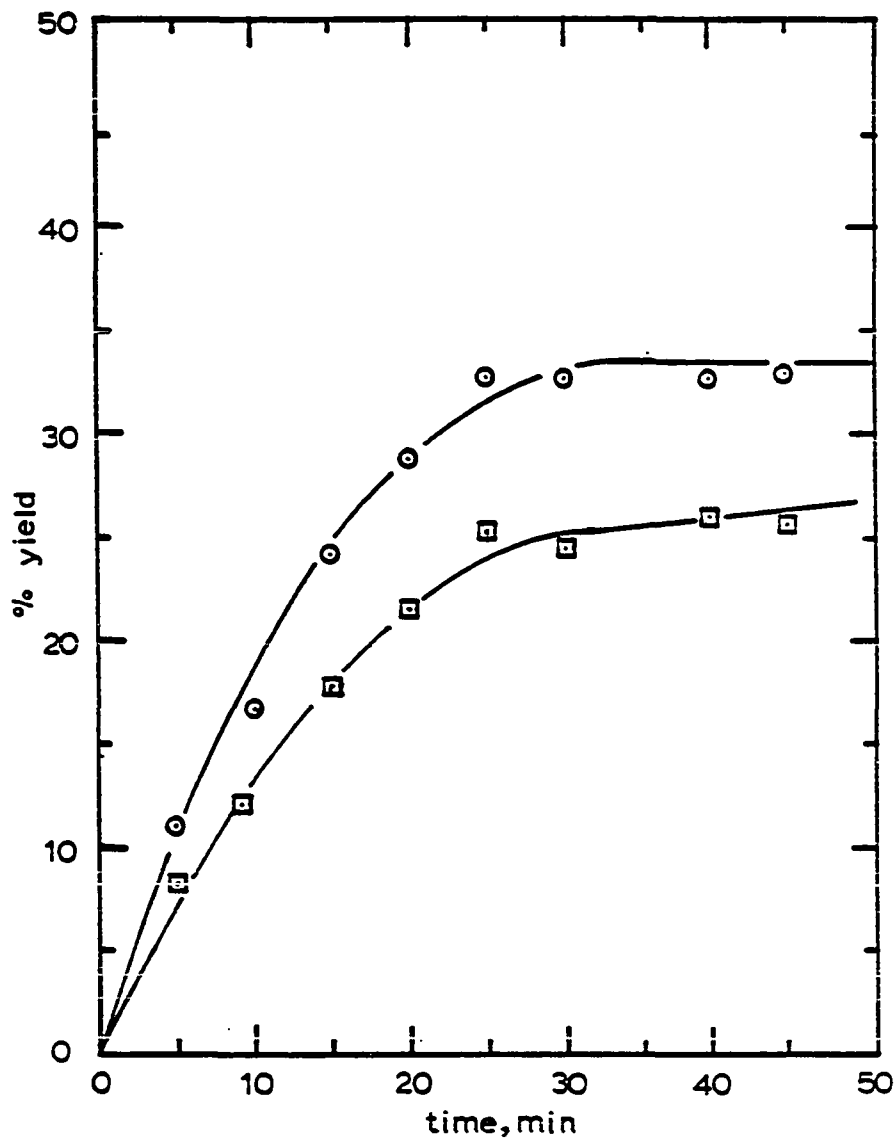


Figure 19. A plot of the yield of diethyl phenylphosphonate (24) (circle) and diphenyl sulfide (29) (square) versus time for the reaction of diethyl phosphite ion/thiophenoxide with iodobenzene (experiment A, Table 28)

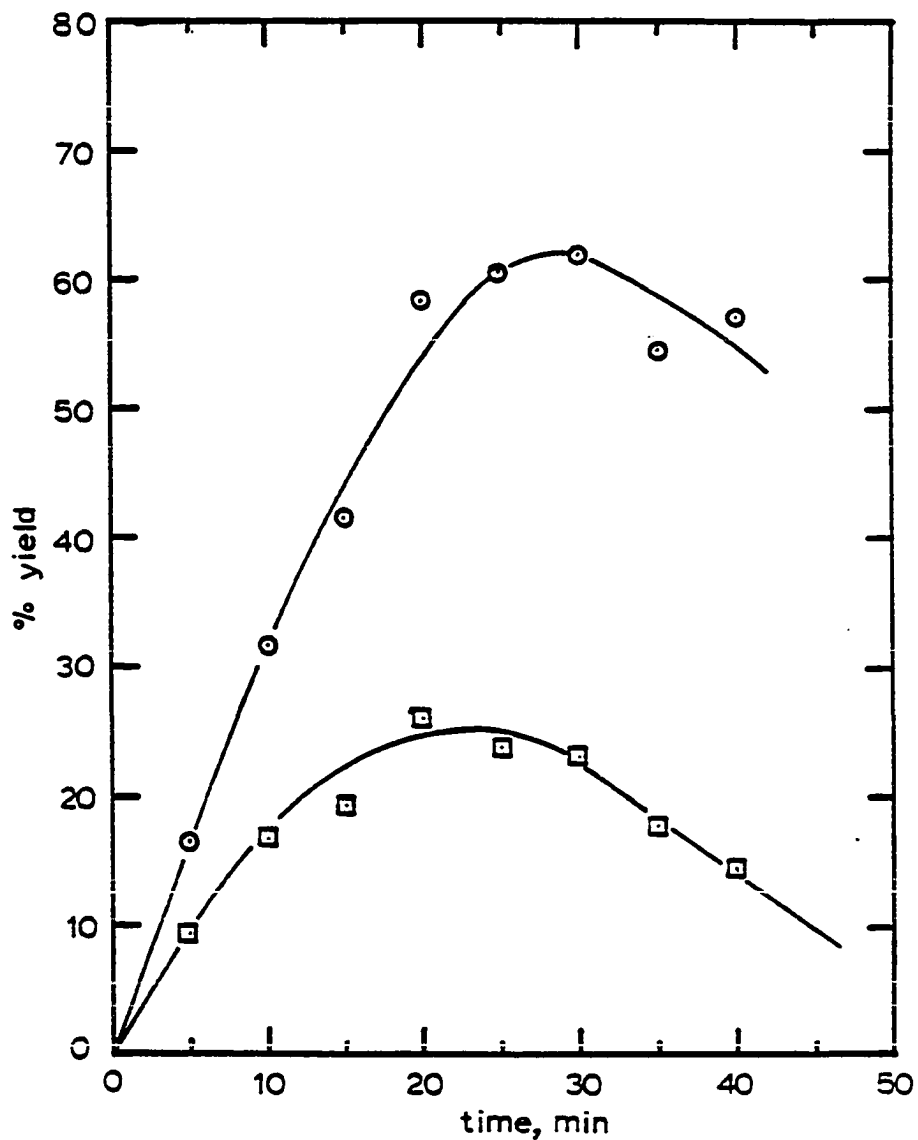


Figure 20. A plot of the yield of diethyl phenylphosphonate (24) (circle) and diphenyl sulfide (29) (square) versus time for the reaction of diethyl phosphite ion/thiophenoxide with iodobenzene (experiment B, Table 28)

Table 29. Initial relative rates for the diethyl phosphite ion/thiophenoxide pair with iodobenzene

exp	$\frac{d_{24}}{dt}$	$\frac{d_{29}}{dt}$	$[(EtO)_2PO^-]$	$[PhS^-]$	k_p/k_s
A	3.5	1.9	0.32	0.34	1.9
B	2.9	1.7	0.30	0.33	1.9
				ave	1.9

(Table 31). The large differences in the relative rates can be contributed to the initiation process of the reaction. Consider Figure 23, the experiment that gave an initial relative rate of 1.1 has only a slight curvature at small times. The experiment that gave a value of 3.8 for the initial relative rate exhibits a large curvature at small times indicating an alternative mode of formation of 25 other than radical-nucleophile coupling (Figure 23). Both reactions were performed under identical conditions. The only explanation is that a small amount of oxygen was present in the reaction that resulted in an initial rate of 3.8. The oxygen would inhibit the free radical chain reaction and would allow the cage recombination process to dominate.

Thiophenoxide versus 1-phenyl-3,3-dimethyl-2-butanone enolate with iodobenzene

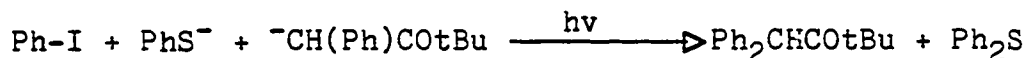


Table 32 summarizes the initial rate results for the thiophenoxide/1-phenyl-3,3-dimethyl-2-butanone enolate pair with iodobenzene. Figures 24 and 25 are the yield versus time plots from which the initial relative rates were calculated. The average initial relative rate of the enolate to thiophenoxide is 0.40 (Table 33).

Figure 26 is the ratio of 26/29 versus time plot for

both experiments. A slight upward curvature at small times indicates formation of 26 by the initiation process discussed earlier.

Diethyl phosphite ion/pinacolone enolate/thiophenoxide with iodobenzene

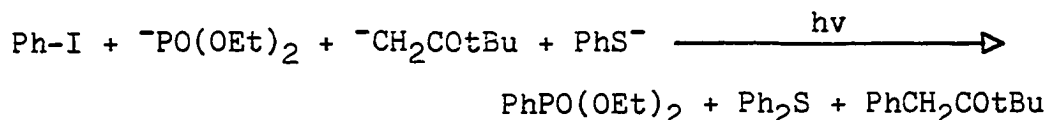


Table 34 summarizes the initial relative rate results for the diethyl phosphite ion/pinacolone enolate/thiophenoxide group with iodobenzene. Figures 27 and 28 are the yield versus time plots from which the relative rates were calculated. The average values for the initial rates are summarized in Table 35.

The k_p/k_s ratio is lower than the independently measured initial relative rates. As presented earlier, diethyl phenylphosphonate decomposes under basic conditions. The decomposition of diethyl phenylphosphonate would result in a lower k_p/k_e ratio. The k_e/k_s ratio would also be effected, resulting in a larger value.

A possible reason for the disagreement between the initial rates is the reaction conditions for the experiment competing three nucleophiles versus each other. As pointed out earlier, diethyl phenylphosphonate is decomposed

Table 30. The yields of diethyl phenylphosphonate (24) and 1,1-diphenyl-3,3-dimethyl-2-butanone (26) from the reaction of diethyl phosphite ion/1-phenyl-3,3-dimethyl-2-butanone enolate with iodobenzene as a function of time

time (min.)	% yield		
	<u>24</u>	<u>26</u>	<u>24/26</u>
exp A ^a			
15	0.7	4.7	6.5
30	4.0	7.7	1.9
45	5.4	10.8	2.0
60	6.0	12.9	2.15
75	4.9	14.0	2.9
90	4.6	14.8	3.2
105	4.3	17.3	4.0
120	3.4	18.2	5.4
exp B ^b			
15	4.4	3.3	.77
30	11.4	6.5	.56
45	11.7	8.4	.71
60	12.3	10.1	.83
75	10.0	11.4	1.13

^a[Ph-I]=0.054 M, [(EtO)₂PO⁻]=0.29 M,
[⁻CH(Ph)COt-Bu]=0.26 M.

^b[Ph-I]=0.054 M, [(EtO)₂PO⁻]=0.33 M,
[⁻CH(Ph)COt-Bu]=0.23 M.

Table 30. continued

time (min.)	% yield		
	<u>24</u>	<u>26</u>	<u>24/26</u>
90	9.5	12.8	0.74
105	7.8	13.9	0.56
120	5.6	11.4	0.49

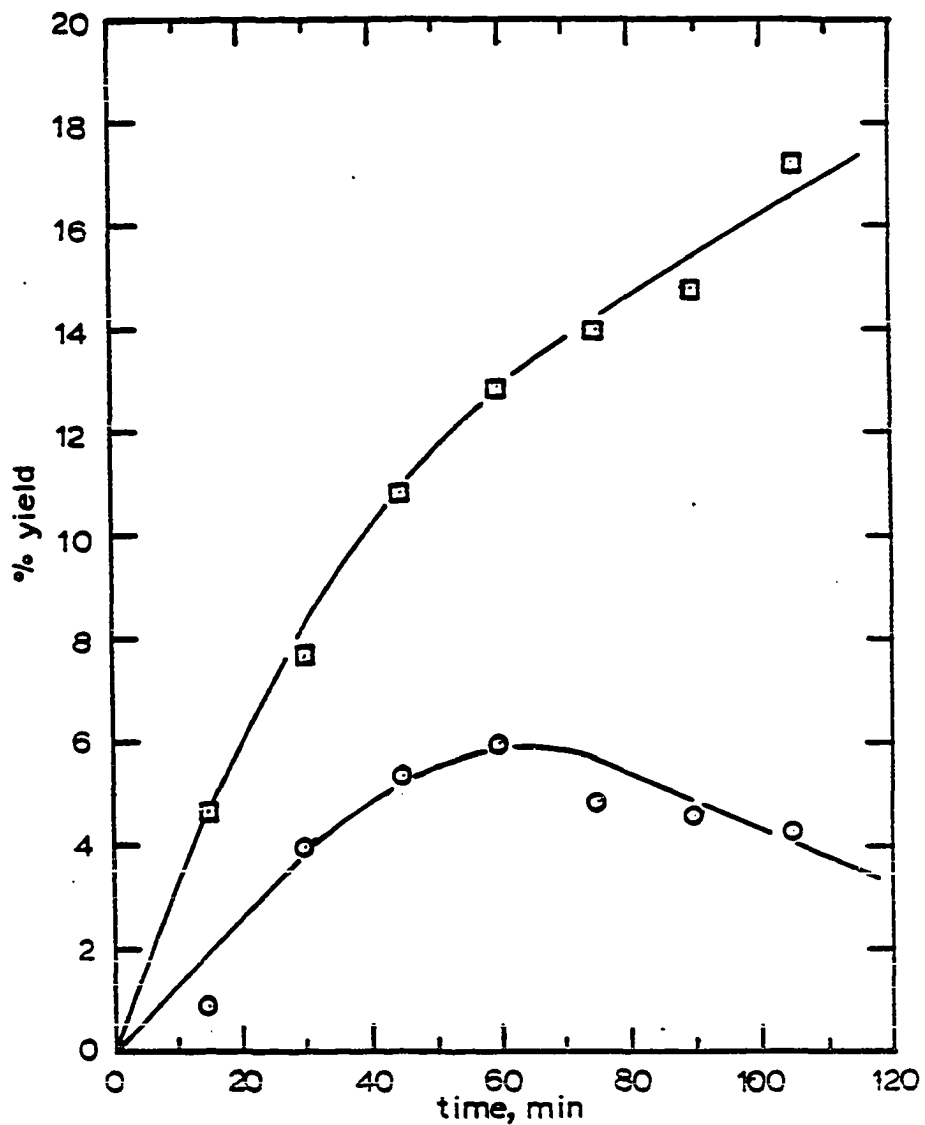


Figure 21. A plot of the yield of diethyl phenylphosphonate (24) (circle) and 1,1-diphenyl-3,3-dimethyl-2-butanone (26) (square) versus time for the reaction of diethyl phosphite ion/1-phenyl-3,3-dimethyl-2-butanone enolate with iodobenzene (experiment A, Table 30)

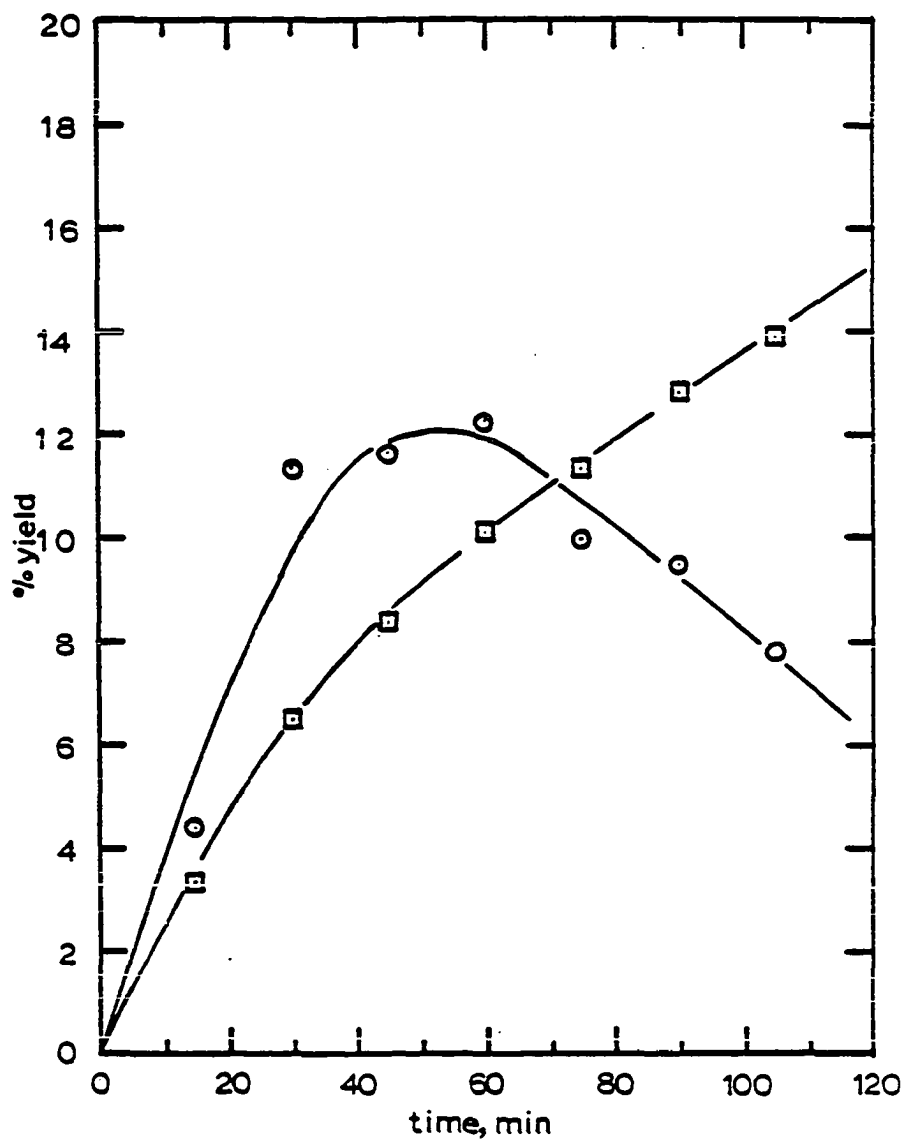


Figure 22. A plot of the yield of diethyl phenylphosphonate (24) (circle) and 1,1-diphenyl-3,3-dimethyl-2-butanone (26) (square) versus time for the reaction of diethyl phosphite ion/1-phenyl-3,3-dimethyl-2-butanone enolate with iodobenzene (experiment B, Table 30)

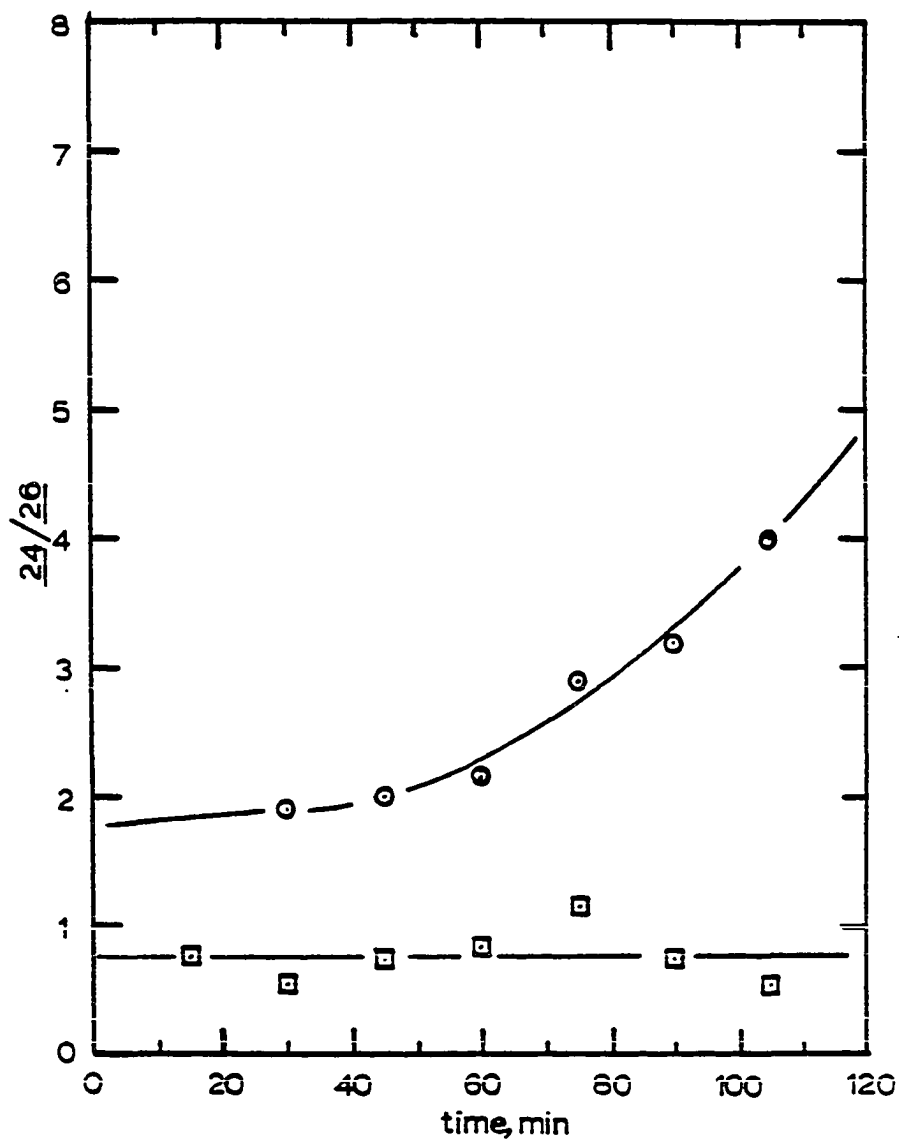


Figure 23. A plot of the ratio of yields of 1,1-diphenyl-3,3-dimethyl-2-butanone (26) to phenyl phosphonate (24) versus time for the reaction of 1-phenyl-3,3-dimethyl-2-butanone enolate/diethyl phosphite ion with iodobenzene (experiments A (circle) and B (square), Table 30)

Table 31. Initial relative rates for the 1-phenyl-3,3-dimethyl-2-butanone enolate/diethyl phosphite ion pair with iodobenzene

exp	d_{26}/dt	d_{24}/dt	$[\text{CH}(\text{Ph})\text{C}(\text{O})\text{t-Bu}]^-$	$[(\text{EtO})_2\text{P}(\text{O})^-]$	k_{e1}/k_p
A	0.25	0.32	0.23	0.33	1.1
B	0.51	0.15	0.15	0.29	3.8

by very basic reaction conditions which could result in unreasonable values for the initial rates. The product formation process from the cage recombination of phenyl radical and α -keto radical may be a minor since the aromatic $S_{RN}1$ reaction can be initiated by all three nucleophiles instead of two.

In this section, the initial relative reactivities for four nucleophiles: diethyl phosphite ion, pinacolone enolate, thiophenoxide, and 1-phenyl-3,3-dimethyl-2-butanone enolate have been presented. The initial reactivities are summarized in Table 36. Evidence has been presented that the initial formation of 1-phenyl-3,3-dimethyl-2-butanone (25) and 1,1-diphenyl-3,3-dimethyl-2-butanone (26) from the reaction of pinacolone enolate with iodobenzene occurs by a process other than radical-nucleophile coupling. The most plausible process is the photolysis of the charge transfer complex between the enolate and iodobenzene. During the early stages of the reaction, the major product formation step appears to be a photochemical electron transfer leading to a cage reaction. However, as time increases, the kinetic chain length increases resulting in formation of the product via the propagation steps of Scheme 4. The formation of iodide ion in the reaction solutions may be involved in the change in mechanism.

Table 32. The yields of diphenyl sulfide (29) and 1,1-diphenyl-3,3-dimethyl-2-butanone (26) from the reaction of thiophenoxide/1-phenyl-3,3-dimethyl-2-butanone enolate with iodobenzene as a function of time

time (min.)	% yield		
	<u>26</u>	<u>29</u>	<u>26/29</u>
exp A ^a			
15	7.1	2.6	0.37
30	13.1	4.6	0.35
45	17.6	6.1	0.35
60	42.8	14.2	0.33
75	46.0	17.0	0.37
90	64.4	24.1	0.37
105	68.7	26.0	0.38
120	64.2	24.0	0.37
exp B ^a			
15	12.3	5.29	0.43
30	26.1	8.8	0.34
45	31.0	10.5	0.34
60	40.9	12.9	0.32
75	73.7	24.0	0.33
90	60.3	21.2	0.35

^a[Ph-I]=0.054 M, [PhS⁻]=0.27 M,
[⁻CH(Ph)Cot-Bu]=0.26 M.

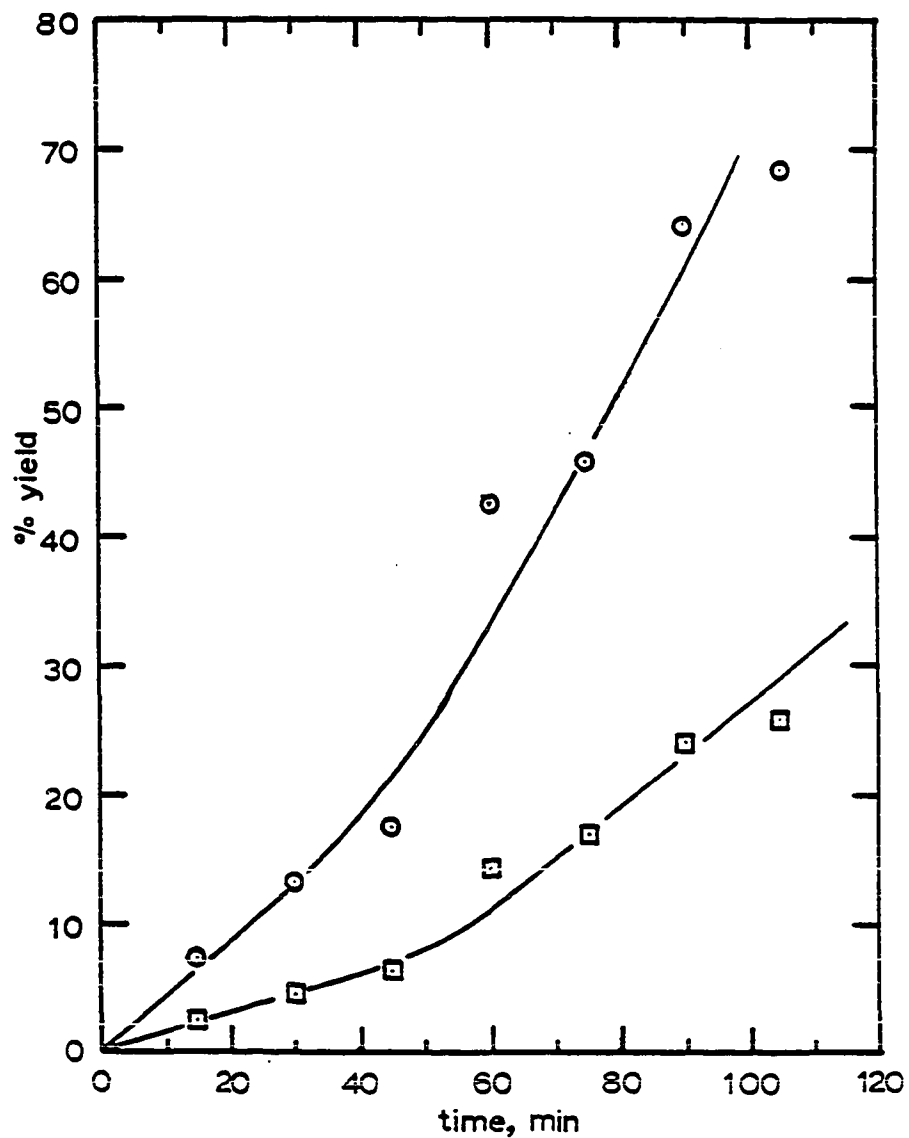


Figure 24. A plot of the yield of 1,1-diphenyl-3,3-dimethyl-2-butanone (26) and diphenyl sulfide (29) versus time for the reaction of 1-phenyl-3,3-dimethyl-2-butanone enolate/thiophenoxide with iodobenzene (experiment A, Table 32)

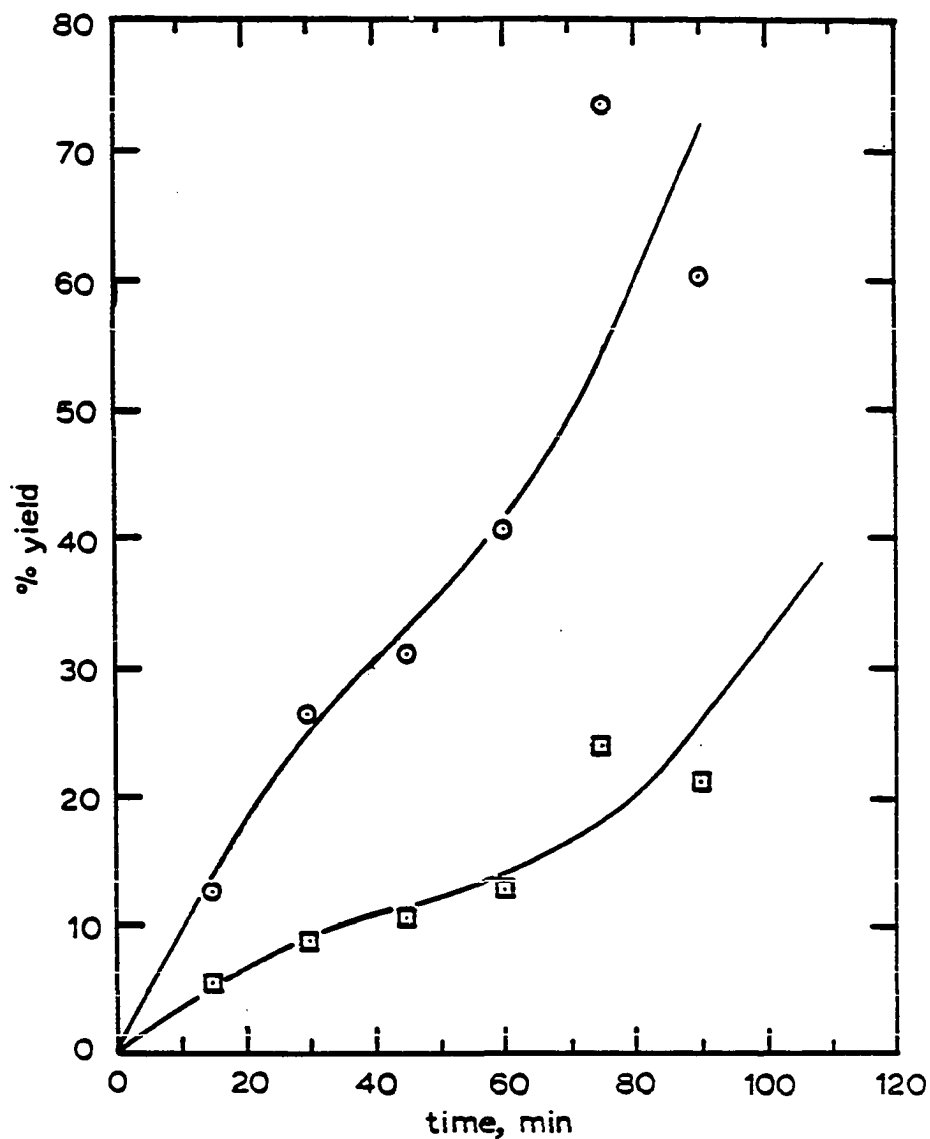


Figure 25. A plot of the yield of 1,1-diphenyl-3,3-dimethyl-2-butanone (26) and diphenyl sulfide (29) versus time for the reaction of 1-phenyl-3,3-dimethyl-2-butanone enolate/thiophenoxide with iodobenzene (experiment B, Table 32)

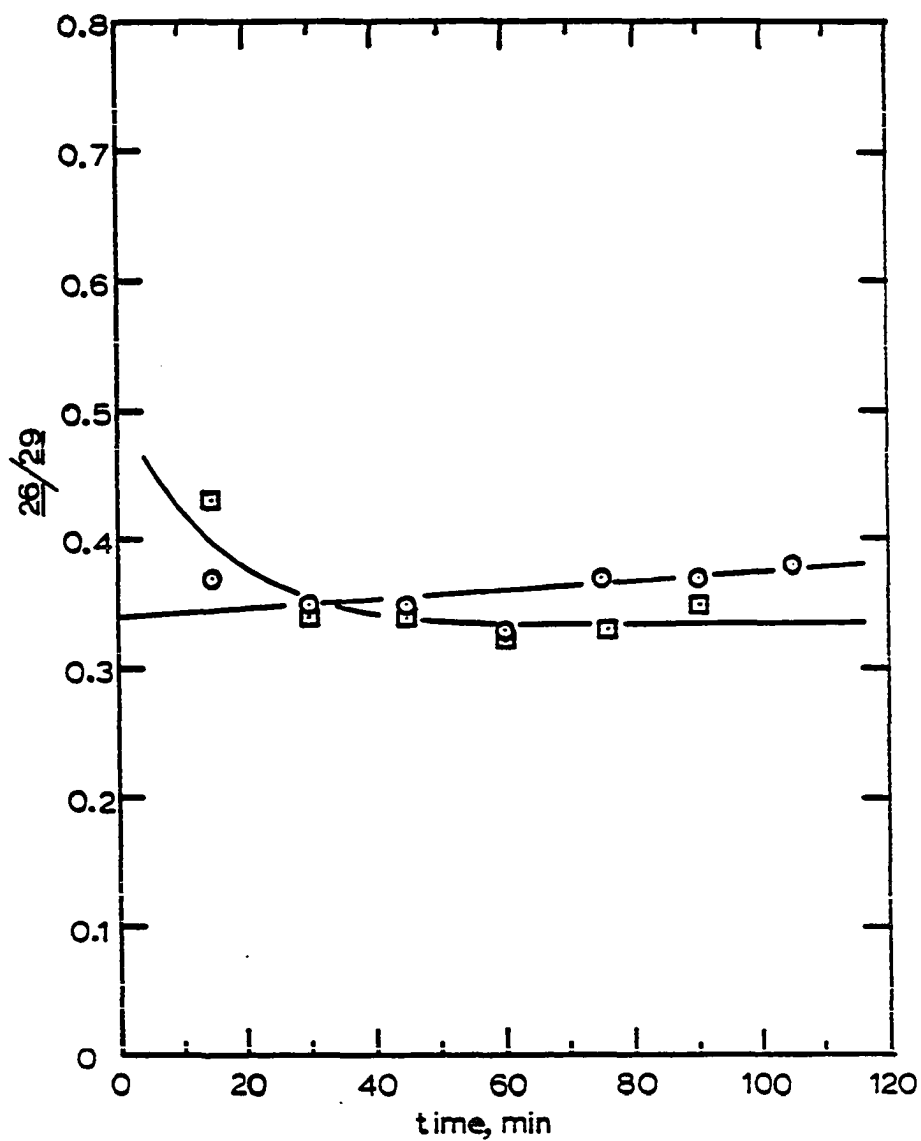


Figure 26. A plot of the yield ratio of 1,1-diphenyl-3,3-dimethyl-2-butanone (26) to diphenyl sulfide (29) for the reaction of 1-phenyl-3,3-dimethyl-2-butanone/thiophenoxide with iodobenzene (experiments A and B, Table 32)

Table 33. Initial relative rates for the thiophenoxide/1-phenyl-3,3-dimethyl-2-butanone enolate pair with iodobenzene

exp	$\frac{d26}{dt}$	$\frac{d29}{dt}$	$[\text{PhS}^-]$	$[\text{}^-\text{CH}(\text{Ph})\text{COT-Bu}]$	k_e/k_s
A	0.43	0.16	0.27	0.26	0.40
B	0.85	0.30	0.27	0.26	0.38
				ave	0.39

Table 34. The yields of 1-phenyl-3,3-dimethyl-2-butanone (25), diethyl phenylphosphonate (24), and diphenyl sulfide (29) from the reaction of pinacolone enolate/diethyl phosphite ion/thiophenoxide with iodobenzene as a function of time

time (min.)	% yield			
	<u>25</u>	<u>26</u>	<u>24</u>	<u>29</u>
exp A ^a				
5	8.4	-	1.3	5.0
10	17.8	0.5	3.4	10.0
15	30.8	1.2	4.4	16.1
20	36.0	1.0	5.1	19.9
25	45.4	2.0	6.4	21.2
30	49.6	2.2	6.5	23.1
35	59.6	2.9	7.1	28.5
40	55.8	1.4	7.1	24.3
45	60.1	2.4	7.5	22.9
exp B ^b				
10	11.7	-	2.4	13.0
15	21.7	1.1	4.0	19.7
20	20.8	1.0	4.5	21.0

^a[Ph-I]=0.054 M, [⁻CH₂COt-Bu]=0.29 M, [(EtO)₂PO⁻]=0.22 M
[PhS⁻]=0.29 M.

^b[Ph-I]=0.054 M, [⁻CH₂COt-Bu]=0.25 M, [(EtO)₂PO⁻]=0.25 M
[PhS⁻]=0.32 M.

Table 34. continued

time (min.)	% yield			
	<u>25</u>	<u>26</u>	<u>24</u>	<u>29</u>
25	35.3	0.7	5.8	28.3
30	33.3	1.4	7.7	24.8
35	40.8	1.7	8.8	28.1
40	36.8	1.7	7.8	24.3
45	40.5	1.7	8.6	27.7

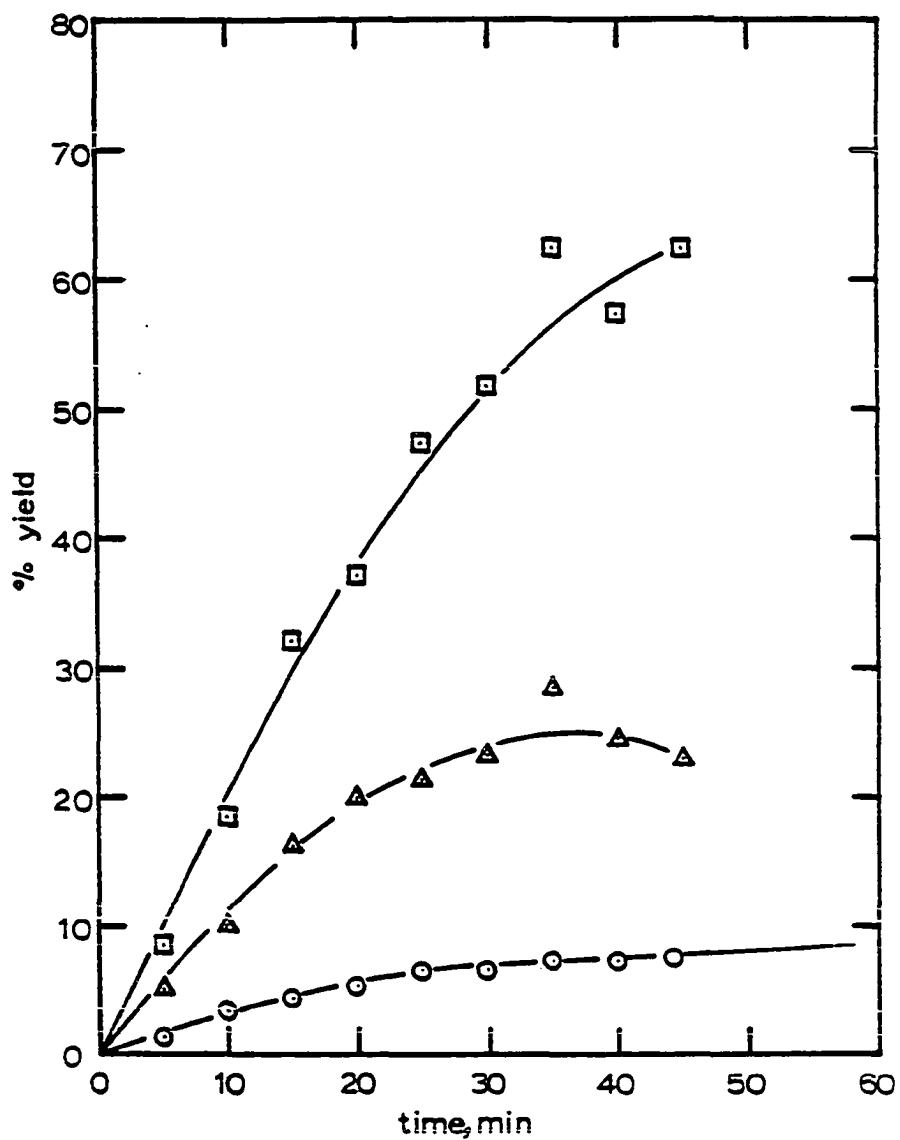


Figure 27. A plot of the yield of diethyl phenylphosphonate (24) (circle), 1-phenyl-3,3-dimethyl-2-butanone (25) (square), and diphenyl sulfide (29) (triangle) versus time for the reaction of diethyl phosphite ion/pinacolone enolate/thiophenoxide with iodobenzene (experiment A, Table 34)

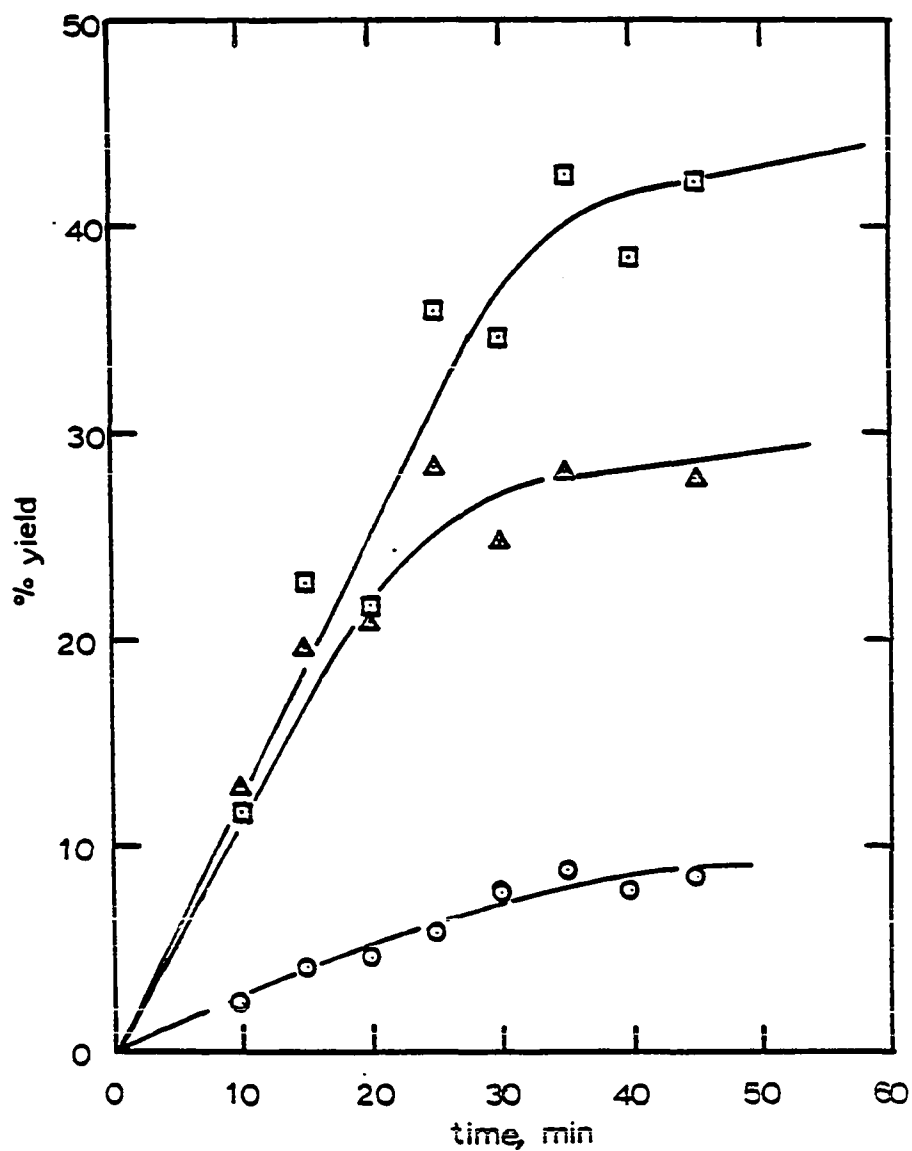


Figure 28. A plot of the yield of diethyl phenylphosphonate (24) (circle), 1-phenyl-3,3-dimethyl-2-butanone (25) (square), and diphenyl sulfide (29) (triangle) versus time for the reaction of diethyl phosphite ion/pinacolone enolate/thiophenoxide with iodobenzene (experiment B, Table 34)

Table 35. Initial relative rates for the pinacolone enolate/diethyl phosphite ion/thiophenoxide group with iodobenzene

exp	d_{25}/dt	d_{24}/dt	d_{29}/dt	$[-CH_2COtBu]$	$[(EtO)_2PO^-]$	$[PhS^-]$	k_e/k_p	k_e/k_s	k_p/k_s
241	1.9	0.3	1.1	0.29	0.22	0.29	3.2	1.7	0.5
242	1.4	0.4	1.4	0.25	0.25	0.32	3.5	1.4	0.4
						ave	3.3	1.5	0.5

Table 36. Initial relative reactivity of nucleophiles in the aromatic $S_{RN}1$ reaction

substrate	A ⁻	B ⁻	k _A /k _B
Ph-I	⁻ CH ₂ CotBu	⁻ PO(OEt) ₂	3.75
	⁻ CH ₂ CotBu	⁻ PO(OEt) ₂	1.95 ^a
Ph-I	⁻ CH ₂ CotBu	⁻ SPh	3.2
Ph [•] (PAT)	⁻ CH ₂ CotBu	⁻ SPh	2.2
Ph-I	⁻ PO(OEt) ₂	⁻ SPh	1.9
Ph-I	⁻ CH(Ph)CotBu	⁻ PO(OEt) ₂	1.1
			3.8
Ph-I	⁻ CH(Ph)CotBu	⁻ SPh	0.39
Ph-I	⁻ CH ₂ CotBu	⁻ PO(OEt) ₂	3.3 ^b
	⁻ CH ₂ CotBu	⁻ SPh	1.5 ^b
	⁻ PO(OEt) ₂	⁻ SPh	0.45 ^b

^aIn the presence of iodide ion.

^bAll three nucleophiles present.

CONCLUSION

Evidence has been presented that supports the existence of only one intermediate in the aromatic $S_{RN}1$ reaction. Competition studies pitting two nucleophiles versus each other with iodobenzene and other substrates resulted in the product ratio being independent of nucleophile concentration at a constant ratio of the two nucleophiles consistent with a one intermediate mechanism. The relative reactivity of nucleophiles competing for an intermediate in the aromatic $S_{RN}1$ reaction and phenyl radical generated from the thermolysis of PAT were very similar.

Initial relative rate studies pitting two nucleophiles versus each other with iodobenzene under $S_{RN}1$ conditions indicate another important product forming step in the early stages of the reaction other than radical-nucleophile coupling. A charge transfer complex between pinacolone or 1-phenyl-3,3-dimethyl-2-butanone enolates and iodobenzene may undergo photoinduced electron transfer to yield a phenyl radical and an alpha-keto radical in a solvent cage. Before the radicals can diffuse out of the cage, they may couple resulting in the formation of the substituted product. As the kinetic chain length increases, perhaps because of the formation of iodide ion, this process becomes less important.

The aromatic $S_{RN}1$ process does not appear to be a

simple reaction. Although the general details of the reaction are clear, the reaction does not usually occur with a sufficiently long kinetic chain length so that the technique of competitive reaction kinetics can be fruitfully applied. Competition occurs between a photochemical process involving electron transfer followed by cage recombination and the photostimulated free radical chain process.

EXPERIMENTAL

General Considerations

All melting points were determined on a Thomas-Hoover capillary melting point apparatus and are uncorrected. GC mass spectra (GCMS) were recorded on a Finnegan 4000 instrument. ^1H NMR were recorded on a Varian EM-360 instrument (60 MHz) or on a Bruker WM-300 (300 MHz). Infrared spectra (IR) were recorded on a Beckman 4250 spectrophotometer.

Irradiations were carried out in a Rayonet RPR-100 photochemical reactor equipped with 10-15 350 nm bulbs or with a 275 W sun lamp. Phenylazotriphenylmethane thermolyses were carried out in a thermostated mineral oil bath at 45 °C.

All glassware, syringes, and needles were dried at 140 °C for at least twelve hours. When removed from the oven, they were allowed to cool in a desiccator.

GLC Analysis

GLC analyses of products were carried out on a Varian 3700 equipped with a thermal conductivity detector and a Hewlett-Packard 3390A integrater. A 1/8 in X 10 ft 7% OV-3 on Chromsorb W column was used. A temperature program of 100 °C to 310 °C at 10 °C/min was used for all product analysis with the exception of benzene. The temperature program used when benzene was being quantified was 50 °C to

310 °C at 5 °C/min. Yields of products were determined by use of internal standards. In all cases, the area ratio was corrected for molar response determined from standard solutions of the products and the internal standards.

General work-up procedure

The following work-up procedure was used for the reaction in this section. All reaction mixtures were poured into 50 mL of distilled water. Benzyl ether (0.0098 g, 4.95×10^{-4} mole) was added as an internal standard. The water layer was extracted three times with 30 mL portions of ethyl ether. The ether extracts were combined and washed with 50 mL of distilled water. The ether was dried (MgSO_4) and removed using a rotatory evaporator. The residue was dissolved in chloroform and analyzed by GLC as described above.

Materials

The dimethyl sulfoxide (DMSO) was obtained from Fisher Scientific and purified by drying for one day over calcium hydride. Sodium amide was added just before vacuum distillation through a Vigreux column (<45 °C). The DMSO was stored in a foil wrapped flask over 4A molecular sieves under an argon atmosphere.⁵² The DMSO was deoxygenated by passing argon through the solvent for one hour. The 4A molecular sieves were activated by heating at 200 °C under

vacuum for one day. The DMSO was transferred by syringe to preclude contact with oxygen.

Diethyl phosphite was obtained from Aldrich Chemical Company and was purified by drying over calcium hydride followed by vacuum distillation. Benzenethiol was obtained from Eastman Organic and was purified by drying over calcium hydride followed by vacuum distillation. Pinacolone and ethyl phenylacetate were obtained from Aldrich Chemical Company and were purified by drying over anhydrous potassium carbonate followed by distillation. Potassium t-butoxide, bromobenzene, diphenyl sulfide, and phenyltrimethylammonium iodide were obtained from Aldrich Chemical Company and were used without further purification. Iodobenzene was obtained from Eastman Organic and was distilled, the colorless liquid was stored in a foil wrapped brown bottle. The preparation of phenylazotriphenylmethane (PAT),⁴⁷ 1-phenyl-3,3-dimethyl-2-butanone,¹³ 1,1-diphenyl-3,3-dimethyl-2-butanone,¹³ diethyl phenylphosphonate,¹⁵ and ethyl diphenylacetate⁵³ has been described in the literature.

Competition Experiments

Typical procedure for halobenzene substrates

The following procedure was used for iodobenzene, bromobenzene, diphenyl sulfide, and phenyltrimethylammonium iodide. A 100 mL volumetric flask was charged with potas-

sium t-butoxide (8.10 g, 0.066 mole) and fitted with a septum. The flask was purged with argon and 50 mL of DMSO was syringed into the flask. The flask was swirled until all of the base had dissolved. Diethyl phosphite (4.33 g, 0.031 mole) and pinacolone (3.14 g, 0.031 mole) were syringed into the flask. The flask was swirled for 5 mins. DMSO was syringed into the flask to bring the total solution volume to 100 mL. Four test tubes fitted with septa and flushed with argon were charged with the following amounts of the standard solution prepared above via syringe: 20 mL, 14 mL, 10 mL, and 8 mL. DMSO was injected into each tube to adjust the volume of the solution to 20 mL. The concentration of each nucleophile in the test tubes was calculated to be 0.31 M, 0.20 M, 0.15 M, and 0.12 M. Iodobenzene (0.018 g, 9.0×10^{-4} mole) was syringed into each tube just prior to irradiation. The test tube containing the nucleophiles and iodobenzene was placed within 6 inches of a 275 W sunlamp for three minutes. Immediately after irradiation, the reaction mixture was poured into 30 mL of water containing benzyl ether (0.010 g, 5.1×10^{-5} mole) as an internal standard. The water layer was extracted three times with 30 mL portions of diethyl ether. The ether extracts were combined, washed with 50 mL water, and dried (MgSO_4). The ether was stripped off at room temperature using a rotary evaporator. The residue was dissolved in

chloroform and the solution analyzed by GLC.

Typical competition procedure for PAT

A 50 mL volumetric flask was charged with potassium t-butoxide (1.35 g, 0.011 mole), fitted with a septum, and flushed with argon. Dry DMSO, 30 mL, was syringed into the flask. Benzenethiol (0.55 g, 0.005 mole) and ethyl phenylacetate (0.78 g, 0.0048 mole) were syringed into the flask. Dry DMSO was syringed into the flask to adjust the volume to 50 mL. A test tube was charged with phenyazotriphenylmethane (0.05807 g, 1.67×10^{-4} mole), fitted with a septum, and flushed with argon. A 20 mL aliquot from the above standard solution was syringed into the test tube. The test tube was placed into an oil bath at 45 °C for 22 hours. The tube was removed, worked up and analyzed as described above.

Initial Rates

Typical procedure for iodobenzene

A test tube equipped with a stirring bar was charged with potassium t-butoxide (1.82 g, 1.49×10^{-3} mole). The test tube was fitted with a septum and flushed with argon. DMSO, 10 mL, was syringed into the tube, the solution was stirred until all of the base was dissolved. The potassium ion was complexed by syringing 18-crown-6 (4.81 g, 0.0132 mole) into the tube. Benzenethiol (0.97 g, 0.0088 mole) and diethyl phosphite (1.00 g, 0.0072 mole) was syringed into the

tube. The solution was stirred for 5 mins. DMSO was syringed into the tube to adjust the volume of the solution to 25 mL. Iodobenzene (0.28 g, 0.0014 mole) was syringed into the tube. The test tube was placed in the Rayonet Reactor and 2 mL aliquots were removed by syringe under a positive pressure of argon. Each aliquot was worked up and analyzed as described earlier.

Typical procedure for PAT

A 50 mL volumetric flask was charged with potassium t-butoxide (4.60 g, 0.0376 mole), fitted with a septum, and flushed with argon. DMSO, 15 mL, was syringed into the flask. The potassium was complexed by syringing 18-crown-6 (9.96 g, 0.0377 mole) into the flask. Benzenethiol (1.73 g, 0.016 mole) and pinacolone (1.77 g, 0.018 mole) were syringed into the flask. The volume of the solution was adjusted to 50 mL by injecting DMSO. A 50 mL round bottomed flask equipped with a stirring bar was charged with PAT (0.47 g, 0.00135 mole), fitted with a septum, and flushed with argon. Syringed into the 50 mL round bottomed flask was 20 mL of the standard solution prepared above. The round bottomed flask was placed in an oil bath at 45 °C and 2 mL aliquots were removed by syringe under a positive pressure of argon. Each aliquot was worked up and analyzed as described earlier.

General Procedures

Determination of benzene

A 25 mL volumetric flask was charged with potassium t-butoxide (1.00 g, 0.0082 mole), fitted with a septum, and flushed with argon. Dry DMSO, 10 mL, was syringed into the flask. The potassium was complexed by syringing 18-crown-6 (2.62 g, 0.0099 mole) into the flask. Pinacolone (0.87 g, 0.0087 mole) was syringed into the flask and the volume was adjusted to 25 mL by injecting dry DMSO. An ampoule (10 mL in volume) was charged with PAT (0.10 g, 0.00029 mole), attached to a vacuum line, and flushed with argon. An 8 mL aliquot of the above solution was syringed into the ampoule via a side arm on the neck of the ampoule. The solution in the ampoule was frozen under vacuum using liquid nitrogen, then warmed to room temperature under argon. This procedure was repeated two times. After the freeze-pump-thaw cycles, the solution was frozen and the ampoule was sealed under vacuum using a torch. The sealed ampoule was placed in an oil bath at 45 °C for 22 hours. After this heating period, the solution in the ampoule was frozen and then opened. While still frozen, a septum was fitted to the neck of the ampoule and securely fastened. Once at room temperature, toluene (0.05 g, 0.00054 mole) was injected into the ampoule and was used as the internal standard for the quantitation of benzene. A 10 uL aliquot of the reaction mixture was

injected into the GLC instrument using the conditions outlined above to quantify benzene. After the quantification was complete, the reaction mixture was worked up and analyzed as described earlier.

Thermolysis of PAT in the presence of diethyl phosphite ion

A 25 mL volumetric flask was charged with potassium t-butoxide (1.00 g, 8.18×10^{-3} mole), fitted with a septum, and flushed with argon. DMSO, 15 mL, and diethyl phosphite (1.00 g, 7.24×10^{-3} mole) was syringed into the flask. The solution was brought to volume by injecting dry DMSO. Two ampoules were attached to a vacuum line and flushed with argon as described above. A 10 mL aliquot of the above solution was syringed into each ampoule. The ampoules were sealed under vacuum and placed in an oil bath for 24 hrs. After the heating period, the ampoule was opened and benzene was quantified as described above. The reaction mixture was worked up and analyzed using the general procedure outlined above. Benzene, 17.1 %, was the only product detected.

Thermolysis of PAT in the presence of 4-iodoanisole and diethyl phosphite ion

A 25 mL volumetric flask was charged with potassium t-butoxide (1.01 g, 8.26×10^{-3} mole), fitted with a septum, and flushed with argon. DMSO, 15 mL, and diethyl phosphite (1.04 g, 7.53×10^{-3} mole) was syringed into the flask. The

solution was then brought to volume. An ampoule was charged with PAT (0.10077 g, 2.89×10^{-4} mole) and 4-iodoanisole (0.07673 g, 3.28×10^{-4} mole), attached to a vacuum line and flushed with argon. A 10 mL aliquot of the above standard solution was syringed into the ampoule. The solution was subjected to three freeze-pump-thaw cycles. The ampoule was then sealed under vacuum using a torch. The ampoule was placed in an oil bath at 45°C for 20 hrs. Benzene and product analyses were done as described above. The only products detected were benzene, 14.0%, and anisole, 65.3%.

Thermolysis of PAT in the presence of 4-iodoanisole and diethyl phosphite ion under $S_{RN}1$ conditions

A 10 mL volumetric flask was charge with potassium t-butoxide (0.40 g, 3.3×10^{-3} mole), fitted with a septum, and flushed with argon. DMSO, 5 mL, and diethyl phosphite (0.41 g, 3.0×10^{-3} mole) was syringed into the flask. The solution was brought to volume. A test tube was charged with PAT (0.11089 g, 3.19×10^{-4} mole), 4-iodoanisole (0.08578 g, 3.6×10^{-4} mole), fitted with a septum and flushed with argon. The standard solution above was syringed into the test tube. The test tube was placed in the Rayonet Photochemical Reactor for 22 hrs. The solution was worked up as described above and analyzed by GLC. The only product detected was anisole, 35.8%.

Dark reaction between diethyl phosphite ion and 4-iodoanisole

A 10 mL volumetric flask was charged with potassium t-butoxide (0.40 g, 3.3×10^{-3} mole), fitted with a septum and flushed with argon. DMSO, 5 mL, and diethyl phosphite (0.40 g, 3.0×10^{-3} mole) were syringed into the flask. The solution was brought to volume. A test tube was charged with 4-iodoanisole (0.1056 g, 4.5×10^{-4} mole), fitted with a septum and flushed with argon. The above standard solution was syringed into the test tube. The test tube was wrapped with aluminum foil and placed in an oil bath at 45 °C for 22 hrs. The reaction mixture was worked up as described earlier and analyzed by GLC. The only product detected was anisole, 63.4 %, and unreacted starting material, 20.9 %.

Reaction of diethyl phosphite ion with 4-iodoanisole under $S_{RN}1$ conditions

The same procedure was followed as described for the dark reaction with this exception. The test tube was placed in the Rayonet Photochemical Reactor for 2.5 hrs. The only product detected was diethyl p-methoxyphenylphosphonate, 40%.

Time study of reaction of diethyl phenylphosphonate with excess potassium t-butoxide

A 100 mL round bottomed flask equipped with a magnetic stirring bar was charged with potassium t-butoxide (2.05 g, 1.7×10^{-2} mole), fitted with a septum and flushed with argon. DMSO, 50 mL, and diethyl phosphite (2.13 g, 3.1×10^{-2} mole) was syringed into the flask. The solution was allowed to stir for 5 mins. and was placed in an oil bath at 45 °C. Diethyl phenylphosphonate (0.30 g, 1.4×10^{-3} mole) was syringed into the solution. Aliquots, 2 mL, were removed from the solution at certain time intervals. Each aliquot was worked up as described earlier and analyzed by GLC. The diethyl phenylphosphonate was decomposed under these reaction conditions.

Time study of diethyl phenylphosphonate in the presence of excess diethyl phosphite

A 100 mL round bottomed flask was charged with potassium t-butoxide (0.91 g, 7.5×10^{-3} mole), fitted with a septum and flushed with argon. DMSO, 25 mL, and diethyl phosphite (1.00 g, 7.24×10^{-3} mole) was syringed into the flask. The solution was placed in an oil bath at 45 °C. Phenyl phosphonate (0.15 g, 7.0×10^{-4} mole) was syringed into the flask. Aliquots, 2 mL, were removed at certain time intervals and worked up as described earlier. The aliquots were analyzed by GLC. The diethyl phenylphosphonate was stable to the reaction conditions.

Measurement of nitrogen produced from the thermolysis of PAT in the presence of diethyl phosphite ion

A 25 mL volumetric flask was charged with potassium t-butoxide (0.60 g, 4.91×10^{-3} mole), fitted with a septum and flushed with argon. DMSO, 15 mL, and diethyl phosphite (0.58 g, 4.20×10^{-3} mole) was syringed into the flask. The solution was brought to volume. A 50 mL three necked round bottomed flask was equipped with a magnetic stirring bar and gas inlet tube in one neck. The flask was charged with PAT (1.00 g, 2.9×10^{-3} mole), fitted with septa in the two remaining necks, and flushed with argon. A 20 mL aliquot of the above solution was syringed into the flask. A large recrystallization dish was filled with water. A 100 mL graduated cylinder was filled with water and was inverted such that the lip of the cylinder was below the water level in the crystallization dish. Care was taken such that no air was allowed into the cylinder during the inversion. A piece of tygon tubing was connected to the gas inlet tube on the round bottomed flask. The other end of the tubing was placed inside the graduated cylinder. A drying tube filled with Drierite was placed between the inlet tube and the graduated cylinder. The flask was then heated at 45°C for 22 hrs. The nitrogen produced from the thermolysis was collected in the graduated cylinder. The water temperature was noted along with the atmospheric pressure. The pressure was corrected for the vapor pressure of water at the tem-

perature noted. The amount of nitrogen was calculated by using the ideal gas law. The amount of nitrogen produced was 84.9%.

PART II. THE DETERMINATION OF ABSOLUTE RATE CONSTANTS
FOR THE COUPLING OF PHENYL RADICAL WITH VARIOUS
NUCLEOPHILES

INTRODUCTION

The generation and reactions of the phenyl radical has been studied extensively in solution.⁵⁴ Phenyl radicals have been shown to add to aromatic rings,⁵⁴ double bonds,⁵⁴ trivalent phosphorous,⁵⁵ and divalent sulfur.⁵⁶ They have also been shown to abstract univalent atoms H, Cl, Br, and I.⁵⁴

The relative reactivity of a variety of substrates toward phenyl radical have been determined using the competition technique. Tables 37, 38, and 39 summarize the relative reactivity of phenyl radical for hydrogen atom abstraction, halogen atom abstraction and addition reactions for a select number of substrates relative to chlorine atom abstraction from carbon tetrachloride.

Kryer and coworkers⁴⁸ reported the first absolute rate constants for the reaction of phenyl radical with common radical scavengers in solution. The rate constants were calculated by using competition data. The rate constant for hydrogen atom abstraction from mineral oil was determined from competition experiments at high solvent viscosity using the assumption that the scavenging rate constant is equal to the diffusion limited value. Table 41 summarizes the absolute rate constants determined.

Janzen et al.⁵⁷ and Janzen and Evans⁵⁸ determined the absolute rate constant for hydrogen atom abstraction by

Table 37. Relative reactivity of phenyl radical toward hydrogen atom abstraction relative to chlorine atom abstraction from carbon tetrachloride

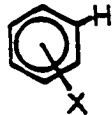
substrate	temp.	k_H/k_{Cl}	ref
			
X= <u>m</u> -CH ₃	80	0.21	59
H	80	0.21	59
<u>m</u> -Cl	80	0.29	59
<u>m</u> -CN	80	0.22	59
<u>m</u> -NO ₂	80	0.33	59
<u>p</u> -OCH ₃	80	0.39	59
<u>p</u> -CH ₃	80	0.27	59
<u>p</u> -Cl	80	0.28	59
<u>p</u> -CN	80	0.27	59
<u>p</u> -NO ₂	80	0.65	59
pentane	60	0.60	47
hexane	60	0.80	47
heptane	60	0.96	47
octane	60	1.15	47
cyclopentane	60	1.04	47

Table 37. continued

substrate	temp.	k_H/k_{Cl}	ref
cyclohexane	60	1.08	47
cyclohexene	60	4.40	47
toluene	60	0.27	47
ethylbenzene	60	0.84	47
cumene	60	0.93	47
diphenylmethane	60	1.40	47
triphenylmethane	60	3.5	47
chloroform	60	3.20	47
acetone	60	0.17	47
iso-propyl ketone	60	1.30	47
ethyl acetate	60	0.09	47
acetonitrile	60	0.29	47
tetramethylsilane	60	0.29	47
2-nitropropane	60	0.25	47
nitromethane	60	0.05	47
$(CH_3O)_2CH_2$	100	2.9	60
$(CH_3CH_2O)_2CH_2$	100	3.1	60
$(PrO)_2CH_2$	100	3.5	60
$(CH_3O)_2CHCH_3$	100	4.4	60
$(CH_3CH_2O)_2CHCH_3$	100	4.8	60
$(PrO)_2CHCH_3$	100	5.2	60

Table 37. continued

substrate	temp.	k_H/k_{Cl}	ref
$C_6H_5CH_3$	100	0.3	60
$C_6H_5CH_2CH_3$	100	1.1	60
$C_6H_5CH(CH_3)_2$	100	1.4	60
$C_6H_5CH_3$	60	0.36	61
C_6H_5SH	60	518	61
$(CH_3O)_3PO$	60	0.05	62
$(CH_3CH_2O)_3PO$	60	0.26	62
$(i-PrO)_3PO$	60	0.31	62
$CH_3PO(OCH_3)_2$	60	0.06	62
$C_2H_5PO(OEt)_2$	60	0.18	62
$(C_2H_5)_3PO$	60	0.36	62
$C_6H_5PO(OEt)_2$	60	0.15	62
CH_3CCl_3	80	0.06	63
$(CH_3)_2CCl_2$	80	0.06	63
$(CH_3)_3CCl$	80	0.04	63
$(CH_3)_3CCN$	80	0.03	63

Table 38. Relative reactivity of phenyl radical toward halogen abstraction relative to chlorine atom abstraction from carbon tetrachloride


substrate	temp.	k_X/k_{Cl}	ref
			
Y= <u>m</u> -NO ₂	60	42.7	64
<u>p</u> -NO ₂	60	22.9	64
<u>m</u> -Br	60	33.1	64
<u>m</u> -COCH ₃	60	26.9	64
<u>p</u> -Br	60	21.4	64
<u>m</u> -OCH ₃	60	21.4	64
<u>m</u> -CH ₃	60	19.5	64
<u>p</u> -C ₆ H ₅	60	13.8	64
<u>p</u> -CH ₃	60	13.5	64
<u>p</u> -OCH ₃	60	10.0	64
<u>m</u> -CN	60	38.0	64
<u>p</u> -CHO	60	28.2	64
<u>m</u> -CF ₃	60	28.2	64
<u>m</u> -CHO	60	27.5	64
<u>m</u> -CO ₂ CH ₃	60	25.1	64
<u>p</u> -COCH ₃	60	18.2	64

Table 38. continued

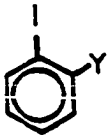
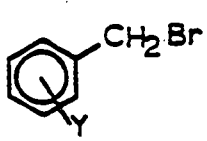
substrate	temp.	k_X/k_{Cl}	ref
<u>m</u> -NH ₂	60	17.8	64
<u>p</u> -NH ₂	60	8.3	64
1-iodonaphthalene	60	22.0	65
2-iodonaphthalene	60	17.4	65
2-iodopyridine	60	106.0	65
3-iodopyridine	60	25.6	65
4-iodopyridine	60	31.2	65
iodobenzene	60	17.0	65
2-iodothiophene	60	4.6	65
3-iodothiophene	60	4.0	65
			
Y=NH ₂	60	7.6	66
CH ₃ O	60	8.3	66
EtO	60	8.5	66
F	60	14.5	66
CH ₃	60	16.9	66
H	60	17.0	66

Table 38. continued

substrate	temp.	k_X/k_{Cl}	ref
C_2H_5	60	19.7	66
$2'-CH_3S-C_6H_4$	60	24.9	66
Cl	60	25.9	66
C_6H_5	60	34.0	66
Br	60	50.0	66
I	60	77.0	66
CF_3	60	103.0	66
NO_2	60	186.0	66



The diagram shows a benzene ring with a CH_2Br group attached to the top carbon and a substituent Y attached to the bottom carbon.

Y= <u>p</u> - CH_3	60	6.17	67
<u>m</u> - CH_3	60	3.54	67
H	60	3.70	67
<u>m</u> -Cl	60	4.2	67
<u>p</u> -Cl	60	5.8	67
<u>m</u> - NO_2	60	4.5	67
<u>p</u> - NO_2	60	7.0	67

Table 39. Relative reactivity of phenyl radical toward addition relative to chlorine atom abstraction from carbon tetrachloride

substrate	temp.	k_A/k_{Cl}	ref
MeSSMe	60	31.0	56a, 68
EtSSEt	60	17.4	68
PrSSPr	60	16.0	68
iPrSSiPr	60	3.3	68
tBuSStBu	60	0.2	68
CH ₂ =CHCH ₃	60	2.0	69
CH ₂ =CHO(O)P(OMe) ₂	60	3.0	69
CH ₂ =CHOC ₂ H ₅	60	3.5	69
C ₆ H ₅ PO(OEt) ₂	60	0.3	62
C ₆ H ₅ PO(OMe) ₂	60	0.3	62
(C ₆ H ₅ O) ₂ PO(OMe)	60	0.5	62
(MeO) ₃ PO	60	0.1	62
CH ₂ =C(CH ₃) ₂	60	7.22	69
CH ₂ =CHSi(OEt) ₃	60	10.0	69
CH ₂ =CHPO(OEt) ₂	60	11.8	69
CH ₂ =CCl ₂	60	26.4	69
CH ₂ =CHPh	60	31.0	69
CH ₂ =CHCO ₂ H	60	31.0	69
CH ₂ CHCOCH ₃	60	31.0	69
CH ₂ =CH(CH ₃)Ph	60	40.5	69
CH ₂ =CHCN	60	35.4	69

Table 40. Absolute rate constants for the reaction of phenyl radical with radical scavengers

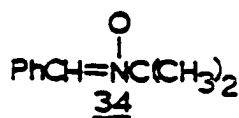
substrate	reaction	solvent	$k, M^{-1}s^{-1}$	ref
PhCl	addition	PhCl-mineral oil	1.3×10^6	48
PhH	addition	PhH-PhCl	1.0×10^6	48
CCl ₄	Cl transfer	PhH-CCl ₄	5.8×10^6	48
CCl ₄	Cl transfer	CCl ₄	2.7×10^6	48
CCl ₄	Cl transfer	CCl ₄	3.3×10^6	48
CBr ₄	Br transfer	PhCl	4.0×10^9	48
CBr ₄	Br transfer	PhCl	5.0×10^9	48
CBr ₄	Br transfer	CCl ₄	5.5×10^9	48
I ₂	I transfer	PhCl	1.5×10^{10}	48
I ₂	I transfer	PhH	1.2×10^{10}	48
i-PrI	I transfer	PhH	8.3×10^8	48
i-PrI	I transfer	CCl ₄	1.2×10^9	48
i-PrI	I transfer	CCl ₄	1.3×10^9	48
BrCCl ₃	Br transfer	PhH	1.5×10^9	48

Table 40. continued

substrate	reaction	solvent	k, M ⁻¹ s ⁻¹	ref
BrCCl ₃	Br transfer	CCl ₄	1.9 X 10 ⁹	48
BrCCl ₃	Br transfer	CCl ₄	1.7 X 10 ⁹	48
BrCCl ₃	Br transfer	CCl ₄	1.9 X 10 ⁹	48
O ₂	addition	CCl ₄	4.4 X 10 ⁹	48
O ₂	addition	c C ₆ H ₁₂	4.7 X 10 ⁹	48
(MeO) ₂ P(O)H	H-trans	CCl ₄	1.1 X 10 ⁷	48
(MeO) ₃ P	addition	TMP-DMP ^a	3.5 X 10 ⁸	48

^aTMP=trimethyl phosphite, DMP=dimethyl phosphite.

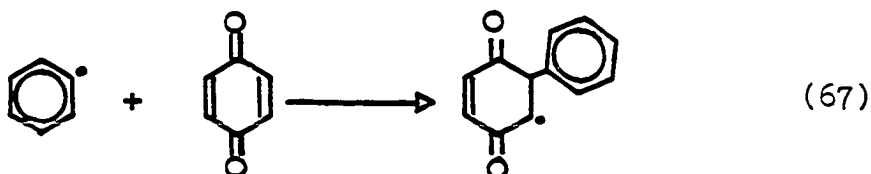
phenyl radical from methanol, ethanol, and iso-propanol via competition studies. The reference rate constant was the attack of phenyl radical on to the spin trap 34 (PBN). The rate constant for the trapping of phenyl radical by PBN was assumed to be similar to the rate constant for the trapping of the *p*-methylphenyl radical by PBN determined by Packer et al.⁷⁰ The rate constants are summarized in Table 41.



Scaiano and Ingold⁷¹ measured the rate constant for the attack of phenyl radical on dimethyl and diethyl selenide at $-30\text{ }^\circ\text{C}$. The rate constants were calculated from competition experiments using the rate constant for hydrogen atom abstraction from cyclopentane as the standard. The attack of phenyl radical on to dimethyl and diethyl selenide was $6.0 \times 10^6 \text{ M}^{-1}\text{s}^{-1}$ (Equation 65) and $1.4 \times 10^8 \text{ M}^{-1}\text{s}^{-1}$ (Equation 66) respectively.



Veltivisch⁷² determined the rate constant for attack of phenyl radical on 1,4-quinone ($k=1.2 \times 10^9 \text{ M}^{-1}\text{s}^{-1}$, Equation 67). The phenyl radical was formed by pulse radiolysis and the addition adduct observed by optical absorption spectroscopy.

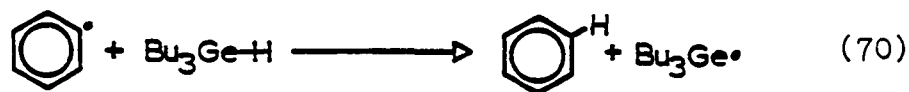
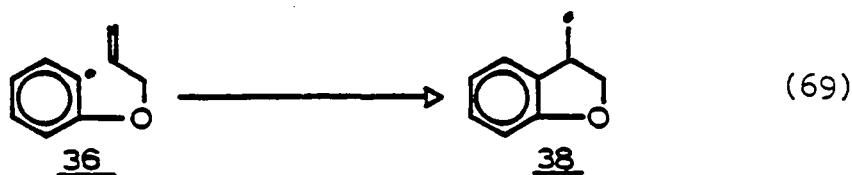
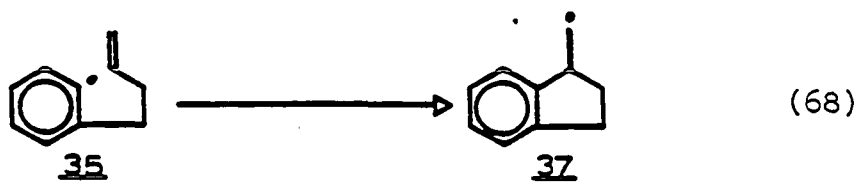


Scaiano and Stewart⁷³ determined absolute rate constants for a variety of substrates using laser flash photolysis in Freon 113 at 25 °C. Benzoyl peroxide was photolyzed to form phenyl radicals. The rate constants determined are summarized in Table 42.

Burkey and coworkers⁷⁴ measured the rate constant for attack of phenyl radical on to furan, thiophene, and 1-hexene in hydrocarbon solvent at 25 °C. The technique used was kinetic electron spin resonance and laser flash photolysis using beta-methylstyrene as a probe. Table 43 summarizes the rate constants determined.

Johnson and coworkers⁷⁵ determined the rate constant for cyclization of radicals 35 and 36 to yield radicals 37 and 38 using flash laser photolysis. The rate constants are $4.0 \times 10^8 \text{ s}^{-1}$ and $6.3 \times 10^9 \text{ s}^{-1}$ at 30 °C for Equations 68 and

69 respectively. Also measured was the rate constant for hydrogen atom abstraction by phenyl radical from dibutyl germanium and tin hydride in benzene at 29 °C. The rate constants determined were $2.6 \times 10^6 \text{ M}^{-1}\text{s}^{-1}$ for germanium hydride (Equation 70) and $5.2 \times 10^6 \text{ M}^{-1}\text{s}^{-1}$ for the tin hydride (Equation 71).



Lustzyk and Ingold⁷⁶ measured the rate constant of the addition of phenyl radical on hexafluorobenzene at 25 °C using ESR and laser flash photolysis (Equation 72). The

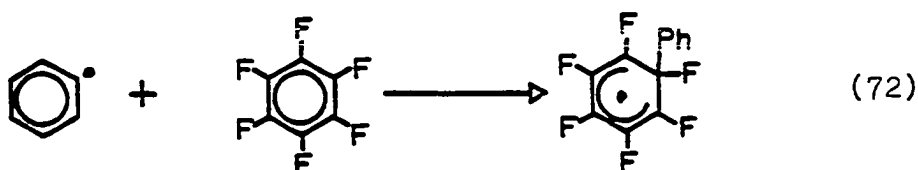
Table 41. Absolute rate constants for hydrogen atom abstraction by phenyl radical at 25 °C

substrate	solvent	$k_H, M^{-1}s^{-1}$	ref
CH ₃ OH	CH ₃ OH	1.2 X 10 ⁷	57, 58
C ₆ H ₆	C ₆ H ₆	4.0 X 10 ⁷	57, 58
CH ₃ CH ₂ OH	CH ₃ CH ₂ OH	2.3 X 10 ⁵	57, 58
(CH ₃) ₂ CHOH	(CH ₃) ₂ CHOH	4.1 X 10 ⁵	57, 58

Table 42. Absolute rate constants for the reaction of phenyl radical with various substrates in Freon 113 at 25 °C

substrate	k, M ⁻¹ s ⁻¹	ref
benzene	4.5 X 10 ⁵	73
chlorobenzene	1.18 X 10 ⁶	73
styrene	1.10 X 10 ⁸	73
B-methylstyrene	3.0 X 10 ⁷	73
methyl methacrylate	1.8 X 10 ⁸	73
cyclohexene	2.8 X 10 ⁸	73
toluene	1.7 X 10 ⁶	73
cumene	1.4 X 10 ⁷	73
p-xylene	2.4 X 10 ⁶	73
isopropanol	1.4 X 10 ⁶	73
benzhydrol	2.0 X 10 ⁷	73
acetonitrile	1.0 X 10 ⁵	73
tetrahydrofuran	4.8 X 10 ⁶	73
carbon tetrachloride	7.8 X 10 ⁶	73
2-bromobutane	2.3 X 10 ⁶	73
1-bromopropane	1.1 X 10 ⁶	73
benzoyl peroxide	2.1 X 10 ⁷	73
furan	2.7 X 10 ⁶	74
thiophene	6.4 X 10 ⁶	74
1-hexene	2.8 X 10 ⁸	74

rate constant was determined to be $1.2 \times 10^6 \text{ M}^{-1}\text{s}^{-1}$.



The determination of rate constants for the coupling of aryl radicals with nucleophiles has been reported recently. Amatore et al.^{19,27} have studied the aromatic $S_{RN}1$ reaction electrochemically. The absolute rate constants for the coupling of phenyl and other aryl radicals with thiophenoxide, diethyl phosphite ion, and acetone enolate in liquid ammonia at -38°C have been determined using redox catalysis, electrochemical competition or direct electrochemical measurements. Table 43 summarizes the rate constants determined electrochemically. Inspection of Table 43 reveals that the coupling of aryl radicals with nucleophiles are below the diffusion limit.

Tanko¹⁰ studied the coupling of phenyl radical with nucleophiles in dimethyl sulfoxide (DMSO) at 45°C . The phenyl radicals were generated from the thermolysis of phenylazotriphenylmethane (PAT). Competition studies were carried out pitting two nucleophiles versus each other,

thiophenoxide and nitronate ions. The rate constants were based upon the rate constant for attack of phenyl radical on carbon tetrachloride.⁷³ Hydrogen atom abstraction from nitronate, 18-crown-6, and benzenethiol were also determined. Table 44 summarizes the rate constants determined.

This section of the thesis will be an extension of the work carried out by Tanko.¹⁰ Absolute rate constants for the coupling of phenyl radical with a variety of nucleophiles have been determined via competition studies.

Table 43. Absolute rate constants for the coupling of aryl radicals with nucleophiles determined electrochemically in liquid ammonia at -38°C

radical	rate constant, $\text{M}^{-1}\text{s}^{-1}$			ref
	PhS^-	$(\text{EtO})_2\text{PO}^-$	$\text{CH}_3\text{COCH}_2^-$	
2-cyano	1.4×10^{10}	8.0×10^9	2.4×10^{10}	27
3-cyano	1.5×10^{10}	7.5×10^9	9.0×10^9	27
4-cyano	3.4×10^{10}	1.4×10^9	2.6×10^9	27
1-naphthyl	2.0×10^{10}	3.2×10^{10}	4.2×10^{10}	27
3-quinolyl	1.9×10^9	7.6×10^8	3.8×10^9	27
4-quinolyl	3.2×10^9	1.6×10^9	5.4×10^9	27
2-quinolyl	1.4×10^7	1.7×10^7	1.0×10^8	27
3-pyridyl	1.0×10^{10}	7.0×10^9	1.6×10^{10}	27
2-pyridyl	1.0×10^8	-	-	27
phenyl	2.6×10^7	3.8×10^8	-	19

Table 44. Absolute rate constants for the reaction of phenyl radical with various substrates in DMSO at 45 °C based on the rate constant of chlorine atom abstraction from carbon tetrachloride⁷³

substrate	reaction	solvent	k, M ⁻¹ s ⁻¹	ref
DMSO	H-abst.	DMSO	3.0 X 10 ⁵	10
D ₆ -DMSO	D-abst	DMSO	4.3 X 10 ⁴	10
Me ₂ =NO ₂ ^{-a}	coupling	DMSO	1.2 X 10 ⁹	10
Me ₂ =NO ₂ ⁻	H-abst.	DMSO	2.8 X 10 ⁸	10
PhS ^{-a}	coupling	DMSO	2.2 X 10 ⁸	10
PhS ⁻ K ⁺	coupling	DMSO	5.7 X 10 ⁷	10
PhSSPh	S _H 2	DMSO	1.3 X 10 ⁸	10
PhSSPh	S _H 2	CCl ₄	3.0 X 10 ⁸	10
PhSH	H-abst.	DMSO	5.1 X 10 ⁸	10
PhSH	H-abst.	CCl ₄	4.1 X 10 ⁹	10
18-crown-6	H-abst.	CCl ₄	3.8 X 10 ⁷	10

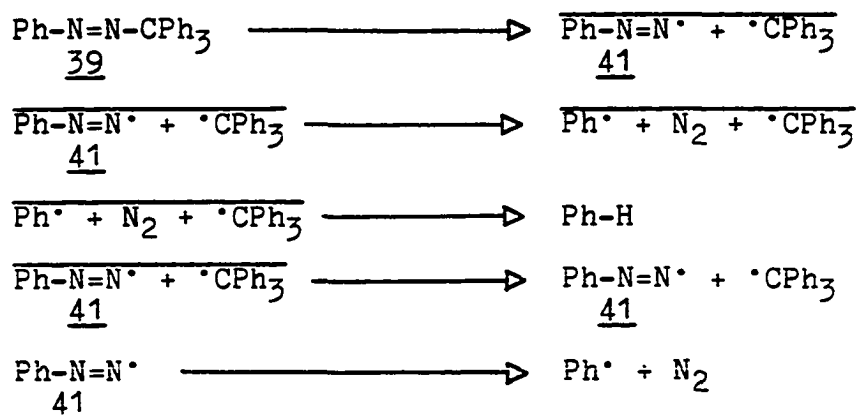
^aPotassium complexed by 18-crown-6.

RESULTS AND DISCUSSION

Mechanism of PAT Thermolysis

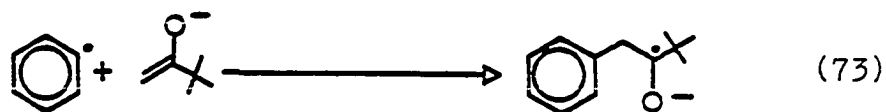
The thermolysis of phenylazotriphenylmethane (39) (PAT) yields phenyl radicals in greater than 90%.^{10,47,48,49,50} Other than benzoyl peroxide, the thermolysis of PAT has been used to study the reactivity of various substrates toward phenyl radical. PAT was chosen as a precursor to phenyl radical because of its thermal decomposition takes place under mild reaction conditions.

The mechanism for the thermolysis of PAT is outlined in Scheme 23. Thermolysis of PAT in solution results in the formation of trityl radical (40) and diazenyl radical (41) in a solvent cage. The phenyl radical can be formed in the solvent cage by loss of nitrogen from 41. While in the solvent cage, the phenyl radical can abstract a hydrogen atom to yield benzene. In the absence of any hydrogen atom donating species, 5.4% benzene is formed from the cage reaction. All benzene yields reported are corrected by subtracting 5.4% from the measured amount of benzene. The diazenyl radical and trityl radical can diffuse out of the cage yielding phenyl radical after loss of nitrogen from the diazenyl radical (41). The rate constant for the loss of nitrogen from the diazenyl radical is $1.6 \times 10^5 \text{ s}^{-1}$ ($k_d = 1.6 \times 10^5 \text{ s}^{-1}$).

Scheme 23.

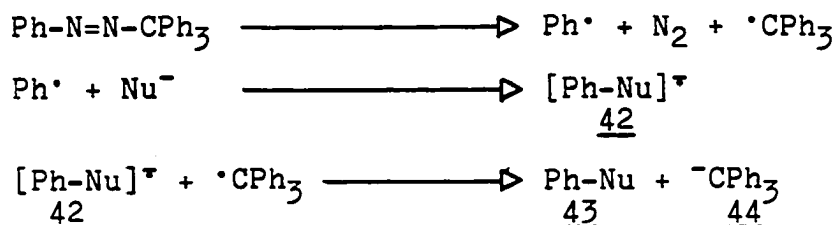
Mechanism for the Coupling of Phenyl Radical Generated From the Thermolysis of PAT in the Presence of a Nucleophile

It is believed that a sigma phenyl radical is the sole intermediate in the aromatic $S_{RN}1$ reaction.⁹ In the aromatic $S_{RN}1$ reaction a phenyl radical couples with a nucleophile, such as pinacolone enolate, to yield a radical anion (Equation 73). The radical anion usually transfers the odd electron back to the substrate. A few absolute rate constants have been determined electrochemically under $S_{RN}1$ conditions for the coupling of aryl radicals with thiophenoxide, diethyl phosphite ion, and acetone enolate in liquid ammonia.^{17,25} However, no absolute rate constants have been reported for the coupling process when phenyl radical is generated unambiguously.



PAT is known to yield phenyl radical in greater than 90% and can be thermolyzed in the presence of nucleophiles in DMSO. Scheme 24 outlines the proposed mechanism for the coupling of phenyl radical, generated from PAT, and a nucleophile. The phenyl radical couples with nucleophile Nu^- to form radical anion 42. Radical anion 42 is then oxidized by the trityl radical to give the substituted product 43, and trityl anion (44).

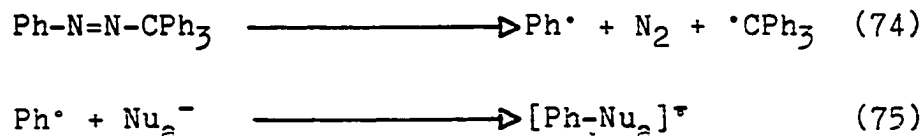
Scheme 24.

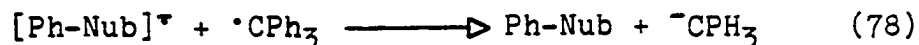
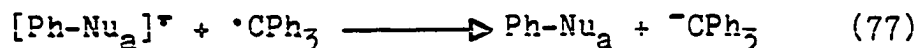
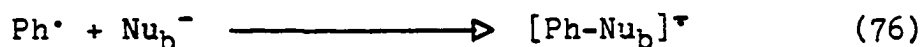


Relative Reactivities

Competition studies between two nucleophiles for phenyl radical can be conveniently carried out when PAT is used as the phenyl radical precursor. Scheme 25 outlines the mechanism for the competition of two nucleophiles for phenyl radical.

Scheme 25.



Scheme 25. continued

The relative reactivities were calculated from the expression

$$\frac{k_A}{k_B} = \frac{[\text{Nu}_a\text{-Ph}] [\text{Nu}_b]}{[\text{Nu}_b\text{-Ph}] [\text{Nu}_a]}$$

This approach can be justified only if: (a) the kinetics of reaction 75 and 76 are first order in Nu_a and Nu_b and are the same kinetic order in phenyl radical, (b) reaction 75 and 76 are the only source of Ph-Nu_a and Ph-Nu_b , (c) the ratio of $[\text{Nu}_b]/[\text{Nu}_a]$ remains constant, (d) reactions 77 and 78 are fast and irreversible.

Assumptions (a) and (b) have been shown to be valid.⁹ By choice of the reaction conditions it was possible to hold the ratio $[\text{Nu}_a]/[\text{Nu}_b]$ constant.

Competition reactions were run in dry deoxygenated DMSO at 45 °C. The concentration of the nucleophiles were 7 to 11 time larger than the PAT concentrations such that assumption (c) was valid. All samples were worked up and analyzed as described in the experimental section. The results of the competition studies are presented in Table

45. The mean values for the measured relative reactivities are summarized in Table 46.

A few relative reactivities can not be measured directly, but can be calculated using a reference nucleophile. The pairs are: pinacolone enolate/diethyl phosphite ion, pinacolone enolate/1-phenyl-3,3-dimethyl-2-butanone enolate, pinacolone enolate/thiophenoxide, acetophenone enolate/deoxybenzoin enolate, and diethyl phosphite ion/thiophenoxide. The relative reactivities were calculated using Equation 79 and are summarized in Table 47. The reference nucleophile was the enolate of ethyl phenylacetate.

$$\frac{k_B}{k_C} = \frac{k_B}{k_A} \times \frac{k_A}{k_C} \quad (79)$$

Diethyl phosphite ion/thiophenoxide and pinacolone enolate/diethyl phosphite ion pairs can not be measured since diethyl phenylphosphonate is destroyed by the enolate and thiophenoxide during the reaction. Table 48 presents the results from subjecting the diethyl phenylphosphonate to the reaction conditions when diethyl phosphite ion and thiophenoxide were present.

The product from the coupling of phenyl radical with thiophenoxide is diphenyl sulfide (Equation 80). Pinacolone enolate reacts with diphenyl sulfide via the aromatic $S_{RN}1$ reaction under thermal conditions to yield 1-phenyl-3,3-

Table 45. Relative reactivity of various nucleophiles toward phenyl radical in DMSO at 45 °C

[PAT]	[Nu _A]	[Nu _B]	% yield			k _A /k _B
			Ph-Nu _A	Ph-Nu _B	Ph ₃ CH	
Nu _A ⁻ SPh; Nu _B ⁻ CH(Ph)COtBu						
0.011	0.10	0.092	36.1	29.3	87.6	1.13
0.010	0.10	0.092	43.3	34.2	108.3	1.15
					ave	1.15
Nu _A ⁻ CH(Ph)COtBu; Nu _B ⁻ CH(Ph)COPh						
0.010	0.084	0.10	13.5	51.0	-	0.32
0.010	0.084	0.10	12.4	53.8	-	0.27
					ave	0.30
Nu _A ⁻ CH ₂ COtBu; Nu _B ⁻ CH(Ph)CO ₂ Et						
0.0082	0.098	0.11	45.8	17.1	89.8	3.00
0.0087	0.098	0.11	43.4	18.4	94.5	2.65
					ave	2.83

Table 45. continued

[PAT]	[Nu _A]	[Nu _B]	% yield			k _A /k _B
			Ph-Nu _A	Ph-Nu _B	Ph ₃ CH	
Nu _A = ⁻ CH ₂ COPh; Nu _B = ⁻ CH(Ph)CO ₂ Et						
0.0070	0.097	0.098	47.4	13.6	95.9	3.52
0.0070	0.097	0.098	47.8	13.6	96.5	3.55
					ave	3.53
Nu _A = ⁻ CH(CO ₂ Et)CO ₂ Et; Nu _B = ⁻ CH ₂ COtBu						
0.0075	0.089	0.096	0	57.1	84.2	0
0.0078	0.089	0.096	0	55.9	85.8	0
Nu _A = ⁻ CH(CO ₂ Et)CO ₂ Et; Nu _B = ⁻ P(O)(OEt) ₂						
0.0077	0.088	0.13	0	67.8	73.9	0
0.0073	0.088	0.13	0	67.8	76.2	0
Nu _A = ⁻ CH(Ph)CO ₂ Et; Nu _B = ⁻ P(O)(OEt) ₂						
0.0088	0.093	0.13	13.3	32.8	86.4	0.57

Table 45. continued

[PAT]	[Nu _A]	[Nu _B]	% yield			k _A /k _B
			Ph-Nu _A	Ph-Nu _B	Ph ₃ CH	
0.0098	0.093	0.13	13.2	34.0	86.7	0.54
						ave 0.56
Nu _A = ⁻ CH(Ph)CO ₂ Et; Nu _B = ⁻ CH(Ph)COPh						
0.0083	0.10	0.10	25.8	41.1	81.0	0.63
0.0088	0.10	0.10	25.5	40.3	77.9	0.63
						ave 0.63
Nu _A = ⁻ SPh; Nu _B = ⁻ CH(Ph)CO ₂ Et						
0.0084	0.10	0.095	28.2	32.3	83.8	0.83
0.0086	0.10	0.095	28.5	32.0	84.5	0.85
						ave 0.84
Nu _A = ⁻ CH ₂ COtBu; Nu _B = ⁻ CH(Ph)COPh						
0.0078	0.10	0.10	52.1	18.7	79.0	2.79

Table 45. continued

[PAT]	[Nu _A]	[Nu _B]	% yield			k _A /k _B
			Ph-Nu _A	Ph-Nu _B	Ph ₃ CH	
0.0078	0.10	0.10	53.1	19.1	79.4	2.78
						ave 2.79
Nu _A = ⁻ P(O)(OEt) ₂ ; Nu _B = ⁻ CH(Ph)CO ₂ Et						
0.0075	0.094	0.11	33.6	19.4	96.0	2.03 ^a
0.0075	0.094	0.11	37.7	21.9	97.0	2.01 ^a
						ave 2.02 ^a
Nu _A = ⁻ CH ₂ COtBu; Nu _B = ⁻ CH(Ph)CO ₂ Et						
0.0078	0.089	0.12	48.0	16.4	90.7	3.95 ^a
0.0074	0.089	0.12	46.8	16.7	96.0	3.78 ^a
						ave 3.87 ^a

^apotassium complexed by 18-crown-6.

Table 45. continued

[PAT]	[Nu _A]	[Nu _B]	% yield			k _A /k _B
			Ph-Nu _A	Ph-Nu _B	Ph ₃ CH	
Nu _A = ⁻ CH ₂ COtBu; Nu _B = ⁻ CH ₂ COPh						
0.012	0.094	0.11	35.4	53.1	92.9	0.78
0.011	0.094	0.11	37.4	54.6	93.1	0.80
						ave 0.79
Nu _A = ⁻ CH ₂ COPh; Nu _B = ⁻ SPh						
0.014	0.10	0.10	80.4	15.8	94.7	5.09
0.012	0.10	0.10	82.3	16.8	91.6	4.90
						ave 5.00
Nu _A = ⁻ CH(Ph)COtBu; Nu _B = ⁻ CH ₂ COPh						
0.010	0.092	0.11	8.1	72.3	99.1	0.13
0.011	0.092	0.11	7.0	63.8	98.2	0.11
						ave 0.12

Table 45. continued

[PAT]	[Nu _A]	[Nu _B]	% yield			k _A /k _B
			Ph-Nu _A	Ph-Nu _B	Ph ₃ CH	
Nu _A = ⁻ CH(Ph)COtBu; Nu _B = ⁻ P(O)(OEt) ₂						
0.011	0.09	0.11	7.9	66.0	94.9	0.15
0.011	0.09	0.11	7.8	63.9	92.6	0.15
					ave	0.15
Nu _A = ⁻ CH(Ph)CO ₂ Et; Nu _B = ⁻ CH(Ph)CN						
0.0073	0.10	0.10	15.7	51.9 ^b	87.9	0.30
0.0072	0.10	0.10	14.3	51.8 ^b	88.1	0.28
					ave	0.29
Nu _A = ⁻ CH(Ph)CO ₂ Et; Nu _B = ⁻ CH(Ph)COtBu						
0.0076	0.10	0.088	35.5	12.0	94.1	2.60
0.0080	0.10	0.088	34.3	11.0	93.1	2.74
					ave	2.67

^bDiphenyl methane is produced.

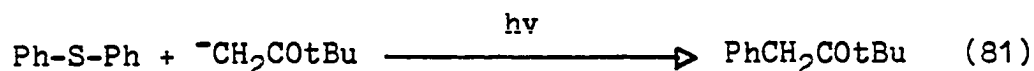
Table 46. Mean values of relative reactivities of nucleophiles toward phenyl radical in DMSO at 45 °C

rate constant ratio	relative reactivity ^a
$k\text{-SPh}/k\text{-CH(Ph)CotBu}$	1.15
$k\text{-CH(Ph)CotBu}/k\text{-CH(Ph)COPh}$	0.30
$k\text{-CH}_2\text{CotBu}/k\text{-CH(Ph)CO}_2\text{Et}$	2.83
$k\text{-CH}_2\text{COPh}/k\text{-CH(Ph)CO}_2\text{Et}$	3.53
$k\text{-CH(Ph)CO}_2\text{Et}/k\text{-P(O)(OEt)}_2$	0.58
$k\text{-CH(Ph)CO}_2\text{Et}/k\text{-CH(Ph)COPh}$	0.63
$k\text{-SPh}/k\text{-CH(Ph)CO}_2\text{Et}$	0.84
$k\text{-CH}_2\text{CotBu}/k\text{-CH(Ph)COPh}$	2.79
$k\text{-CH}_2\text{CotBu}/k\text{-CH}_2\text{COPh}$	0.79
$k\text{-CH}_2\text{COPh}/k\text{-SPh}$	5.00
$k\text{-CH(Ph)CotBu}/k\text{-CH}_2\text{COPh}$	0.12
$k\text{-CH(Ph)CO}_2\text{Et}/k\text{-CH(Ph)CN}$	0.29
$k\text{-CH(Ph)CO}_2\text{Et}/k\text{-CH(Ph)CotBu}$	2.67
$k\text{-CH(Ph)CotBu}/k\text{-P(O)(OEt)}_2$	0.15
$k\text{-P(O)(OEt)}_2/k\text{-CH(Ph)CO}_2\text{Et}$	2.02 ^b
$k\text{-CH}_2\text{CotBu}/k\text{-CH(Ph)CO}_2\text{Et}$	3.87 ^b

^a±0.05.

^bpotassium complexed by 18-crown-6.

The pinacolone enolate reacts with diphenyl sulfide via the aromatic $S_{RN}1$ reaction to yield 1-phenyl-3,3-dimethyl-2-butanone (Equation 81).⁹ The destruction of diphenyl sulfide during the course of the reaction would not allow a reliable relative reactivity to be measured.



Absolute Rate Constants

Absolute rate constants can be calculated from the relative reactivity data if one of the rate constants is known. From earlier work, the rate constant for the coupling of phenyl radical with thiophenoxide was determined to be $5.7 \times 10^7 \text{ M}^{-1}\text{s}^{-1}$.¹⁰ This rate constant was based on the rate constant for chlorine atom abstraction from carbon tetrachloride by phenyl radical.⁷³ Using the value of $5.7 \times 10^7 \text{ M}^{-1}\text{s}^{-1}$ for thiophenoxide, the rate constants for other nucleophiles coupling with phenyl radical can be calculated from the relative reactivity data. Table 49 presents the absolute rate constants for the coupling of various nucleophiles with phenyl radical.

The rate constant for coupling of phenyl radical with pinacolone enolate can also be calculated from the competition of phenyl radical abstracting a hydrogen atom

Table 47. Calculated relative reactivities

rate constant ratio	relative reactivity
$k\text{-CH}_2\text{CotBu}/k\text{-P(O)(OEt)}_2$	1.61
$k\text{-CH}_2\text{CotBu}/k\text{-CH(Ph)CotBu}$	7.56
$k\text{-CH}_2\text{CotBu}/k\text{-SPh}$	3.37
$k\text{-CH}_2\text{CotBu}/k\text{-CH(Ph)COPh}$	2.22
$k\text{-P(O)(OEt)}_2/k\text{-SPh}$	2.13

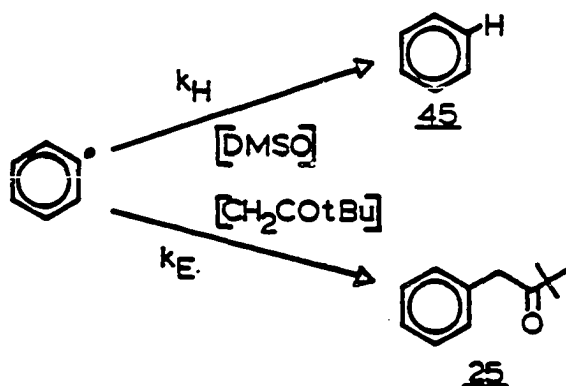
Table 48. Time study of the decomposition of diethyl phenylphosphonate in the presence of diethyl phosphite ion and thiophenoxide^a

time, min	% PhP(O)(OEt) ₂
30	92.3
60	89.0
160	61.4
360	28.5
1260	1.6

^a[Ph⁻]=0.35 M; [⁻P(O)(OEt)₂]=0.32 M
[PhP(O)(OEt)₂]=0.026 M.

from the solvent, DMSO, and the coupling process. Consider the mechanism outlined in Scheme 26.

Scheme 26.



The relative reactivity of hydrogen atom abstraction to nucleophile coupling (k_H/k_E) was calculated using the expression

$$\frac{k_H}{k_E} = \frac{[\text{Ph-H}] [\text{^-CH}_2\text{C(OtBu)}]}{[\text{Ph-E}] [\text{DMSO}]}$$

Table 50 presents the results of the competition. Using the average yields of benzene (45), 1-phenyl-3,3-dimethyl-2-butanone (25), and the concentration of reactants, the relative reactivity for hydrogen atom abstraction of coupling was 1.14×10^{-3} ($k_H/k_E=0.00114$). The rate constant for hydrogen atom abstraction from DMSO has been determined to be $3.0 \times 10^5 \text{ M}^{-1}\text{s}^{-1}$ ($k_H=3.0 \times 10^5 \text{ M}^{-1}\text{s}^{-1}$).¹⁰ Therefore,

Table 49. Absolute rate constants for the coupling of phenyl radical with nucleophiles in DMSO at 45 °C

nucleophile	relative rate	rate constant	k, M ⁻¹ s ⁻¹
⁻ CH(Ph)CO ₂ Et	k-CH(Ph)CO ₂ Et/k-SPh=1.19	k-SPh=5.7 X 10 ⁷	6.8 X 10 ⁷
⁻ CH(Ph)COtBu	k-CH(Ph)COtBu/k-SPh=0.87	k-SPh=5.7 X 10 ⁷	5.0 X 10 ⁷
⁻ CH(Ph)COtBu	k-CH(Ph)COtBu/k-CH(Ph)CO ₂ Et=0.37	k-CH(Ph)CO ₂ Et=6.8 X 10 ⁷	2.5 X 10 ⁷
⁻ CH ₂ COPh	k-CH ₂ COPh/k-SPh=5.00	k-SPh=5.7 X 10 ⁷	2.9 X 10 ⁸
⁻ CH ₂ COPh	k-CH ₂ COPh/k-CH(Ph)CO ₂ Et=3.53	k-CH(Ph)CO ₂ Et=6.8 X 10 ⁷	2.4 X 10 ⁸
⁻ CH ₂ COPh	k-CH ₂ COPh/k-CH(Ph)COtBu=8.33	k-CH(Ph)COtBu=5.0 X 10 ⁷	4.1 X 10 ⁸
⁻ CH ₂ COtBu	k-CH ₂ COtBu/k-CH(Ph)CO ₂ Et=2.83	k-CH(Ph)CO ₂ Et=6.8 X 10 ⁷	1.9 X 10 ⁸
⁻ CH ₂ COtBu	k-CH ₂ COtBu/k-CH ₂ COPh=0.78	k-CH(Ph)CO ₂ Et=6.8 X 10 ⁷	2.3 X 10 ⁸
⁻ P(O)(OEt) ₂	k-PO(OEt) ₂ /k-CH(Ph)CO ₂ Et=1.79	k-CH(Ph)CO ₂ Et=6.8 X 10 ⁷	1.2 X 10 ⁸
⁻ P(O)(OEt) ₂	k-PO(OEt) ₂ /k-CH(Ph)COtBu=8.33	k-CH(Ph)COtBu=5.0 X 10 ⁷	3.3 X 10 ⁸
⁻ CH(Ph)COPh	k-CH(Ph)COPh/k-CH(Ph)CO ₂ Et=1.59	k-CH(Ph)CO ₂ Et=6.8 X 10 ⁷	1.1 X 10 ⁸

Table 49. continued

nucleophile	relative rate	rate constant	k, M ⁻¹ s ⁻¹
⁻ CH(Ph)COPh	k-CH(Ph)COPh/k-CH(Ph)COtBu=6.67	k-CH(Ph)COtBu=5.0 X 10 ⁷	3.3 X 10 ⁸
⁻ CH(Ph)CN	k-CH(Ph)CN/k-CH(Ph)CO ₂ Et=3.45	k-CH(Ph)CO ₂ Et=6.8 X 10 ⁷	2.3 X 10 ⁸
⁻ O ₂ N=CMe ₂			1.2 X 10 ^{9a}

^aReference 10.

the rate constant for coupling is $2.6 \times 10^8 \text{ M}^{-1}\text{s}^{-1}$ ($k_E = 2.6 \times 10^8 \text{ M}^{-1}\text{s}^{-1}$). This value is in good agreement with the values obtained by nucleophile competitions.

The absolute rate constants for the coupling of nucleophiles diethyl phosphite ion, ethyl phenylacetate enolate, and pinacolone enolate with phenyl radical when the counter ion potassium is complexed by 18-crown-6 can be determined. Consider the mechanism outlined in Scheme 27. The rate constant for coupling of phenyl radical with pinacolone enolate can be calculated from the competition of hydrogen atom abstraction from DMSO and 18-crown-6 relative to coupling.

Scheme 27.

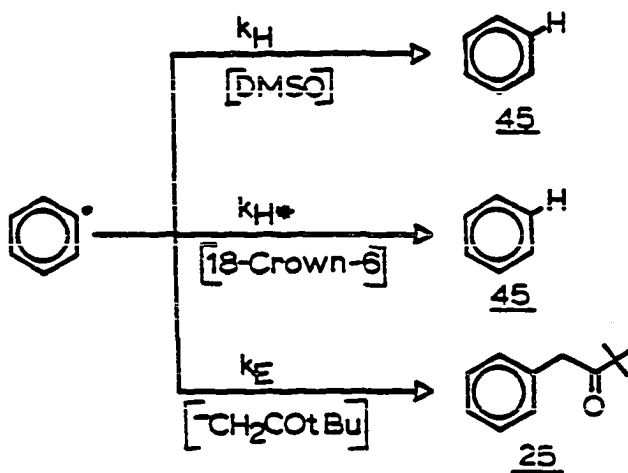


Table 50. The yields of benzene and 1-phenyl-3,3-dimethyl-2-butanone from the reaction of phenyl radical with pinacolone enolate at 45 °C in DMSO

exp	% yield	
	Ph-H	Ph-CH ₂ CotBu
A	1.4	89 ^a
B	8.0	87 ^a
ave	4.7	88

^a[PAT]=0.030 M; [DMSO]=14 M; [⁻CH₂CotBu]=0.30 M.

Applying the steady state assumption to the mechanism in Scheme 27, a kinetic expression relating the ratio of the yields of benzene (45)/1-phenyl-3,3-dimethyl-2-butanone (25) (Y_H/Y_E) to concentration of reactants and rate constants can be derived (Equation 82). Equation 82 can be rearranged to relate the rate constant k_E to known quantities (Equation 83). The results of the competition are summarized in Table 51.

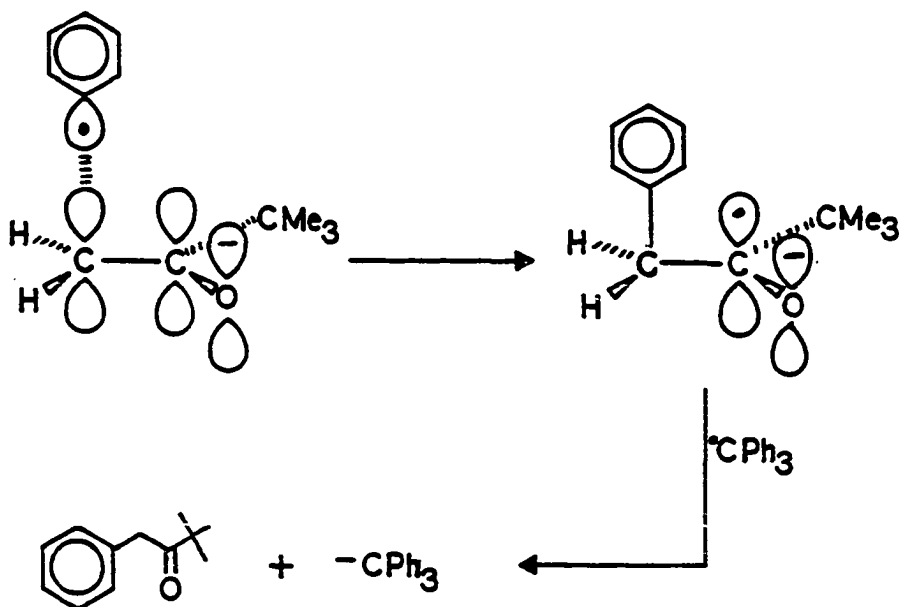
$$\frac{Y_H}{Y_E} = \frac{k_H [\text{DMSO}] + k_{H^*} [\text{18-crown-6}]}{k_E [\text{^-CH}_2\text{CotBu}]} \quad (82)$$

$$k_E = \frac{Y_E \{k_H [\text{DMSO}] + k_{H^*} [\text{18-crown-6}]\}}{Y_H [\text{^-CH}_2\text{CotBu}]} \quad (83)$$

The rate constant for hydrogen atom abstraction from 18-crown-6 has been determined to be $3.8 \times 10^7 \text{ M}^{-1} \text{ s}^{-1}$ ($k_{H^*} = 3.8 \times 10^7 \text{ m}^{-1} \text{ s}^{-1}$).¹⁰ Substituting the known values into Equation 83, the rate constant k_E is calculated to be $3.3 \times 10^8 \text{ m}^{-1} \text{ s}^{-1}$ ($k_E = 3.3 \times 10^8 \text{ M}^{-1} \text{ s}^{-1}$). Using this rate constant, the other rate constants can be calculated using the relative reactivities obtained earlier. The absolute rate constants for the coupling of phenyl radical with pinacolone enolate, diethyl phosphite ion, and ethyl phenyl acetate enolate when potassium is complexed by 18-crown-6 are presented in Table 52.

Discussion of Nucleophile Reactivities

Coupling of a phenyl radical with a ketone enolate can be thought of as a radical attacking a substituted alkene. The radical approaches the enolate ion perpendicular to the alkene plane forming a ketyl radical (46) after coupling. The ketyl 46 is then oxidized by the trityl radical to give the trityl anion and the product.



Coupling of phenyl radical with diethyl phosphite ion may be similar to the attack of phenyl radical on a trivalent phosphorous compound.⁵⁵ The diethyl phosphite ion has two resonance structures, 47 and 48. Attack of phenyl radical on structure 48 would result in radical anion 49 which is then oxidized by trityl radical to give the

Table 51. The yields of benzene and 1-phenyl-3,3-dimethyl-2-butanone from the reaction of phenyl radical with pinacolone enolate when potassium is complexed by 18-crown-6 at 45 °C in DMSO

exp	% yield	
	Ph-H	Ph-CH ₂ COtBu
A	11.4	70.3
B	13.3	74.5
ave	12.3	72.4

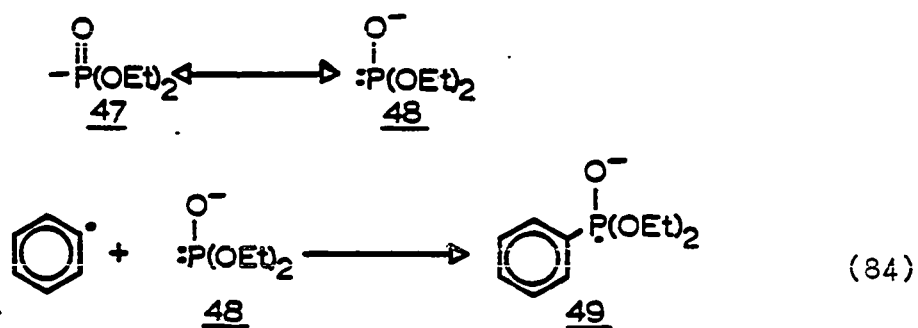
^a[PAT]=0.036 M; [DMSO]=14.0 M, [⁻CH₂COtBu]=0.35 M;
[18-crown-6]=0.40 M.

Table 52. Absolute rate constants for the coupling of phenyl radical with nucleophiles in DMSO at 45 °C when potassium is complexed by 18-crown-6

nucleophile	relative rate	rate constant	k, M ⁻¹ s ⁻¹
CH_2COtBu	see text	see text	3.3×10^8
$\text{CH(Ph)CO}_2\text{Et}$	$k\text{-CH}_2\text{COtBu}/k\text{-CH(Ph)CO}_2\text{Et}=3.87$	$k\text{-CH}_2\text{COtBu}=3.3 \times 10^8$	8.5×10^7
P(O)(OEt)_2	$k\text{-P(O)(OEt)}_2/k\text{-CH(Ph)CO}_2\text{Et}=2.02$	$k\text{-CH(Ph)CO}_2\text{Et}=8.5 \times 10^7$	1.7×10^8
$\text{O}_2\text{N=CMe}_2$			1.2×10^9 ^a

^aReference 10.

substituted product (Equation 84).



The reactivity of nucleophiles toward phenyl radical appears to be dependent upon the basicity of the nucleophile and the stability of the radical anion formed by coupling of the radical with the nucleophile. The pKa's of the conjugate acids of the nucleophiles used along with the rate constants for coupling are presented in Table 53.

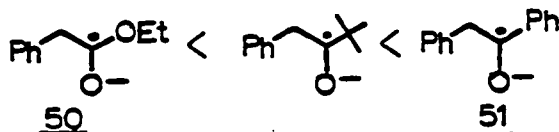
There appears to be a correlation between reactivity and basicity of the nucleophile. Thiophenoxide has a low reactivity toward phenyl radical and also has a low basicity. Pinacolone enolate, acetophenone enolate, and benzyl cyanide ion have nearly the same basicity in DMSO and their reactivity toward phenyl radical is nearly identical.

Table 53. The basicities of the nucleophiles⁷⁷

nucleophile	k, M ⁻¹ s ⁻¹	pKa
⁻ SPh	5.7 X 10 ⁷	10.3
⁻ CH(Ph)COtBu	3.8 x 10 ⁷	19.9 ^a
⁻ CH(Ph)CN	2.3 X 10 ⁸	21.9
⁻ CH(Ph)CO ₂ Et	6.8 X 10 ⁷	22.6
⁻ CH ₂ COPh	3.1 X 10 ⁸	24.5
⁻ CH ₂ COtBu	2.1 X 10 ⁸	27.7

^aThe pKa of phenyl acetone in DMSO.

The stability of the ketyl radical formed from the coupling of the nucleophile and phenyl radical is best represented by the following series:



Structure 50 is the least stable while structure 51 is the most stable. The reactivity of the enolates also parallels the stability of the ketyls formed after coupling.

Comparison of Relative Reactivities of Nucleophiles Competing for an Intermediate in the Aromatic $S_{RN}1$ Reaction and Phenyl Radical Generated from PAT

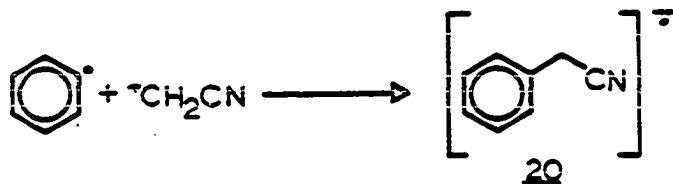
The relative reactivity of pinacolone enolate versus diethyl phosphite ion competing for phenyl radical generated from PAT is 1.6 (Table 47). The relative reactivity of the same two nucleophiles competing for an intermediate in the aromatic $S_{RN}1$ reaction extrapolated to infinite concentration is 1.5 ± 0.5 (Table 13). Also, the relative reactivity of pinacolone enolate versus thiophenoxide competing for phenyl radical is 3.4 (Table 47). The relative reactivity for the same two nucleophiles competing for an intermediate generated from iodobenzene under $S_{RN}1$

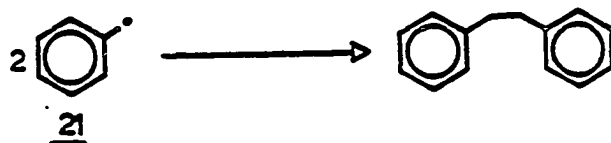
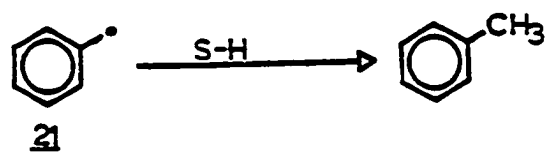
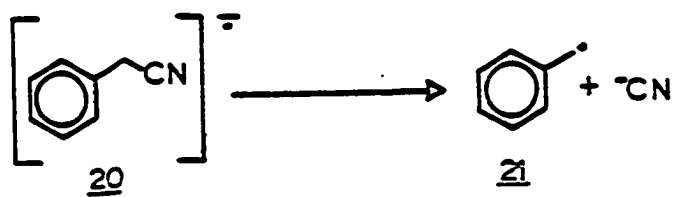
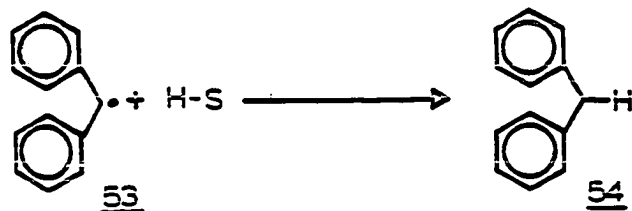
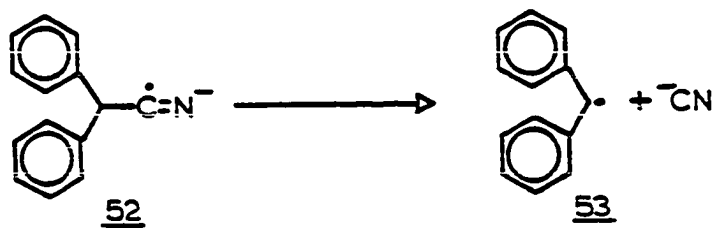
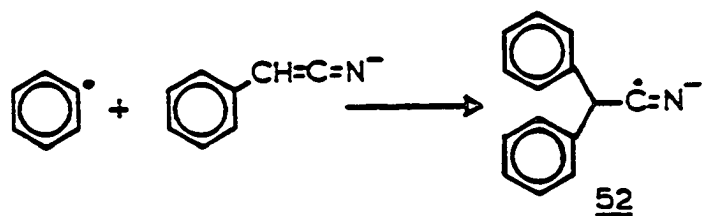
conditions extrapolated to infinite concentration is 3.3 (Table 18). The comparison of the two sets of relative reactivity suggests that a sigma phenyl radical is the sole intermediate involved in the aromatic $S_{RN}1$ reaction.

Reaction of Phenyl Radical with Benzyl Cyanide Ion

The formation of diphenylmethane from the reaction of phenyl radical with benzyl cyanide ion is not surprising. The ion of acetonitrile reacts with bromobenzene under $S_{RN}1$ conditions to give toluene and bibenzyl (Scheme 28).⁴³ The formation of the benzyl radical resulted from the dissociation of the benzyl cyanide radical anion. The formation of diphenylmethane can be justified when considering the above results. Phenyl radical couples with benzyl ion to give radical anion 52 (Scheme 29). Before radical anion 52 can be oxidized by the trityl radical, it dissociates to the diphenylmethyl radical (53) and cyanide ion. The diphenylmethyl radical abstracts a hydrogen atom to give diphenylmethane (54).

Scheme 28.



Scheme 28. continuedScheme 29.

CONCLUSION

The rate constant for the coupling of phenyl radical with a nucleophile is below the diffusion limit value in DMSO at 45 °C. The rate constants measured fall into the 10^7 - 10^8 $\text{M}^{-1}\text{s}^{-1}$ range. The reactivity of nucleophiles toward phenyl radical appears to be related to the basicity of the nucleophile and the stability of the radical anion formed from coupling. For example, thiophenoxide has a low basicity and low reactivity toward phenyl radical. The enolate of acetophenone has a high basicity, forms a stable radical anion after coupling with phenyl radical, and therefore is the most reactive nucleophile toward phenyl radical.

EXPERIMENTAL

General Considerations

All melting points were determined on a Thomas-Hoover capillary melting point apparatus and are uncorrected. GC mass spectra (GCMS) were recorded on a Finnegan 4000 instrument. ^1H NMR were recorded on a Varian EM-360 instrument (60 MHz) or on a Bruker WM-300 (300 MHz). Infrared spectra (IR) were recorded on a Beckman 4250 spectrophotometer. Phenylazotriphenylmethane thermolyses were carried out in a thermostated mineral oil bath at 45 °C. All glassware, syringes, and needles were dried at 140 °C for at least twelve hours. When removed from the oven, they were allowed to cool in a desiccator.

GLC Analysis

GLC analyses of products were carried out on a Varian 3700 equipped with a thermal conductivity detector and a Hewlett-Packard 3390A integrater. A 1/8 in X 10 ft 7% OV-3 on Chromsorb W column was used. A temperature program of 100 °C to 31 °C at 10 °C/min was used for all product analyses with the exception of benzene. The temperature program used when benzene was being quantified was 50 °C to 310 °C at 5 °C/min. Yield of products were determined by use of internal standards. In all cases, the area ratio was corrected for molar response determined from standard

solutions of the products and the internal standards.

General work-up procedure

The following work up procedure was used for the reactions in this section. All reaction mixtures were poured into 50 mL of distilled water. Benzyl ether (0.0098 g, 4.95×10^{-4} mole) was added as an internal standard. The water layer was extracted three times with 30 mL portions of ethyl ether. The ether extracts were combined and washed with 50 mL of distilled water. The ether was dried (MgSO_4) and removed using a rotatory evaporator. The residue was dissolved in chloroform and analyzed by GLC as described above.

Materials

The dimethyl sulfoxide (DMSO) was obtained from Fisher Scientific and purified by drying for one day over calcium hydride. Sodium amide was added just before vacuum distillation through a Vigreux column ($<45^\circ\text{C}$). The DMSO was stored in a foil wrapped flask over 4A molecular sieves under an argon atmosphere.⁵² The DMSO was deoxygenated by passing argon through the solvent for one hour. The 4A molecular sieves were activated by heating at 200°C under vacuum for one day. The DMSO was transferred by syringe to preclude contact with oxygen.

Diethyl phosphite was obtained from Aldrich Chemical

Company and was purified by drying over calcium hydride followed by vacuum distillation. Benzenethiol was obtained from Eastman Organic and was purified by drying over calcium hydride followed by vacuum distillation. Pinacolone and ethyl phenylacetate were obtained from Aldrich Chemical Company and were purified by drying over anhydrous potassium carbonate followed by distillation. Potassium t-butoxide, diphenyl methane, benzyl cyanide and deoxybenzoin were obtained from Aldrich Chemical Company and were used without further purification. The preparation of phenylazotriphenylmethane (PAT),⁴⁷ 1-phenyl-3,3-dimethyl-2-butanone,¹³ 1,1-diphenyl-3,3-dimethyl-2-butanone,¹³ diethyl phenylphosphonate,¹⁵ 1,2,2-triphenylethanone⁷⁸ and ethyl diphenylacetate⁵³ has been described in the literature.

General Procedures

Typical competition procedure for PAT

A 50 mL volumetric flask was charged with potassium t-butoxide (1.35 g, 0.011 mole), fitted with a septum, and flushed with argon. Dry DMSO, 30 mL, was syringed into the flask. Benzenethiol (0.55 g, 0.005 mole) and ethyl phenylacetate (0.78 g, 0.0048 mole) were syringed into the flask. Dry DMSO was syringed into the flask to adjust the volume to 50 mL. A test tube was charged with phenylazotriphenylmethane (0.05807 g, 1.67×10^{-4} mole), fitted with a septum,

and flushed with argon. A 20 mL aliquot from the above standard solution was syringed into the test tube. The test tube was placed into an oil bath at 45 °C for 22 hours. The tube was removed, worked up and analyzed as described above.

Typical competition procedure when one nucleophile is diethyl phosphite ion

A 50 mL volumetric flask was charged with potassium t-butoxide (1.35 g, 1.10×10^{-2} mole), fitted with a septum and flushed with argon. DMSO, 30 mL was syringed into the flask and the flask was swirled until all of the base had dissolved. Ethyl phenylacetate (0.76 g, 4.63×10^{-3} mole) and diethyl phosphite (1.02 g, 7.89×10^{-3} mole) were syringed into the flask. The solution was brought to volume. A test tube was charged with PAT (0.06113 g, 1.76×10^{-4} mole), fitted with a septum and flushed with argon. A 20 mL aliquot of the above solution was syringed into the test tube. The test tube was placed in an oil bath at 45 °C for 22 hours. The reaction mixture was worked-up and analyzed as described earlier.

Typical competition procedure for PAT when potassium is complexed by 18-crown-6

A 50 mL volumetric flask was charged with potassium t-butoxide (1.22 g, 1.0×10^{-2} mole), fitted with a septum and flushed with argon. DMSO, 30 mL, was syringed into the flask. 18-Crown-6 (3.52 g, 1.3×10^{-2} mole) was syringed

into the flask. The flask was swirled until all of the base had dissolved. Ethyl phenylacetate (0.87 g, 5.3×10^{-3} mole) and diethyl phosphite (0.82 g, 5.9×10^{-3} mole) were syringed into the flask. The solution was brought to volume. A test tube was charged with PAT (0.05232 g, 1.5×10^{-4} mole), fitted with a septum and flushed with argon. A 20 mL aliquot from the above solution was syringed into the test tube. The test tube was placed in an oil bath at 45°C for 22 hrs. The reaction mixture was worked-up and analyzed as described earlier.

Determination of benzene

A 25 mL volumetric flask was charged with potassium t-butoxide (1.00 g, 0.0082 mole), fitted with a septum, and flushed with argon. Dry DMSO, 10 mL, was syringed into the flask. The potassium was complexed by syringing 18-crown-6 (2.62 g, 0.0099 mole) into the flask. Pinacolone (0.87 g, 0.0087 mole) was syringed into the flask and the volume was adjusted to 25 mL by injecting dry DMSO. An ampoule (10 mL in volume) was charged with PAT (0.10 g, 0.00029 mole), attached to a vacuum line, and flushed with argon. An 8 mL aliquot of the above solution was syringed into the ampoule via a side arm on the neck of the ampoule. The solution in the ampoule was frozen under vacuum using liquid nitrogen, then warmed to room temperature under argon. This procedure was repeated two times. After the freeze-pump-thaw cycles,

the solution was frozen and the ampoule was sealed under vacuum using a torch. The sealed ampoule was placed in an oil bath at 45 °C for 22 hours. After this heating period, the solution in the ampoule was frozen and then opened. While still frozen, a septum was fitted to the neck of the ampoule and securely fastened. Once at room temperature, toluene (0.05 g, 0.00054 mole) was injected into the ampoule and was used as the internal standard for the quantitation of benzene. A 10 uL aliquot of the reaction mixture was injected into the GLC instrument using the conditions outlined above to quantify benzene. After the quantification was complete, the reaction mixture was worked up and analyzed as described earlier.

Time study of phenyl phosphonate in the presence of excess diethyl phosphite and thiophenoxide

A 100 mL round bottomed flask equipped with a magnetic stirring bar was charged with potassium t-butoxide (1.83 g, 1.5×10^{-2} mole), fitted with a septum and flushed with argon. DMSO, 20 mL, was syringed into the flask. Thiophenol (0.96 g, 8.7×10^{-3} mole) and diethyl phosphite (1.11 g, 8.04×10^{-3} mole) were syringed into the flask and the volume of the solution adjusted to 25 mL. Aliquots, 2 mL, were removed at certain time intervals and worked-up and analyzed as described earlier.

GENERAL SUMMARY

Evidence has been presented that supports the existence of only one intermediate in the aromatic $S_{RN}1$ reaction. The relative reactivity of nucleophiles competing for an intermediate in the aromatic $S_{RN}1$ reaction and phenyl radical generated from the thermolysis of PAT were very similar.

Initial relative rate studies competing two nucleophiles versus each other with iodobenzene under $S_{RN}1$ conditions indicate another important product forming step in the early stages of the reaction other than radical nucleophile coupling. It appears that a competition occurs between a photochemical process involving electron transfer followed by cage recombination and the photostimulated free radical chain process. The only nucleophiles that appear to form a charge transfer complex with iodobenzene were the enolates of pinacolone and 1-phenyl-3,3-dimethyl-2-butanone.

The rate constant for the coupling of phenyl radical with various nucleophiles is below the diffusion limit value in DMSO at 45 °C. The reactivity of nucleophiles toward phenyl radical appears to be related to the basicity of the nucleophile and the stability of the radical anion formed from coupling.

REFERENCES

1. Kornblum, N.; Michel, R. E.; Keriber, R. C. J. Am. Chem. Soc. 1966, 88, 5662.
2. Russell, G. A.; Danen, W. C. J. Am. Chem. Soc. 1966, 88, 5663.
3. Kornblum, N. Angew. Chem. Int. Ed. Engl. 1975, 14, 734.
4. Kim, J. K.; Bunnett, J. F. J. Am. Chem. Soc. 1970, 92, 7463.
5. Kim, J. K.; Bunnett, J. F. J. Am. Chem. Soc. 1970, 92, 7464.
6. Beletskaya, I. P.; Drozd, V. N. Russian Chem. Rev. 1979, 48, 431.
7. Bunnett, J. F. Acc. Chem. Res. 1978, 11, 413.
8. Wolfe, J. F.; Carver, D. R. Org. Prep. Proc. Int. 1978, 10, 225.
9. Rossi, R. A.; de Rossi, R. H. "Aromatic Substitution by the $S_{RN}1$ Mechanism"; American Chemical Society: Washington D.C., 1981.
10. Tanko, J. M. Ph.D. Dissertation, Iowa State University, Ames, IA, 1985.
11. Saveant, J. M. Acc. Chem. Res. 1980, 13, 323.
12. Swartz, J. E.; Stenzel, T. T. J. Am. Chem. Soc. 1984, 106, 2520-24.
13. Scamehorn, R. G.; Bunnett, J. F. J. Org. Chem. 1977, 42, 1449-57.
14. Galli, C.; Bunnett, J. F. J. Org. Chem. 1984, 49, 3041-42.
15. Hoz, S.; Bunnett, J. F. J. Am. Chem. Soc. 1977, 99, 4690-99.
16. Fox, M. A.; Younathan, J.; Fryxell, G. E. J. Org. Chem. 1983, 48, 3109-12.

17. Bunnett, J. F.; Creary, X. J. Org. Chem. 1974, 39, 3612.
18. Bunnett, J. F.; Shafer, S. J. J. Org. Chem. 1978, 43, 1877.
19. Amatore, C.; Combellas, C.; Pinson, J.; Oturan, S. R.; Saveant, J. M.; Thiebault, A. J. Am. Chem. Soc. 1985, 107, 4846-53.
20. Andrieux, C. P.; Dumas-Bouchrat, J. M.; Saveant, J. M. J. Electroanal. Chem. 1978, 88, 43.
21. Kigawa, H.; Takamuku, S.; Toki, S.; Kimmira, N.; Takeda, S.; Tsumori, K.; Sakurai, H. J. Am. Chem. Soc. 1981, 103, 5176.
22. Behan, D.; Neta, P. J. Am. Chem. Soc. 1981, 103, 2280.
23. Neta, P.; Behar, D. J. Am. Chem. Soc. 1981, 103, 103.
24. Houser, K. J.; Bartak, D. E.; Hawley, M. D. J. Am. Chem. Soc. 1973, 95, 6033.
25. Bartak, D. E.; Houser, K. J.; Rudy, B. C.; Hawley, M. D. J. Am. Chem. Soc. 1972, 94, 7526.
26. Amatore, C.; Pinson, J.; Saveant, J. M.; Thielbault, A. J. Electroanal. Chem. 1980, 107, 59.
27. Amatore, C.; Oturan, M. A.; Pinson, J.; Saveant, J. M.; Thiebault, A. J. Am. Chem. Soc. 1985, 107, 3451-59.
28. Gores, G. J.; Koeppi, C. E.; Bartak, D. E. J. Org. Chem. 1979, 44, 380.
29. Nadigo, L.; Saveant, J. M. J. Electroanal. Chem. 1971, 30, 41.
30. Aalstad, B.; Parker, V. D. Acta Chem. Scand. 1982, B 36, 47.
31. Danen, W. C.; Kensler, T. T.; Lawless, J. G.; Marcus, M. F.; Hawley, M. D. J. Phys. Chem. 1969, 73, 4389.
32. Lawless, J. G.; Hawley, M. D. J. Electroanal. Chem. 1969, 21, 365.
33. Tilset, M.; Parker, V. D. Acta Chem. Scand. 1982, B 36, 311.

34. Parker, V. D. Acta Chem. Scand. 1981, B 35, 655.
35. Nelson, R. F.; Carpenter, A. K.; Seo, E. T. J. Electrochem. Soc. 1973, 120, 206.
36. Amatore, C.; Pinson, J. Chanssand, J.; Saveant, J. M.; Theibault, A. J. J. Am. Chem. Soc. 1979, 101, 6012.
37. M'Halla, F.; Pinson, J.; Saveant, J. M. J. Am. Chem. Soc. 1980, 102, 4120.
38. Galli, C.; Bunnett, J. F. J. Am. Chem. Soc. 1981, 103, 7140-47.
39. Rossi, R. A.; Bunnett, J. F. J. Org. Chem. 1973, 38, 1407.
40. Bunnett, J. F.; Traber, R. P. J. Org. Chem. 1978, 43, 1867.
41. Swartz, J. E.; Bunnett, J. F. J. Org. Chem. 1979, 44, 340.
42. Rossi, R. A.; de Rossi, R. H.; Pierini, A. B. J. Org. Chem. 1979, 44, 2662.
43. Bunnett, J. F.; Gloor, B. F. J. Org. Chem. 1973, 38, 4156.
44. Scamehorn, R. G.; Hardacre, J. M.; Lukauick, J. M.; Sharpe, L. R. J. Org. Chem. 1984, 49, 4881-83.
45. Pierini, A. B.; Peirenory, A. B.; Rossi, R. A. J. Org. Chem. 1984, 49, 486-90.
46. Bunnett, J. F.; Shafer, S. J. J. Org. Chem. 1978, 43, 1873.
47. Bridger, R. F.; Russell, G. A. J. Am. Chem. Soc. 1963, 85, 3754.
48. Kryer, R. G.; Lorand, J. P.; Stevens, N. R.; Herron, N. R. J. Am. Chem. Soc. 1977, 99, 7589.
49. Porter, N. A.; Dubay, G. R.; Green, J. G. J. Am. Chem. Soc. 1978, 100, 920.
50. Suehiro, T.; Nakausa, R.; Kobayash, M.; Date, M.; Toshimako, M. Chem. Lett. 1982, 1191.

51. Bunnett, J. F.; Sundberg, J. E. J. Org. Chem. 1976, 41, 1702-6.
52. Ritchie, C. D.; Skinner, G. A.; Badding, V. G. J. Am. Chem. Soc. 1967, 89, 2069.
53. Vorlander, D.; Rach, E. Berichte 1923, 56, 1126.
54. (a) Walling, C. "Free Radicals in Solution"; Wiley: New York, N. Y., 1957. (b) Pryor, W. A. "Free Radicals"; McGraw-Hill: New York, N. Y., 1966; Chapter 12. (c) Nonheblel, D. C.; Walton, J. C. "Free Radical Chemistry"; Cambridge University Press: Cambridge, 1974.
55. (a) Fu, J. J. L.; Benturde, W. G. J. Am. Chem. Soc. 1972, 94, 7710. (b) Fu, J. J. L.; Bentrude, W. G. J. Am. Chem. Soc. 1972, 94, 7717.
56. (a) Pryor, W. A.; Guard, H. J. Am. Chem. Soc. 1964, 86, 1150. (b) Kampmeier, J. A.; Geer, R. P.; Meskin, A. J.; D'Silvia, R. M. J. Am. Chem. Soc. 1966, 88, 1257. (c) Kampmeier, J.; Evans, T. R. J. Am. Chem. Soc. 1966, 88, 4096.
57. Janzen, E. G.; Nuter, Jr., D. E.; Evans, C. A. J. Phys. Chem. 1975, 79, 1983-4.
58. Janzen, E. G.; Evans, C. A. J. Am. Chem. Soc. 1975, 97, 205-6.
59. Suehiro, T.; Suzuki, A.; Tsuchida, Y.; Yamazaki, J. Bull. Chem. Soc. Jpn. 1977, 50, 3324-8.
60. Batyrbaev, N. A.; Zorin, V. V.; Imashev, V. B.; Zolotski, S. S.; Ralchmankulov, D. L. Zh. Org. Khim. (Engl. Trans.) 1980, 16, 1351.
61. Pryor, W. A.; Echols, Jr., J. T.; Smith, K. J. Am. Chem. Soc. 1966, 88, 1189-98.
62. Levin, Y. A.; Trutneva, E. K.; Ivanov, B. E. Zh. Obslich Khim. (Engl. Trans.) 1974, 44, 1418.
63. Takayama, K.; Kosugi, M.; Migita, T. Chem. Lett., 1973, (2), 193-5.
64. Tanner, D. D.; Reed, D. W.; Setilciani, B. P. J. Am. Chem. Soc. 1982, 104, 3917-23.

65. Danen, W. C.; Saunders, D. G.; Rose, K. A. J. Am. Chem. Soc. 1974, 96, 4558-62.
66. Danen, W. C.; Saunders, D. G.; Rose, K. A. J. Am. Chem. Soc. 1973, 95, 1612-15.
67. Migita, T.; Nagai, T.; Abe, Y. Chem. Lett. 1975, (6), 543-6.
68. Pryor, W. A.; Smith, K. J. Am. Chem. Soc. 1970, 92, 2731-38.
69. Levin, Y. A.; Abulkhanov, G. G.; Nefedov, V. P.; Skorobogatova, B. E. Dokl. Akad. Nauk. SSSR (Engl. Trans.) 1977, 235, 629.
70. Packer, J. E.; House, D. B.; Rasburn, E. J. J. Chem. Soc. B, 1971, 1574.
71. Scaiano, J. C.; Ingold, K. U. J. Am. Chem. Soc. 1977, 99, 2079-84.
72. Veltivisch, D.; Asums, K. D. J. Chem. Soc. Perkin Trans II, 1982, (9), 1147.
73. Scaiano, J. C.; Stewart, L. C. J. Am. Chem. Soc. 1983, 105, 3609-14.
74. Burkey, T. J.; Griller, D.; Lunauyzi, L.; Nazran, A. S. J. Org. Chem. 1983, 48, 3704-7.
75. Johnson, L. J.; Lusztyk, J.; Wayner, D. D. M.; Abeywickreyma, A. N.; Beckwith, A. L. J.; Scaiano, J. C.; Ingold, K. U. J. Am. Chem. Soc. 1985, 107, 4594-6.
76. Lusztyk, J.; Ingold, K. U. J. Phys. Chem. 1985, 89, 1865-9.
77. Bordwell, F. G., Department of Chemistry, Northwestern University, private communication.
78. Kakis, F. J.; Brase, D.; Oshima, A. J. Org. Chem. 1971, 36, 4117.

ACKNOWLEDGEMENTS

The investigator would like to thank Dr. Glen A. Russell for his support and guidance throughout this study. He also thanks the members of the Russell group for their support and suggestions during the course of this study. The investigator wishes to thank the faculty, staff, and graduate students of the Department of Chemistry of Iowa State University for their support resulting in three and a half enjoyable years.

He would like to thank most of all his wife Nancy, who has withstood the trials and tribulations of the last three years. Her understanding and love has made the completion of this degree possible. This thesis is dedicated to her.